



The University
of Milano
Bicocca

**THE
PhD
PROGRAM
DIMET**

The PhD Program in
Translational and Molecular
Medicine (DIMET)
is an inter-departmental
project between the School
of Medicine and the Faculty
of Science, organized
by the University of
Milano-Bicocca.



PhD

**PROGRAM IN TRANSLATIONAL
AND MOLECULAR MEDICINE**

DIMET

**UNIVERSITY OF MILANO-BICOCCA
SCHOOL OF MEDICINE AND FACULTY OF SCIENCE**

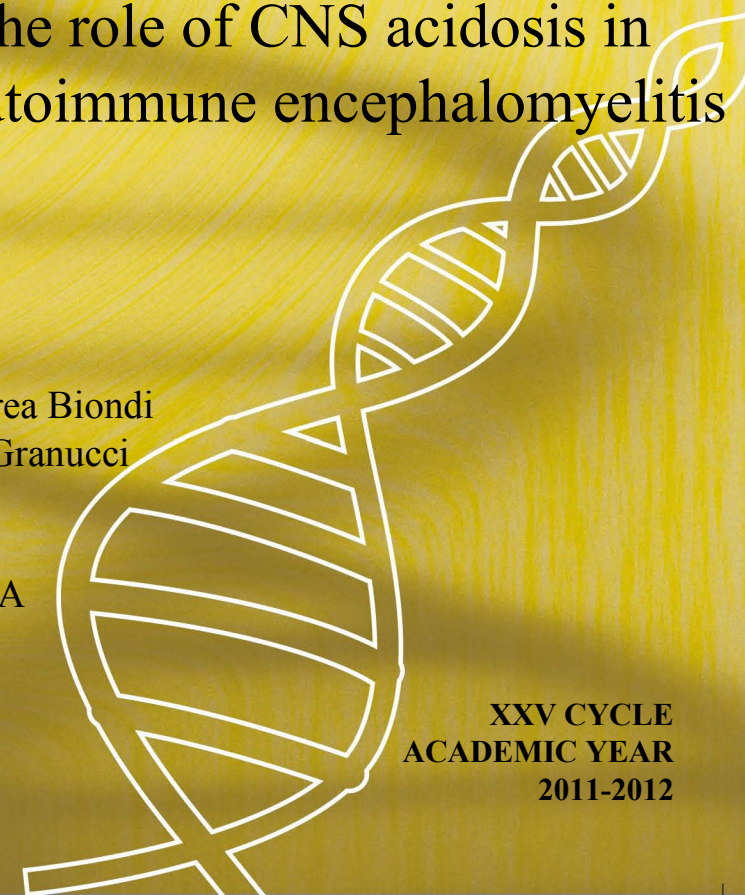
**Unraveling the role of CNS acidosis in
experimental autoimmune encephalomyelitis**

**Coordinator: Prof. Andrea Biondi
Tutor: Prof. Francesca Granucci**

**Dr. Roberta DE CEGLIA
Matr. No. 062720**

**XXV CYCLE
ACADEMIC YEAR
2011-2012**

DIMET - Dr. Roberta DE CEGLIA - A.A. 2011-12



Dimet

Ph.D. Program
Translational and
Molecular Medicine

UNIVERSITY OF MILANO – BICOCCA
SCHOOL OF MEDICINE AND SCHOOL OF SCIENCE



**UNRAVELING THE ROLE OF CNS ACIDOSIS IN
EXPERIMENTAL AUTOIMMUNE ENCEPHALOMYELITIS**

Coordinator: Prof. Andrea Biondi

Tutor: Prof. Francesca Granucci

Dr. Roberta DE CEGLIA

Matr. No. 062720

XXV CYCLE

ACADEMIC YEAR

2011-2012

A chi mi è stato vicino...
... soprattutto nei momenti difficili

*"There isn't a better moment to be happy than this,
happiness is the way not the destination...
Behind every result there is a new challenge.
Go on, even when everybody expects you to give up."*

Mother Teresa from Calcutta

TABLE OF CONTENENT

CHAPTER 1	7
Introduction	7
1. Multiple sclerosis	7
1.1. History, aetiology and risk factors	7
1.2. MS form and Clinical feature	12
1.3. MS lesions	14
1.4. MS immunological mechanisms	18
1.5. Therapies.....	22
2. Animal model of MS	27
2.1. The experimental autoimmune encephalomyelitis (EAE) model	28
2.2. The MOG-induced EAE model	30
3. Inflammation-acidification in CNS during EAE.....	32
3.1. Neurodegeneration in EAE: the role of inflammation	32
3.2. Acidification in CNS: the role of ASICs	34
4. Scope of the thesis.....	43
5. References	44
CHAPTER 2	53
CNS acidosis in Experimental Autoimmune Encephalomyelitis; role of ASIC channels.....	53
CHAPTER 3	109
Impaired striatal GABA transmission in experimental autoimmune encephalomyelitis.....	109
CHAPTER 4	149

Summary, conclusions and future perspectives	149
References	154
CHAPTER 5	156
Publications.....	156
Acknowledgements	157

CHAPTER 1

Introduction

1. Multiple sclerosis

1.1. History, aetiology and risk factors

Multiple sclerosis (MS), also known as *disseminated sclerosis* or *encephalomyelitis disseminata*, is an autoimmune inflammatory disorder of the brain and spinal cord in which focal lymphocytic infiltration leads to damage of myelin and axons (Compston & Coles 2008). The name multiple sclerosis refers to scars (*sclerae*, better known as plaques or lesions) particularly in the white matter of the brain and spinal cord. This pathology was primarily described by Robert Carswell in 1838 as “a remarkable lesion of the spinal cord accompanied with atrophy”, anticipating the first official identification of MS done in 1868 by Charcot. However, personal diaries and historical works push back descriptions of the disease at least 50, and perhaps 500, years earlier (lucidly summarized at <http://ms-society.ie/pages/historical-overview/>). In the 20th century, the monograph *Multiple Sclerosis* (1955) published by Douglas McAlpine, Nigel Compston and Charles Lumsden defined the name of this pathology, starting to be universally known as *multiple sclerosis* (MS) (Thompson 1955). MS affects principally young adults between

the age of 20 and 50 with an average age of onset of 29.2 (WHO 2008), however it can occur also in young children and older adults (nationalmssociety.org). MS shows a chronic and often debilitating course, and carries a large burden of suffering and expense for approximately 2.5 million affected worldwide (WHO report 2008). Although the aetiology is still unknown, the disease certainly appears to develop in population with a specific genetic profile as a consequence of environmental exposures (*Fig.1* and 2). Indeed, MS is more common in Caucasian (50-100 people each 100'000) than in other ethnic groups where the incidence is lower as in African

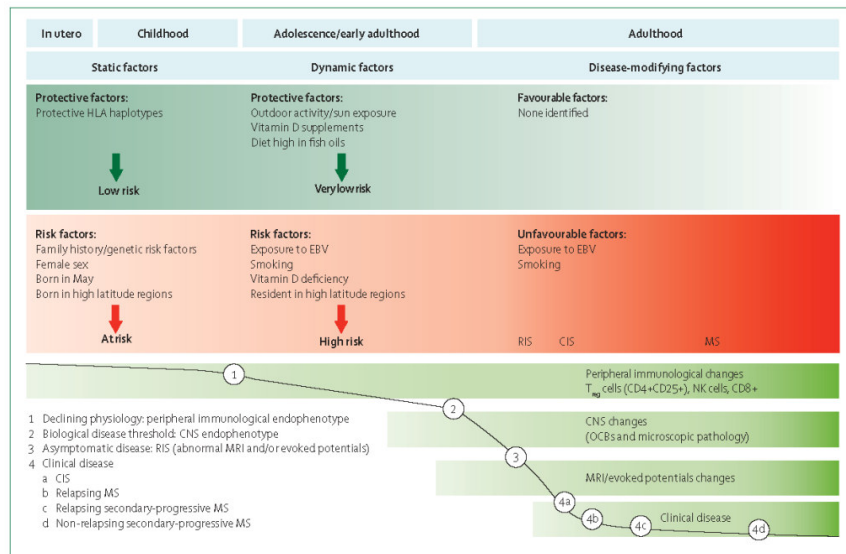


Fig.1 Risk factors in MS (Ramagopalan et al 2010).

Americans, Native Americans, Mexicans, Puerto Ricans, and Japanese, and a virtual absence of the disease in Chinese and Filipinos (Ramagopalan et al 2010).

In addition genetic factor seems to be associated with MS disease. Genome-wide association studies (GWAS) found that the most common alleles associated with MS are human leukocyte antigen HLA haplotype, which encode for molecules that present antigen to CD4⁺ T cells, the interleukin (IL)-2 receptor α and IL-7 receptor α (CD127) genes (Libbey & Fujinami 2010). Until now the experimental evidences are not sufficient to demonstrate that these genes are the only origin of the disease. Furthermore, it is described a maternal parent-of-origin effect supporting that a genetic predisposition is real, but the mechanism of this increased risk factor remains to be elucidated (Ramagopalan et al 2010). Also the gender appears to be involved in MS susceptibility. Globally, the median estimated male/female ratio is 0.5, or 2 women for every 1 man (WHO 2008). Certainly for specific country, such as Denmark and Canada, the ratio is almost three women affected for each man (Koch-Henriksen & Sørensen 2010) and for the northern Europe is over 3.5 (Trojano et al 2012), thus suggesting that hormones play an important role in triggering this pathology.

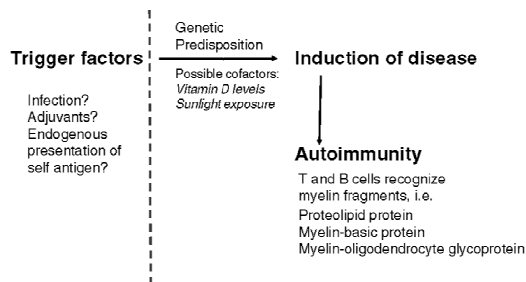


Fig.2 Multistep induction of MS (Weissert 2013)

Another aspect to be discussed is the presence of a variety of infectious agents, in particular viruses, that maybe involved in MS onset. The

herpes viruses, influenza virus, paramyxoviruses, picornaviruses and

Epstein–Barr virus (EBV) were studied in MS patients, but until now there is not a definitive proof that directly links any one of these viruses to the autoimmune reaction that is believed to be responsible for the demyelination seen in MS. Recent studies suggest that the pathology starts when a multiple viral infection occurs (Cusick 2013). The idea is that one virus infection may enhance another virus replication and as a consequence while the first virus prime the immune system or damage the CNS defence (i.e. disrupting the blood-brain-barrier), the second virus trigger the disease onset. However for the moment it is just a speculation, more studies are needed to prove this hypothesis. A recent study demonstrated that also the commensal gut flora, in the absence of pathogenic agents, is essential in triggering immune processes in animal models of MS. These new findings highlighted the idea that the MS pathogenesis originates in the immune system rather than in changes in the CNS target (Berer et al 2011).

Other increasing risk factors described in recent studies are the Vitamin D and the sunlight exposure. These two aspects well correlate because vitamin D is the mediator of the sunlight effect, so an inadequate intake of this vitamin and a low exposition to sunlight, especially in country with increased latitude, may be a co-factor to trigger MS. Indeed vitamin D supplemented diet in people that risk to develop MS may reduce it of 40% (Ascherio & Marrie 2012).

Traditionally MS has been considered an autoimmune disease T cells mediated, specifically deregulated auto-reactive T cell coming from

the periphery in concert with B cells and macrophages destroy specific elements of the CNS -i.e. myelin-.

Beyond the environmental and genetic risk factors, evaluating only the biological system, two models were speculated about the pathophysiology of MS (*Fig.3*). The first model is the “outside-in model” which supposes that the initial failure starts inside the CNS, as the most common neurodegenerative disease (Alzheimer and Parkinson). The latter “inside-out model” foresees a cellular specific damage (probably at the expense of oligodendrocyte–myelin complex) that release highly antigenic constituents that subsequently triggered a strong inflammatory and autoimmune response in predisposed host (Stys et al 2012).

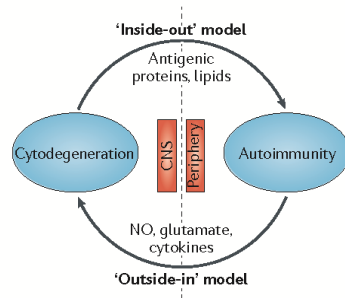


Fig.3 The two hypothetical models of MS aetiologies (Stys et al 2012).

Although both models are pertinent and may describe the onset of the disease, further studies are needed to establish the precise pathophysiology of MS. Nevertheless, it appears clear from the recent literature, that MS is a multifactor pathology and its onset probably depend on genetic predisposition, environmental

factors and infectious agents. However, one of these factors without the complicity of the others is not sufficient to induce the onset and the development of the disease.

1.2. MS form and Clinical feature

MS is further complicated by the fact that is hard to identify the early stages, as well as the first evident sign of its appearance –i.e. clinically isolated syndrome (CIS)- which is defined by a distinct first neurological event with observed demyelination involving the optic nerve, cerebrum, cerebellum, brainstem, or spinal cord (Miller et al 2005). However, it is possible to recognize signs of the disease even

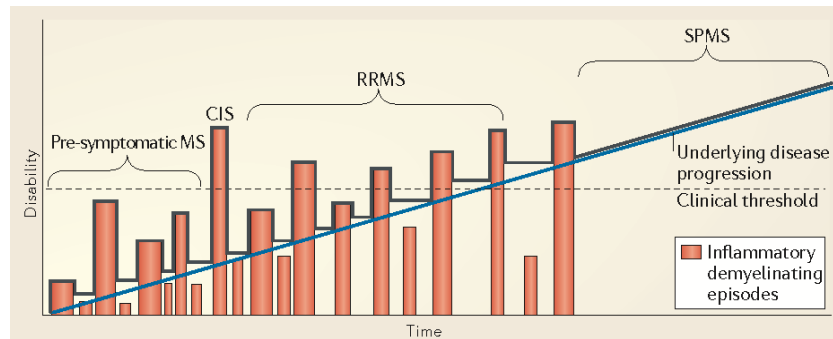


Fig.4 Clinical form of MS (Stys et al 2012).

before the CIS by identifying radiological abnormalities. This status is called radiologically isolated syndrome (RIS) and often precedes MS onset (Fig.4).

MS patients present several common pattern symptoms that are associated with a specific inflammatory response. The most common form of MS is the relapsing-remitting (RRMS) form that affects 85% of newly diagnosed patients. RRMS patients experienced a worsening of the neurological function (called relapse or exacerbation) that can occur in the brain, in the spinal cord and/or in the optic nerve. This attack is followed by periods of remission in which the neurological functionality is partially recovered within weeks to months.

Neurological abnormalities revealed by magnetic resonance scanning, highlight multifocal lesions that are typically, but not exclusively, placed in the white matter. The majority of patients affected by RRMS enter into a phase of non-relapsing secondary progressive MS (SPMS) in which CNS inflammation is reduced, but a slowly progressive neurological decline and CNS atrophy are occurring. Interestingly, a minority court of patients assumes a relatively non-inflammatory progressive course from the onset. In this form, the disease is called primary progressive MS (PPMS). It is also interesting to note that, although the initial courses of RRMS and PPMS are very different, the progression of both forms of MS is somehow similar (*Table 1.*).

Table 1 Stages of MS

Stage	Initiation	Latency	Disease onset (CIS)	Inflammatory phase (RR-MS)	Transitional phase	Neurodegenerative phase (SP-MS)
Stage number	1	2	3	4a	4b/5a	5b
Disease-modifying therapies	None	None	Anti-inflammatory therapies effective	Anti-inflammatory therapies effective	Anti-inflammatory therapies less effective	None
Clinical events	None	None	Single symptomatic episode of inflammatory demyelination	Intermittent symptomatic attacks, often with satisfactory recovery; stable neurological baseline	Neurological baseline becomes unstable; recovery from attacks may be incomplete	Steady progression occasionally punctuated by attacks; variable periods of stability without marked improvement
Proposed pathogenesis	Activation of autoreactive lymphocytes: molecular mimicry; superantigen; altered lymphocyte physiology due to EBV and low vitamin D	Stochastic intrathecal accumulation of inflammatory cells and asymptomatic demyelinating lesions	Inflammatory demyelination of cortex and white matter often triggered by systemic stimuli such as URI	Recurrent bouts of demyelination with axonal injury; cortical pathology; variable repair	Failure of repair and compensation as axonal injury reaches threshold	Widespread glial activation; progression of cortical pathology; ongoing axonal degeneration; meningeal inflammation
Typical age (range)	13–15 (5–20)	15–30 (10–50)	30 (20–50)	30–45 (<70)	45–55	45–75

CIS, clinically isolated syndrome; RR, relapsing-remitting; SP, secondary progressive; EBV, Epstein-Barr virus; URI, upper respiratory infection.

Table 1.Stages of MS (Ransohoff 2012)

MS patient disabilities were clinically evaluated by using the Extended Disability Status Scale (EDSS) (Kurtzke, 1983) that defines the neurological disability of the patients focused mainly on the ability to walk and giving a score that ranges from 0 to 10. Lower numbers indicate less severe disability, while higher numbers reflect a greater degree of disability. This scale is complemented by the

Functional System Score (FSS) that measures the gait, the use of assistive devices and observes also functions like problems with speech, visual function, mental functions, ect.. Together EDSS, FSS and also magnetic resonance imaging (MRI) of CNS allow the clinicians to have a good framework of neurological impairments of MS patients.

1.3. MS lesions

Lesions in the MS brain are continuously forming, although some of them may regress during the course of the disease. Indeed, also patients with a long story of disease might experience the onset of new lesions. Some lesions look essentially similar to scars but they contain a centre surrounded by a rim of foamy lipid-laden macrophages that reflect the advanced myelin phagocytosis; others appear as a solid ball of foamy macrophages. However, pathological hallmark of these lesions is the presence of perivascular lymphocytes, altered numbers of oligodendrocytes and activation of astrocytes. In MS pathology, lesions are staged according to inflammatory activity into active, chronic active, and chronic inactive. Degree of inflammation is determined by the density and distribution of macrophages or microglia. Indeed, the principal hallmark of the active lesions is the presence of a massive number of macrophages engulfing myelin debris and activated microglia associated with a low grade of infiltrating lymphocytes. Chronic active lesions are lesions with an inactive core, surrounded by a narrow rim (usually

thinner than active lesions) of microglia activation, macrophages infiltration and a moderate lymphocytic infiltration. Finally, chronic inactive lesions are hypocellular scar-like lesions that show demyelination and a limited number of inflammatory infiltrates (van der Valk & Amor 2009).

Furthermore, the development of new MRI technologies allowed clinicians to identify specific white and gray matter regions that are not presenting lesion signs, but they are predisposed to develop them.

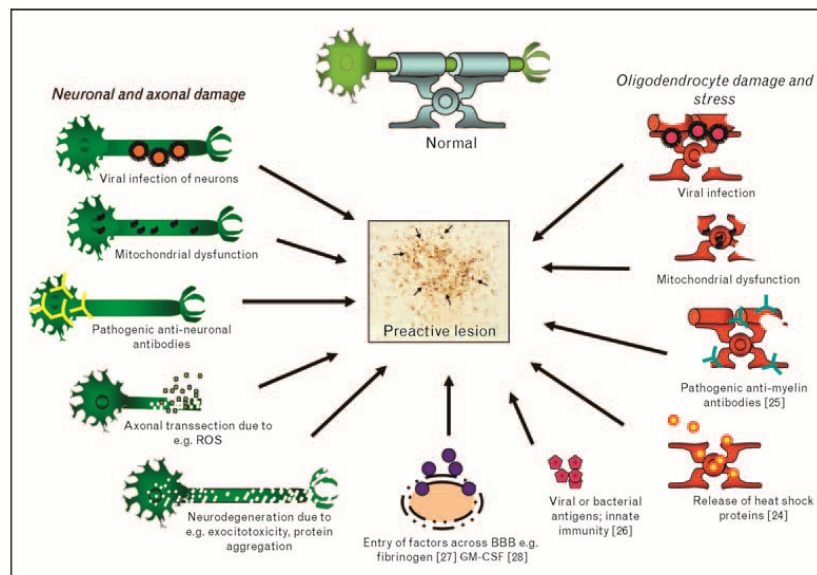


Fig.5 Schematic representation of lesion development in MS (Allen et al 2001).

Indeed, these areas, known as normal-appearing white matter (NAWM) and normal-appearing grey matter, show a normal appearance of myelin, although they also display signs of microglia and astrocytes activation (Fig.5). NAWM features are not well

established yet, even if there is a large consensus that sustain the idea that these areas are preferentially exposed to lesion manifestation (Allen et al 2001).

Recently, the demyelination of cerebral cortex, which is possibly associated to the development of cortical atrophy, has been recognized as important component of MS pathology (Lassmann 2012). Cortical lesions are divided in three types: combined cortico/subcortical lesions, perivascular intracortical lesions and band-like subpial lesions, which affect the cerebral cortex over several adjacent gyri and sulci (Bø 2003). Initially, it was thought that cortical lesions developed only in the progressive phase of the pathology and that they were different from the white matter lesions by the absence of perivascular and parenchymal infiltrates of T- and B-lymphocytes, as well as vascular inflammation and blood–brain barrier disturbance. In 2011 Lucchinetti and co-workers demonstrated that also gray matter lesions appeared since the early stage of the disease and were rich of lymphocytic infiltration as white matter lesions. In addition, also the meninges are full of inflammatory cells and this condition well correlates with the appearance of active cortical plaques, in SPMS and PPMS too. These findings support the hypothesis that meningeal inflammation drives tissue damage in the cortex by two different mechanisms: on one side, T and B activated lymphocytes directly influences the cells within the infiltrated area; on the other side, soluble factors –i.e. cytokines and chemokines- released by lymphocytes, macrophages and microglia can diffuse deepest in the tissue, disrupting cells

homeostasis and inducing neurodegeneration and demyelination also in distant area from the infiltration zone (Choi et al 2012, Haider et al 2011).

Demyelination, however, might be repaired by endogenous mechanisms fostering the generation of new myelin and promoting the formation of the so called “shadow plaques”. These areas appear distributed as typical MS lesions, but are characterized by thin myelin sheaths with widened internodes. The remyelination process depends on the status of the disease and on the location of the lesion. For example, lesions in the subcortical white matter or in the cortex are in general more prone to remyelination, if compared to periventricular lesions (Albert et al 2007, Patrikios et al 2006).

Another important aspect to bear in mind is the axonal loss within the lesions. Actually, about 22% axonal loss at sites distal to a fatal brain stem lesion was reported in MS patient (Bjartmar et al 2001) and more than 11,000 transected axons per mm^3 tissue were found in highly inflamed lesions, 3000 transected axons per mm^3 in the edge of chronic active lesions and 875 transected axons per mm^3 in the core of chronic active lesions, whereas fewer than 1 transected axon/ mm^3 tissue was found in control white matter (Trapp & Nave 2008). The identification of significant axonal transection in patients with short disease duration (when inflammatory demyelination is predominant) established the concept that axonal loss occurs also at disease onset in MS. The strong correlation between inflammatory activity and axonal damage suggests that inflammation is able to modulate axonal derangement in MS patients. However, initial

axonal loss does not have an immediate clinical impact during early stages of RRMS, but with time and the accumulation of additional lesions, it can drive irreversible neurological disabilities, which are typical of MS progression. Indeed, the conversion of RRMS to SPMS is therefore thought to occur when the brain exhausts its capacity to compensate for further axonal loss (Nave & Trapp 2008). As a consequence, strategies for the promotion of remyelination and restoration of saltatory conduction are functional only if axons are spared. In this scenario, understanding the cellular and molecular mechanisms of axonal transection with disease progression is imperative for the development of neuroprotective therapies (Dutta & Trapp 2011).

All these data suggest that the disease mechanisms change along the natural course of MS and often correlate with acute, relapsing or progressive MS phases that are featured by significant differences in inflammation as well as in distributions of the lesions.

1.4. MS immunological mechanisms

Immunological mechanisms involved in MS onset and disease progression are various and not entirely understood yet. Certainly, T cells are central in the development of this autoimmune inflammatory disease. Accordingly, autoreactive T cells against Myelin Basic Protein (MBP) were found in patients as well as in experimental autoimmune encephalomyelitis (EAE) MS animal models. Furthermore, adoptive transfer of an expanded population

of myelin-reactive encephalitogenic CD4⁺ cells in healthy recipient mice induced mice to develop the EAE. Furthermore the innate immunity captured the researchers' attention after the discovery of abnormally activated (mature) antigen-presenting DCs in MS patients. DCs increase in number during specific phase of MS course, accumulate in MS lesions and show impairment in the maturation process (Nuyts et al 2013). Generally, DC activation (maturation) results in the increased production of proinflammatory cytokines, which lead to the aberrant activation of Th1 and Th17 proinflammatory responses. In MS, these aberrant DCs, prime encephalitogenic adaptive immune effectors (such as Th1 cells, Th17 cells, CD8⁺ cells, and B cells) that up-regulate the expression of specific receptor to cross the blood-brain barrier (BBB) and enter into the CNS. Once in the CNS, the myelin-reactive T cells are reactivated upon encounter of resident APCs, including DCs, presenting myelin-derived epitopes on their MHC II. Subsequently, these perivascular T cells will secrete proinflammatory cytokines allowing recruitment of other inflammatory cells and activating the resident one (astrocytes and microglia). Finally, this inflammatory cascade will lead to the production of reactive oxygen species, excitotoxicity, autoantibody production, and direct cytotoxicity, which are all involved in the demyelination and axonal and neuronal damage, thereby causing the sensory and motor symptoms of MS (*Fig.6*).

Effector T cells play a well-recognized role in the initiation of autoimmune tissue inflammation, and autoreactive CD4⁺ T cells have an established association with the pathogenesis of MS disorder

(Zamvil & Steinman 1990). Different subsets of CD4⁺ effective T cells can be generated from naïve T cells and they all are developed in thymus from a common precursor T cells.

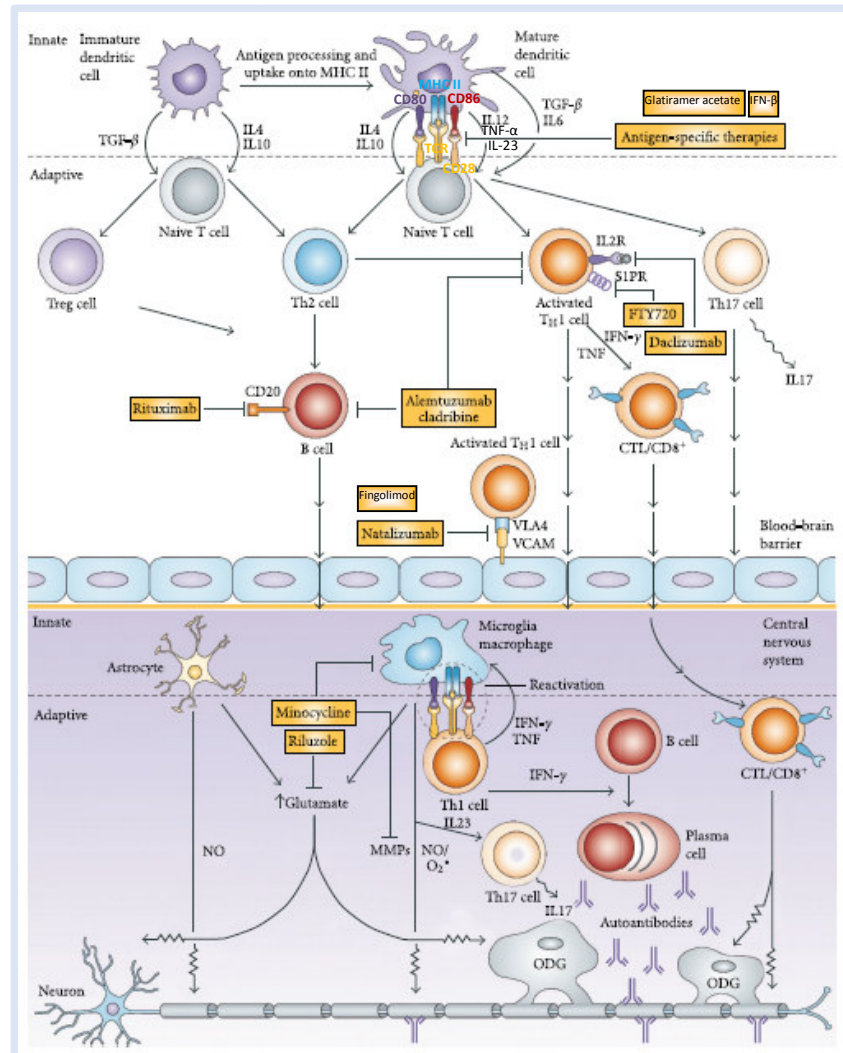


Fig. 6 MS immunopathogenesis and therapeutic targets - adapted from (Chen et al 2012).

CD4 differentiation is regulated by cytokines and extracellular signals present in the microenvironment. Recently, it has been discovered that these cells are also able to switch from one lineage to another during inflammation and tolerance process, and that this plasticity is probably due to miRNAs (Sethi et al 2013).

Based on the cytokine secretion and function, these cells are classified as Th1, Th2, Th9, Th17, follicular helper T cells (T_{FH}) and regulatory CD4 T cell (Treg). In EAE/MS relapse were found increased levels of Th1 cytokines, whereas during remission phases increased Th2 cytokines. Interestingly, different Th1/Th17 ratio seems to modulate EAE induction and Th1 cells have the potential to reciprocally regulate Th17 cells during EAE (Chen et al 2012).

Although MS is believed to be a $CD4^+$ T-cell-mediated autoimmune disease, $CD8^+$ T cells may be involved in MS pathogenesis due to their being the predominate leukocyte in the lesions of MS patients (Cusick 2013). Furthermore, these large numbers of autoreactive $CD8^+$ cytotoxic T lymphocyte (CTL) are found to be clonally expanded in sites of active demyelination and produce tumor necrosis factor (TNF)- α and some also produced IFN- γ .

Also plasmacitoid B cells producing antibody against myelin were found in EAE/MS pathology and seem to have a relevant role in the pathology, indeed their pharmacological inhibition reduces the appearance of new lesion and the relapse events in MS patients. Both innate and adaptive immunities are implicated in triggering and modulating MS pathology. However, further investigations are

needed to better understand the fine tuning of this complicated mechanism in this pathology.

1.5. Therapies

Virtually all available therapies for MS aim to modulate the immune system and are prevalently indicated to treat RRMS which are

Name	Substance	Type	Application
Betaseron TM	Interferon-beta-1b	NBE	s.c., qad
Avonex TM	Interferon-beta-1a	NBE	i.m., 1x/week
Rebif TM	Interferon-beta-1a	NBE	s.c., 3x/week
Extavia TM	Interferon-beta-1b	NBE	s.c., qad
Copaxone TM	Glatirameracetate	NBE	s.c., qd
Tysabri TM	Natalizumab	NBE	i.v., 1x/month
Gilenya TM	Fingolimod	NCE	Oral, qd
Aubagio TM	Teriflunomide	NCE	Oral, qd
Tecfidera TM	Dimethylfumarate	NCE	Oral, qd
Ralenova TM	Mitoxantrone	NCE	i.v., every 3 rd month
Fampyra TM	Fampridine	NCE	Oral, bid

Table 2. Currently marketed therapeutics for MS (Weissert 2013)

featured by active inflammation. So far no effective treatment is available for MS progressive forms in which inflammatory episodes are rare or even not present. The principal pharmacological MS targets are: the initial development of the pathogenic cell population inhibition (pre-clinical approach), the block

of immune cells migration into the site of inflammation and the neutralization of the effector molecules produced by activated immune cells.

However, in the last few decades, new biological entities (NBE) were identified and used to reduce relapse rates and severity in MS (*Table 2.*). The NBE list includes monoclonal antibodies (mAbs) or therapeutic proteins such as insulin and cytokines, showing multiple effects on the immune system. In parallel, we observed the extensive

development of small chemical molecules –i.e. new chemical entities (NCEs)- that are operating on the immune system as NBE. In the early '90 the first NBE introduced in MS was the Interferon- β . IFN β has antiviral, antiproliferative and immunomodulator effects and probably for these multiple roles is able to harness the MS relapse. The second NBE introduced was Glatiramer (1995) that is a polypeptide of about 50 randomly mixed aminoacids containing glutamic acid, lysine, alanine, and tyrosine. Glatimer affects antigen presentation and cytokine balance, thus modulating the immune response. Both IFN β and Glatiramer have a very good long term safety profile and are used in RRMS but also in CIS and early MS (Weissert 2013). In 2006, was introduced the Natalizumab, which is the first therapeutic antibody used in MS targeting and blocking VLA-4 adesion protein on migrating T cells. Furthermore, recent promising Phase II results has been described in march 2013 report in Expert Review of Neurotherapeutics using Secukinumab (AIN457), an antibody that blocks one of the most important T cell- secreted cytokine in MS, the IL-17A (Deiß et al 2013).

A variety of mAbs have been produced against B-cell, in particular mAbs blocking CD20 protein seems to be effective in MS patients (Barun & Bar-Or 2012). CD20 function is not yet elucidated, however it has described having features of a calcium channel with possible roles in B cell activation and differentiation. Rituximab (Rituxan, Genentech and BiogenIdec, RTX) represents the first genetically engineered chimeric anti-CD20 mAb that was found to target and efficiently deplete circulating CD20⁺ B cells in humans. Ocrelizumab

and Ofatumumab are two new anti-CD20 molecules showing a fully human IgG1 tail that are able to bind different epitopes respect rituximab. Both the mAbs appear to deplete B cells primarily through antibody-dependent cellular cytotoxicity (ADCC) and in the ongoing clinical trials seems to be efficacious.

The first NCE molecule available for oral medication for MS was Fingolimod that affects T cell transmigration, by acting in periphery on sphingosine-1-phosphate (S1P) receptor (*Table 2.*).

Dimethylfumarate (DMF), approved in the United States for the treatment of patients with relapsing forms of multiple sclerosis (MS), acts through chemical modification of the repressor protein Keap1, allowing stabilization and nuclear translocation of the transcription factor Nrf2, with subsequent downstream activation of a cascade of several cytoprotective and antioxidant pathways. Additionally, suppression of transcription factor NF- κ B-mediated proinflammatory signaling results in the inhibition of proinflammatory responses and induction of anti-inflammatory cytokines. BG-12, an orally administered enteric-coated microtablet preparation of DMF, has demonstrated efficacy based on clinical and magnetic resonance imaging (MRI) endpoints, as well as an acceptable safety and tolerability profile, in two randomized, double-blind, placebo-controlled, multicenter, Phase 3 studies (Bar-Or et al 2013, Phillips & Fox 2013).

All these therapies are active in MS patients featured by active inflammation -i.e. relapse phase-, while in SPMS or even in PPMS the administration of DMT does not affect disease progression. In this

framework, more studies are needed to define and subsequently target molecules or processes that are exerting relevant harmful functions in the disease (Weissert 2013). In particular, available therapeutics do not prevent axonal loss over time in progressive forms of MS indicating that new molecules directed to axonal preservation are necessary to be discovered.

General approach class	Treatment type	Effects in EAE	References
Ion channel-based approaches	Na channel blockers (e.g. lamotrigine, flecainide), Na channel knockout mice	Improvement	(Bechtold <i>et al.</i> , 2004; 2006; Black <i>et al.</i> , 2006; O'Malley <i>et al.</i> , 2009)
	K Channel blockade	Improvement	(Judge <i>et al.</i> , 1997; Strauss <i>et al.</i> , 2000; Becton <i>et al.</i> , 2001; Madsen <i>et al.</i> , 2005; Reich <i>et al.</i> , 2005)
	Ca channel blockade	Improvement	(Brand Schieber and Werner, 2004; Tokuhara <i>et al.</i> , 2010)
	ASIC channel blockers (e.g. amiloride), ASIC knockouts	Improvement	(Friesen <i>et al.</i> , 2007)

Table 3. Pharmacological approaches on ion channels on EAE model (Constantinescu et al 2011)

Although MS is not conceived as a channelopathy, recent experimental evidence demonstrated that a subset of RRMS patients (13%) developed antibodies against the C-terminal of the AQP4 channel (Alexopoulos et al 2013), as happened in autoimmune channelopathy. Furthermore, changing in the expression of non-mutated channel genes, such as the voltage-gated Na^+ channels (in particular Nav1.8) in EAE cerebellar neurons, could defined MS also as a transcriptional channelopathy (Shields et al 2012, Waxman 2001, Waxman 2005). Hence, in the last few years more attention has been paid on channels activity; indeed, the blockage of channels involved in Na^+ , K^+ and Ca^{++} fluxes seem to ameliorate EAE curse, promising new therapeutic approaches (Table 3.).

Because ions flux within channels seems to be unbalanced and

inflammation often is associated with acidification, particular attention was caught by a class of channels that flux Na^+ and Ca^{++} and it is activated by acidic pH: the acid-sensing ion channel family (ASIC). In particular, Asic1a member opens at slight pH drop, near the physiological pH value as occur during EAE inflammatory state (Friesse et al 2007). Few studies demonstrate that pharmacological block of these channels with amiloride ameliorated EAE disabilities and both myelin and neurons were protected from damage in this acute MS mouse model. The same results were obtained inducing EAE in $\text{ASIC1}^{-/-}$ mice (Friesse et al 2007, Vergo et al 2011). Furthermore, recently was published the first translational pilot study on a cohort of PPMS patients treated with amiloride. This study reveals a significant reduction in normalized annual rate of whole-brain volume during the treatment phase, compared with the pretreatment phase, demonstrating that ASIC1a may exert neuroprotective effects also in patients (Arun et al 2013). However, amiloride is a chemical compound that is able to block not only Asic1a, but also the cognate family ENaCs and sodium/hydrogen exchangers; so it is not possible to exclude that the observed effects are due to the broad spectrum of action of this molecule. Further studies using selective blockers of Asic1a are required to finally demonstrate that the inhibition of this specific channel ameliorate the clinical EAE/MS outcome.

All these findings offer opportunities in providing novel suitable therapeutics in the management of MS, which are often targeted only toward immune-mediated mechanisms.

2. Animal model of MS

Unfortunately, spontaneous animal models developing MS-like symptoms do not exist. However, MS researchers developed sophisticated experimental tools for studying MS and challenging new therapeutic approach. Accordingly, several animal models including transgenic mice mutant for myelin proteins, or model featured by chemically-induced lesions, as well as viral and autoimmune models, have been developed to reproduce the principal pathological MS hallmarks.

To study demyelination and physiology of remyelination were used spontaneous myelin mutants, such as the taiep rat, Shiverer (myelin basic protein (MBP) mutant), Rumpshaker and Jimpy (proteolipid protein (PLP) mutants) mice, as well as gene knockout mice for the myelin associated glycoprotein (MAG) that show dysmyelination, altered neurotransmission and in some instances clinical disease. Furthermore, transgenic T cells expressing myelin (MBP, PLP or MOG)-specific T cell receptors (TCR) can lead to spontaneous CNS disease. Also the focal administration of selective toxin -as lysolecithin (Preston et al. 2013) also called lysophosphatidylcholine (LPC) or the ethidium bromide (Huang et al. 2011)- are used to induce demyelination in mice and rats. These focal demyelination models have been extensively used to challenge new therapeutic drugs for their potency to promote remyelination. Instead, the copper chelator cuprizone [bis(cyclohexylidenehydrazide)] is the chemical of choice for systemic administration (Kipp et al. 2009) and

induces complete corpus callosum demyelination in few week of diet (about 8 weeks). Cuprizone model is one of the best models to study demyelination due to its reproducibility, simplicity to induced demyelination and low mortality.

However, also a set of different viruses has been identified which induce demyelination in rodents: Semliki Forest virus and Theiler's murine encephalomyelitis virus (TMEV). One of the major disadvantages of these animal models is the fact that demyelination and remyelination occur simultaneously, making difficult the quantification of remyelinated area at a given time point.

Beyond all these models, the most frequently used to validate new therapy not only in rodents but also in primate is the autoimmune Experimental Allergic Encephalomyelitis (EAE) model.

2.1. The experimental autoimmune encephalomyelitis (EAE) model

The experimental autoimmune encephalomyelitis (EAE) reproduces many of the clinical, neuropathological and immunological aspects of MS, thus representing a classical model for studying MS pathophysiology as well as for drug screening. The origins of EAE date back to the 1920s, when Koritschoner and Schweinburg induced spinal cord inflammation in rabbits by inoculation with human spinal cord in 1925. In the 1930s, Rivers and Beeton established the EAE model on monkey, immunizing them with a central nervous system

(CNS) homogenate and inducing what is now known as EAE. Successively, Jules Freund developed a new mineral oil-based adjuvant that combined with the brain extracts after a single injection, opposing to the repeated ones of Rivers method (80 injection for each animal), results in disease onset. In the 1950s, rats and guinea pigs became the standard species in which to study EAE, when the addition of heat-inactivated mycobacterium tuberculosis to the adjuvant (complete Freund's adjuvant, CFA) was found to enhance the response to sensitization with CNS tissue.

Nowadays a variety of primate and rodent EAE models are available; specifically, mouse EAE can be induced in different

Model	Similarities to human disease	Differences from human disease	Further comments
Lewis rat Active EAE (CNS myelin, MBP, MOG, PLP)	T-cell inflammation and weak antibody response	Monophasic, little demyelination	Reliable model, commonly used for therapy studies. With guinea-pig MBP little demyelination
Adoptive-transfer EAE (MBP, S-100, MOG, GFAP)	Marked T-cell inflammation. Topography of lesions	Monophasic, little demyelination	Homogeneous course, rapid onset. Differential recruitment of T cells/macrophages depending on autoantigen
Active EAE or AT-EAE + co-transfer of anti-MOG antibodies Congenic Lewis, DA, BN strains	T-cell inflammation and demyelination	Only transient demyelination	Basic evidence for role of antibodies in demyelination
Active EAE (recombinant MOG aa 1–125)	Relapsing–remitting disorders, may completely mimic histopathology of multiple sclerosis and subtypes	No spontaneous disease	Chronic disease course, affection of the optic nerve, also axonal damage similar to multiple sclerosis
Murine EAE (SJL, C57BL/6, PL/J, Biozzi ABH) Active EAE (MBP, MOG, PLP and peptides)	Relapsing–remitting (SJL, Biozzi) and chronic-progressive (C57BL/6) disease courses with demyelination and axonal damage	No spontaneous disease	Pertussis (toxin) required for many strains, whilst it is often not needed for SJL and some Biozzi EAE models. Higher variability of disease incidence and course, often cytotoxic demyelination in C57BL/6. With rat MBP inflammatory vasculitis with little demyelination
Murine EAE in transgenic mice or knockout mice (mostly C57BL/6 background)	Specifically addresses role of defined immune molecules/neurotrophic cytokines/ neuroanatomical tracts	Most results obtained with artificial permanent transgenic or knockouts	Extensive backcrossing (>10 times) on C57BL/6 background required. Future work with conditional (cre/loxP) or inducible (e.g. Tet-on) mutants

Table 4. Commonly used rodent EAE models (Gold et al 2006).

strain (SJL, C57BL/6, PL/J, Biozzi ABH), injecting different triggering peptides (Myelin basic protein (MBP) that was the first identified antigenic component, myelin proteolipid protein (PLP) and myelin oligodendroglial glycoprotein (MOG)) and obtaining different

pathology readouts, as shown in *Table 4*. (Gold et al 2006). Thus, depending on the molecule and the strain used for EAE induction, 3 different kind of pathology develops: a monophasic disease, involving an acute paralytic episode followed by complete recovery; a relapsing-remitting disease, which involves multiple cycles of attack interspersed by full or partial recovery; or a chronic disease, where symptoms of the initial attack either stabilize at peak levels or gradually worsen over time.

2.2. The MOG-induced EAE model

MOG peptide, discovered in 1986 by Lebar, is a minor component of the myelin sheath accounting for 0.1% of total myelin protein. Interestingly, it is the unique myelin autoantigen that induces not only an encephalitogenic T-cell response in susceptible species but also a demyelinating response (Lebar R 1986). Moreover, its position on the outermost lamellae of the myelin sheath renders MOG directly accessible to specific antibodies that are detected in MS patients (Reindl et al 1999, Zhou et al 2006). Most studies were performed using C57BL/6 mice, where disease is induced by immunization with MOG peptide, representing residues 35–55, emulsified in Freund’s adjuvant supplemented with *Mycobacterium tuberculosis* extract. Mice are also injected with pertussis toxin on the day of immunization and 2 days thereafter to further foster the immune response. This protocol is extensively used because it is reproducible and allows taking advantage of the transgenic

resources on the C57BL/6 background. However, this EAE model is monophasic without relapses, the T cell component is predominantly CD4⁺ and spinal cord is affected out of proportion to brain, as in most other forms of EAE, but dissimilar to MS. Although this model provides no insight into MS progression and remyelination and relapses cannot be studied, it provides an extremely flexible, potent and rapid platform to investigate immune tolerance, regulation of cytokine/chemokine networks and the pathophysiological outcome of inflammation on axonal survival and regeneration (Centonze et al. 2009a-b). The enormous body of literature in which transgenic approaches were used to investigate EAE provided many unexpected insights into the roles of specific molecules and signalling pathways in disease pathogenesis, such as IFN- γ role (Ferber et al 1996) or IL-4 gene therapy study (Butti et al 2008). EAE model is also used to study neural stem cell transplantation to provide reproducible and robust therapeutic effects when they are injected intravenously or intrathecally (Martino et al 2010, Pluchino et al 2009). Therefore, EAE is a good model for studying MS mechanisms, even more so than for testing, developing or studying the pathophysiological effects of drugs that at the end were introduced in clinical trial, as happened for laquinimod (Brunmark et al 2002, Comi et al 2008, Ruffini et al 2013, Wegner et al 2010), amiloride (Arun et al 2013, Friese et al 2007b, Vergo et al 2011)-.

3. Inflammation-acidification in CNS during EAE

3.1. Neurodegeneration in EAE: the role of inflammation

Excitatory amino acids, in particular glutamate, can at high extracellular levels kill neurons through a process known as *excitotoxicity*. Interestingly, excessive levels of glutamate were identified in acute MS lesions using magnetic resonance spectroscopy (Srinivasan et al 2005) paralleled by AMPA, kainate and NMDA receptors upregulation (Newcombe et al 2008). Glutamate is released not only by unbalanced neurons but also by activated astrocytes and immune cells (Centonze et al 2009a). In addition, glutamate activates ionotropic and metabotropic receptors on neurons, and in less part on oligodendrocytes, inducing the toxic cytoplasmic Ca^{2+} overload that culminates in *excitotoxicity*-mediated cell death. In fact, blockade of AMPA/kainite glutamate receptors with specific antagonists (NBQX, MPQX, GYKI52466, GYKI53773) are capable to attenuate clinical decline, independently of any effect on CNS lymphocyte, increasing oligodendrocytes survival, and reducing axonal damage in EAE (Pitt et al 2000). The same results were obtained using NMDA receptor antagonists memantine, amantadine and MK-801, and for the inhibitor of glutamate transmission riluzole (Grasselli et al 2013, Ohgoh et al 2002, Vercellino et al 2007). Moreover, glutamate-triggered neurodegeneration might be sustained by a concomitant alteration of GABA transmission in MS brains, causing an imbalance between synaptic excitation and

inhibition (Centonze et al 2009b, Mandolesi et al 2012, Rossi et al 2011).

MS inflammatory milieu *per se* drives axonal injury by activating and producing substances such as proteolytic enzymes, cytokines, oxidative products and free radicals. Furthermore, the local inflammation induces the edema formation that interfering with blood supply induces a further ischemic mechanism of axonal degeneration. Cytokines, in particular IL1 β , TNF α and IFN γ are released by activated microglia (Block & Hong 2005, Muzio et al 2007) and are increased in Cerebral Spinal Fluid of MS patient (Rovaris et al 1996). Moreover these cytokines are able to enhance *in vitro* the excitatory synaptic transmission and downregulate GABA synapses (Lai et al 2006, Mizuno et al 2008, Rossi et al 2011, Stellwagen et al 2005), deregulating the electrophysiological behaviour of neurons and sustaining *excitotoxicity* process.

Indeed, iNOS, the enzyme involved in the nitric oxide (NO) synthesis, is upregulated in acute inflammatory MS lesions, thus producing elevated level of NO that have detrimental effects on axonal survival by modifying the action of key ion channels, transporters, and glycolytic enzymes (Smith & Lassmann 2002). NO excess and its metabolites inhibit mitochondrial respiration limiting the axon's ability to generate adenosine triphosphate (ATP) (Brown 2010, Brown & Borutaite 2002) and sustain additional glutamate release (Brown & Bal-Price 2003).

Furthermore, neurons trying to restore the correct nerve conduction in demyelinated axon augmented the voltage-gated Na⁺ channels

number and distributed them along the entire axon length (instead of reside only in the internode areas). This dispersed location increases the ATP energy demand to allow the Na^+/K^+ ATPase function, needed for axolemma repolarization after action potential activity. The lack of ATP impairs Na^+/K^+ ATPase activity causing the augment of intracellular Na^+ that as a consequence inverts the $\text{Na}^+/\text{Ca}^{2+}$ exchanger activity causing axoplasmic Ca^{2+} overload (Nave & Trapp 2008). Ca^{2+} accumulation in the axon will cause: activation of degradative enzymes, impairment of mitochondrial operation, reduce energy production, compromise axonal transport, and more axoplasmic Ca^{2+} overload (Haines et al 2011).

Besides reducing ATP production, mitochondria impairment induces anaerobic glycolysis and consequently the accumulation of intracellular lactate. Lactate is therefore thrown out in the parenchyma, where dissociates producing lactic acid and H^+ protons that induce metabolic tissue acidification. Acidification, disrupting protons homeostasis, activates and over-stimulates specific channels able to sense H^+ variation, inducing further intracellular ions influx and fostering neuronal suffering.

All the processes above described developed concomitantly leading to worse axonal failure and subsequently to neuronal cell death.

3.2. Acidification in CNS: the role of ASICs

Protons modulate physiological functions, especially in the CNS. As a matter of fact, protons have been shown to tune synaptic

transmission, neuronal plasticity, and membrane excitability (Kaila 1998). Indeed, the pH level in synaptic vesicles is 1.5 pH units lower than in cytosol (Liu 1997); the protons released from synaptic vesicles together with neurotransmitters during synaptic transmission, lead to extracellular acidification in the synaptic cleft (Miesenbock et al 1998), thus modulating ion channels, such as voltage-gated calcium channels, N-methyl-D-aspartate, and γ -amino butyric acid(A) receptor channels. In pathological condition, acidification is diffused within the tissue and continuously stimulates the synaptic cleft and proton sensitive receptors situated in the entire cell body. Few receptors are able to detect H^+ , for example the inward-rectifier K^+ channels (KIR) and the non-selective cation channel Transient Receptor Potential Vanilloid receptor-1 (TRPV1), (Gaudet 2007, Mao et al 2002). However, these channels are activated not only by H^+ but also by intracellular and extracellular ligands. For example TRPV1 is activated by severe acidosis resulting in pH values below 6 and by ATP and vanilloids molecules (i.e. capsaicin)(Holzer et al. 2009).

Interestingly, in 1997 was cloned the first channel of a new class of receptors that specifically protons during detect moderate decreases in extracellular pH: the Acid Sensing Ion Channel 1a (ASIC1a) (Waldmann et al 1997). Since this discovery, the conventional view on acidosis-mediated pain and cell injury has been dramatically changed. ASICs are a family of proton-gated cation channels which are expressed primarily in the nervous system. ASICs were cloned based on their homology to the epithelial sodium channel (ENaC)/degenerin (DEG) gene family that represents a class of ion

channels present only in animals (metazoa) with specialized organ functions for reproduction, digestion, and coordination (Kellenberger & Schild 2002). Their wide tissue distribution that includes transporting epithelia as well as neuronal excitable tissues best reflects the functional heterogeneity of the ENaC/DEG family members. Depending on their function in the cell, these channels are either constitutively active like ENaC or activated by mechanical stimuli as postulated for degenerins, or by ligands such as protons in the case of ASICs.

ASICs genes encode at least six different ASIC subunits: ASIC1a and

Gene	Protein	pH ₅₀	Agonist (EC ₅₀)	Antagonist (IC ₅₀)	Ions passed	Localization
ASIC1 (ACCN2)	ASIC1a	6.2–6.8	MitTx (9.4 nM)	PcTx1 (~1 nM)	Na ⁺ > Ca ²⁺	CNS and PNS
				Mambalgin (55 nM)		
				Sevencol (2.2 mM)		
	ASIC1b	~6.0 (mouse) ~6.2 (human)	MitTx (23 nM)	Mambalgin (192 nM)	mouse: Na ⁺ humans: Na ⁺ > Ca ²⁺	PNS, not yet identified in CNS
ASIC2 (ACCN1)	ASIC2a	4.5–4.9	Minimal activation by MitTx	A-317567 (29 μM)	Na ⁺	CNS and PNS
	ASIC2b	N/A			–	CNS and PNS
ASIC3	ASIC3	~6.6	GMQ (0.35 mM)	APETx2 (63 nM)	Na ⁺	Predominately PNS, detected in mechanosensitive trigeminal neurons in the CNS
			MitTx (830 nM)	Sevencol (0.35 mM)		
				A-317567 (9.5 μM)		
ASIC4	ASIC4	N/A			–	
Heteromeric channels	1a + 1b	6.0		Mambalgin (72 nM)	Na ⁺	CNS
	1a + 2a	5.5–6.1		Mambalgin (246 nM)	Na ⁺	
	1a + 2b	Same as ASIC1a		Mambalgin (61 nM) PcTx1 (~3 nM)	Na ⁺ > Ca ²⁺	
	1a + 3	6.3–6.6			Na ⁺	
	1b + 3	6.0			Na ⁺	
	1b + 2a	4.9			Na ⁺	
	2a + 3	5.7–6.1			Na ⁺	
	2b + 3	6.5		APETx2 (117 nM)	Na ⁺	

Note: amiloride is not included in the table because it functions as a universal blocker for ASICs and many other ion channels, such as ENaCs and sodium/hydrogen exchangers.

Table 5. ASICs principal features (modified from (Zha 2013))

ASIC1b are protein products of alternative splicing from the ACCN2 gene, ASIC2a and ASIC2b products of the alternative spliced ACCN1 gene, ASIC3 encoded by ACCN3, ASIC4 encoded by ACCN4 (Table 5)..

In knockout mouse models, lacking an ASIC isoform produces defects in neurosensory mechanotransduction of tissue such as skin, stomach, colon, aortic arch, venoatrial junction and cochlea. The

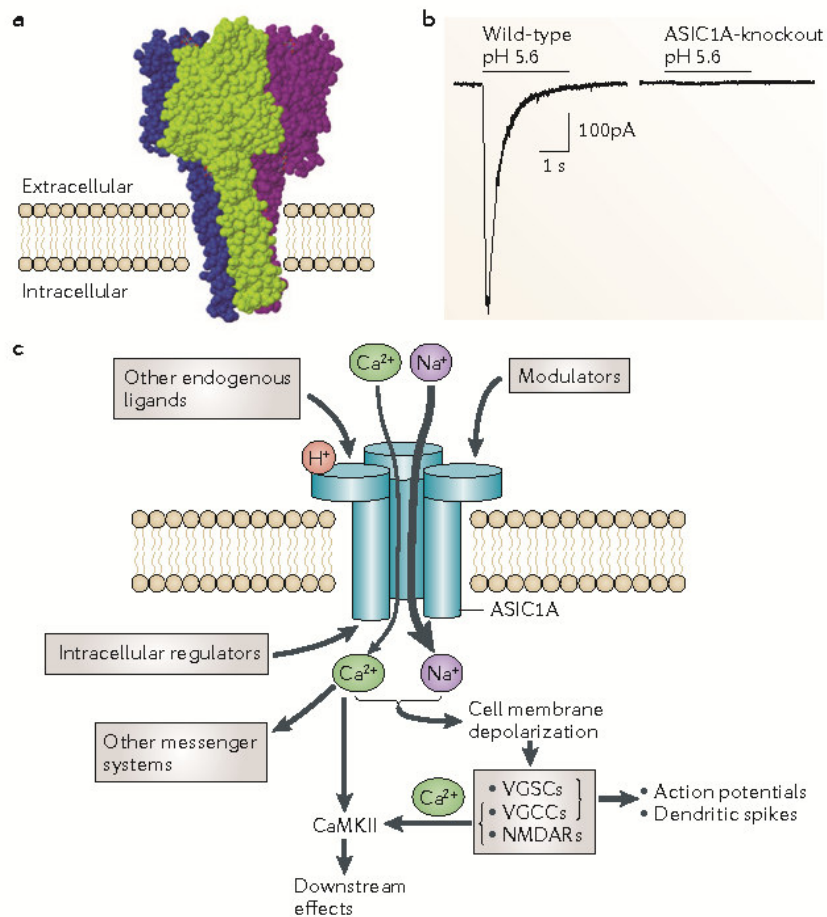


Fig. 7 (a) The crystal structure of the chicken acid-sensing ion channel 1 (ASIC1) indicates that three subunits combine into a trimeric channel complex. (b) Whole-cell voltage-clamp recordings from neurons in acute amygdala slices showing an absence of pH 5.6-evoked current in neurons lacking ASIC1A. (c) schematic representation of ASIC1a channels and its modulators. (voltage-gated Ca²⁺ channels (VGCCs) and voltage-gated Na⁺ channels (VGSCs)). (Wemmie et al 2013)

ASICs are thus implicated in touch, pain, digestive function, baroreception, blood volume control and hearing. ASICs are mainly expressed in all the nervous system and interestingly in the CNS are primarily expresses ASIC1a, ASIC2a, and ASIC2b, with the highest expression levels in the hippocampus, the cerebellum, the neo- and allo-cortical regions, the main olfactory bulb, the habenula, and the basolateral amygdaloid nuclei; whereas ASIC3 is predominantly express in the peripheral nervous system (PNS) almost exclusively in sensory neurons, suggesting a role in pain perception following tissue acidosis. ASIC4 expression was found in the brain but its function is still unclear; however, current evidence suggests that differently from ASIC1a/b, ASIC2a/b and ASIC3 it is not involved in H^+ -sensing (Grunder et al 2000).

ASICs function as homotrimeric or heterotrimeric complexes and conduct mostly Na^+ (Gonzales et al 2009, Jasti et al 2007a, Li et al 2011). Homomeric ASIC1a (*Fig.7*) and human ASIC1b, as well as ASIC1a/2b heteromers, also have a low permeability to Ca^{2+} (Hoagland et al 2011, Zhang & Canessa 2002). Interestingly, at pH 7.25 (but not at pH 5.5), a complex between a truncated chick ASIC1 and its specific inhibitor Psalmotoxin1 (PcTx1) is non-selective to monovalent cations (Baconguis & Gouaux 2012). This result indicates that ion selectivity of ASICs can be altered under specific conditions. ASIC1a and ASIC3 start to open at pH value near physiological pH ranges, specifically at about pH 7 and 7.2, respectively (Babini et al 2002, Yagi et al 2006). Furthermore, ASIC1a starts to saturate their current amplitude at pH 6.0 and the H^+ -concentration response curve

can be fit by a Hill function and yields half-maximal activation at pH 6.5 with a Hill-coefficient of approximately 3 (Babini et al 2002). Recently, many studies were conducted on ASIC1a structure, function and its interplayer –i.e. the scaffold protein Pick1- depicting its importance in physiological and pathological role (Ehling et al 2011). The sub-cellular localization of ASICs is still controversial, but recent findings indicate that these channels operate as a postsynaptic proton receptor. In addition, other studies reveal that ASIC1a regulate dendritic spines during acidosis (the site of most excitatory neurotransmission in the brain (Chu & Xiong 2012, Zha et al 2006)), and are involved in synaptic plasticity, learning/memory, fear conditioning (Wemmie et al 2002).

In view of the fact that in pathological conditions extracellular pH drops are common, ASIC1a may play important roles in a variety of neurological diseases. It was demonstrated that ASIC1a overstimulation seems drive neuronal cell death (Sherwood et al 2011, Wang & Xu 2011) and recently reports describe ASICs

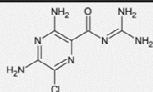
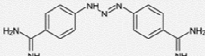
Name	Formula	Inhibition (potency)
Amiloride		Hallmark blocker
Diminazene		Strong inhibition $0.3 \pm 0.1 \mu\text{M}$

Fig 8 . Amiloride and Diminazene chemical structures – adapted from (Chen et al 2010b)

contribution to pain, brain ischemia, multiple sclerosis, seizures as well as anxiety-related disorders (Wemmie et al 2013, Xiong et al 2004a, Zha 2013, Ziemann et al 2008a). In particular, using ASIC1a^{-/-}

transgenic mice or pharmacologically blocking ASIC1a with amiloride in wild type mice was demonstrated that the absence or the inhibition of this receptor reduces EAE severity (Frieze et al 2007, Vergo et al 2011). Amiloride (*Fig 8*), already licensed for treatment of hypertension and congestive heart failure, is a non-selective ASIC1a blocker, that inhibits also ENaC (de la Rosa et al 2000). Using this drug, Frieze and collaborators highlight that amiloride significantly

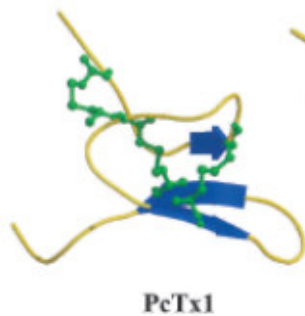


Fig 9 . Three-dimensional structures of PcTx1 (Escoubas et al 2003)

reduces axonal degeneration in EAE. Furthermore, to better define the long-term benefit of amiloride treatment in CNS inflammatory disease, Vergo and colleagues utilizing a chronic relapsing-remitting mouse model of MS, observed a reduction in axonal loss and demyelination in chronic-relapsing EAE that well correlate with a reduction of

mice permanent disability. These findings suggest that blockade of ASIC1 is neuro-protective, therefore drugs that selectively inhibit this channel could be a good pharmaceutical proposal for MS treatment. This hypothesis was also confirmed by the study conducted by Arun and colleagues. They performed an MRI-based pilot study on PPMS patients using amiloride obtaining promising results: a significant reduction in the rate of whole-brain atrophy during the treatment phase thus suggesting the neuroprotective effect of amiloride also in

human. However, amiloride is a non-selective blocker of ASIC1a, thus further studies blocking selectively this channel are required.

In fact other ASIC1a blockers are known: the inhibitory cysteine knot toxin Psalmotoxin1 (PcTx1) (*Fig 9*), from the venom of the tarantula *Psalmopoeus cambridgeia* (Escoubas et al 2003, Escoubas et al 2000a) - that was used in stroke with excellent results (Xiong et al 2004a)- and mambalgin peptide from Black mamba venom (Diochot et al 2012); some non-steroidal anti-inflammatory (Voilley et al 2001). A-317567 and nafamostat mesilate also block native ASIC currents in dorsal root ganglion (DRG) neurons and oocyte-expressing ASICs (Dube et al 2005, Ugawa et al 2007) but do so with relatively low potency; a class of anti-protozoan diarylamidines including diminazene, DAPI, HSB, and pentamidine inhibit ASIC currents in cultured hippocampal neurons with relatively high affinity (Chen et al 2010a, Chen et al 2010b).

Among all blockers, the most potent and selective are PcTx1 and diminazene. Since PcTx1 is derived from venom, it is hard to use it in translational medicine, though it is possible to remodel or copy the structure of this molecule in order to produce synthetic drugs that can selective bind and inhibit ASIC1a.

Diminazene Aceturate (DA) (*Fig.8*) –which commercial name are Diminazene, Berenil, Nozamil, Trypadim, Veriben, Survidim, Diminaveto- is able to inhibits selectively ASIC1a in μM range and it is already used to cure trypanosomosis in human (Grace et al 2009, Soudré et al 2013). Indeed, DA could be a good candidate to be

administered in pathological condition (i.e. MS or stroke) in order to prevent ASIC1a activation.

Increasing evidence indicates the involvement of ASIC channels in both physiological and pathological processes. Therefore understanding the molecular mechanism and its modulation in pathological condition is necessary to establish effective therapeutic interventions.

4. Scope of the thesis

The aim of this thesis is to evaluate two different aspects of inflammation in MOG-EAE mouse model:

In the first work, we explored the inflammation-induced acidosis at the peak of EAE disease and concomitantly the effects of the pharmacological inhibition of the principal sensible proton channel expressed in CNS (ASIC1a) with Diminazene Aceturate (DA). Moreover, to study the electrophysiological effects of acidosis on neurons and the DA specific properties, we performed experiments on *in vitro* networks of neurons coupled with Micro Electrode Array (MEA) devices.

In the second work, realized in collaboration with the laboratory of Prof. Centonze, we combined neurophysiological and morphological investigation to assess how chronic inflammation contribute to alter GABA inhibitory transmission in the brains of EAE mice and in network of neurons.

5. References

- Albert M, Antel J, Brück W, Stadelmann C. 2007. Extensive Cortical Remyelination in Patients with Chronic Multiple Sclerosis. *Brain Pathology* 17: 129-38
- Alexopoulos H, Kampylafka EI, Chatzi I, Travasarou M, Karageorgiou KE, et al. 2013. Reactivity to AQP4 epitopes in relapsing–remitting multiple sclerosis. *Journal of Neuroimmunology* 260: 117-20
- Allen IV, McQuaid S, Mirakhur M, Nevin G. 2001. Pathological abnormalities in the normal-appearing white matter in multiple sclerosis. *Neurol Sci* 22: 141-44
- Arun T, Tomassini V, Sbardella E, de Ruiter MB, Matthews L, et al. 2013. Targeting ASIC1 in primary progressive multiple sclerosis: evidence of neuroprotection with amiloride. *Brain* 136: 106-15
- Ascherio A, Marrie RA. 2012. Vitamin D in MS: A vitamin for 4 seasons. *Neurology* 79: 208-10
- Babini E, Paukert M, Geisler H, Grunder S. 2002. Alternative splicing and interaction with di- and polyvalent cations control the dynamic range of acid-sensing ion channel 1 (ASIC1). *J Biol Chem* 277: 41597 - 603
- Baconguis I, Gouaux E. 2012. Structural plasticity and dynamic selectivity of acid-sensing ion channel-spider toxin complexes. *Nature* 489: 400 - 05
- Bar-Or A, Gold R, Kappos L, Arnold D, Giovannoni G, et al. 2013. Clinical efficacy of BG-12 (dimethyl fumarate) in patients with relapsing–remitting multiple sclerosis: subgroup analyses of the DEFINE study. *Journal of Neurology*: 1-9
- Barun B, Bar-Or A. 2012. Treatment of multiple sclerosis with Anti-CD20 antibodies. *Clinical Immunology* 142: 31-37
- Berer K, Mues M, Koutrolos M, Rasbi ZA, Boziki M, et al. 2011. Commensal microbiota and myelin autoantigen cooperate to trigger autoimmune demyelination. *Nature* 479: 538-41
- Bjartmar C, Kinkel RP, Kidd G, Rudick RA, Trapp BD. 2001. Axonal loss in normal-appearing white matter in a patient with acute MS. *Neurology* 57: 1248-52
- Block ML, Hong J-S. 2005. Microglia and inflammation-mediated neurodegeneration: Multiple triggers with a common mechanism. *Progress in Neurobiology* 76: 77-98
- Bø VC, Nyland HI, Trapp BD, Mørk SJ. 2003. Subpial Demyelination in the Cerebral Cortex of Multiple Sclerosis Patients. *Journal of Neuropathology & Experimental Neurology* 62: 723-32

- Brown G, Bal-Price A. 2003. Inflammatory neurodegeneration mediated by nitric oxide, glutamate, and mitochondria. *Molecular Neurobiology* 27: 325-55
- Brown GC. 2010. Nitric oxide and neuronal death. *Nitric Oxide* 23: 153-65
- Brown GC, Borutaite V. 2002. Nitric oxide inhibition of mitochondrial respiration and its role in cell death. *Free Radical Biology and Medicine* 33: 1440-50
- Brunmark C, Runström A, Ohlsson L, Sparre B, Brodin T, et al. 2002. The new orally active immunoregulator laquinimod (ABR-215062) effectively inhibits development and relapses of experimental autoimmune encephalomyelitis. *Journal of Neuroimmunology* 130: 163-72
- Butti E, Bergami A, Recchia A, Brambilla E, Del Carro U, et al. 2008. IL4 gene delivery to the CNS recruits regulatory T cells and induces clinical recovery in mouse models of multiple sclerosis. *Gene Ther* 15: 504-15
- Centonze D, Muzio L, Rossi S, Cavasinni F, De Chiara V, et al. 2009a. Inflammation Triggers Synaptic Alteration and Degeneration in Experimental Autoimmune Encephalomyelitis. *Journal of Neuroscience* 29: 3442-52
- Centonze D, Muzio L, Rossi S, Furlan R, Bernardi G, Martino G. 2009b. The link between inflammation, synaptic transmission and neurodegeneration in multiple sclerosis. *Cell Death and Differentiation* 17: 1083-91
- Chen S-J, Wang Y-L, Fan H-C, Lo W-T, Wang C-C, Sytwu H-K. 2012. Current Status of the Immunomodulation and Immunomediated Therapeutic Strategies for Multiple Sclerosis. *Clinical and Developmental Immunology* 2012: 16
- Chen X, Orser BA, MacDonald JF. 2010a. Design and screening of ASIC inhibitors based on aromatic diamidines for combating neurological disorders. *European Journal of Pharmacology* 648: 15-23
- Chen X, Qiu L, Li M, Dürrnagel S, Orser BA, et al. 2010b. Diarylamidines: High potency inhibitors of acid-sensing ion channels. *Neuropharmacology* 58: 1045-53
- Choi SR, Howell OW, Carassiti D, Magliozzi R, Gveric D, et al. 2012. Meningeal inflammation plays a role in the pathology of primary progressive multiple sclerosis. *Brain* 135: 2925-37
- Chu X, Xiong Z. 2012. Physiological and pathological functions of Acid-sensing ion channels in the central nervous system. *Curr Drug Targets* 13: 263 - 71
- Comi G, Pulizzi A, Rovaris M, Abramsky O, Arbizu T, et al. 2008. Effect of laquinimod on MRI-monitored disease activity in patients with relapsing-remitting multiple sclerosis: a multicentre, randomised,

- double-blind, placebo-controlled phase IIb study. *The Lancet* 371: 2085-92
- Compston A, Coles A. 2008. Multiple sclerosis. *The Lancet* 372: 1502-17
- Constantinescu CS, Farooqi N, O'Brien K, Gran B. 2011. Experimental autoimmune encephalomyelitis (EAE) as a model for multiple sclerosis (MS). *British Journal of Pharmacology* 164: 1079-106
- Cusick MFL, Jane E.; Fujinami, Robert S. 2013. Multiple sclerosis: autoimmunity and viruses. *Current Opinion in Rheumatology* 25(4): p 496-501
- de la Rosa DA, Canessa CM, Fyfe GK, Zhang P. 2000. Structure and regulation of amiloride-sensitive sodium channels. *Annu. Rev. Physiol.* 62: 573-94
- Deiß A, Brecht I, Haarmann A, Buttmann M. 2013. Treating multiple sclerosis with monoclonal antibodies: a 2013 update. *Expert Review of Neurotherapeutics* 13: 313-35
- Diochot S, Baron A, Salinas M, Douguet D, Scarzello S, et al. 2012. Black mamba venom peptides target acid-sensing ion channels to abolish pain. *Nature* 490: 552 - 55
- Dube G, Lehto S, Breese N, Baker S, Wang X, et al. 2005. Electrophysiological and in vivo characterization of A-317567, a novel blocker of acid sensing ion channels. *Pain* 117: 88 - 96
- Dutta R, Trapp BD. 2011. Mechanisms of neuronal dysfunction and degeneration in multiple sclerosis. *Progress in Neurobiology* 93: 1-12
- Ehling P, Bittner S, Budde T, Wiendl H, Meuth SG. 2011. Ion channels in autoimmune neurodegeneration. *FEBS Letters* 585: 3836-42
- Escoubas P, Bernard C, Lambeau G, Lazdunski M, Darbon H. 2003. Recombinant production and solution structure of PcTx1, the specific peptide inhibitor of ASIC1a proton-gated cation channels. *Protein Science* 12: 1332-43
- Escoubas P, De Weille J, Lecoq A, Diochot S, Waldmann R, et al. 2000. Isolation of a tarantula toxin specific for a class of proton-gated Na⁺ channels. *J Biol Chem* 275: 25116 - 21
- Ferber IA, Brocke S, TaylorEdwards C, Ridgway W, Dinisco C, et al. 1996. Mice with a disrupted IFN-gamma gene are susceptible to the induction of experimental autoimmune encephalomyelitis (EAE). *J. Immunol.* 156: 5-7
- Friese MA, Craner MJ, Etzensperger R, Vergo S, Wemmie JA, et al. 2007. Acid-sensing ion channel-1 contributes to axonal degeneration in autoimmune inflammation of the central nervous system. *Nature Medicine* 13: 1483-89

- Gaudet R. 2007. Chapter 25-Structural Insights into the Function of TRP Channels. CRC Press
- Gold R, Linington C, Lassmann H. 2006. Understanding pathogenesis and therapy of multiple sclerosis via animal models: 70 years of merits and culprits in experimental autoimmune encephalomyelitis research. *Brain* 129: 1953-71
- Gonzales EB, Kawate T, Gouaux E. 2009. Pore architecture and ion sites in acid-sensing ion channels and P2X receptors. *Nature* 460: 599-604
- Grace D, Randolph T, Affognon H, Dramane D, Diall O, Clausen P-H. 2009. Characterisation and validation of farmers' knowledge and practice of cattle trypanosomosis management in the cotton zone of West Africa. *Acta Tropica* 111: 137-43
- Grasselli G, Rossi S, Musella A, Gentile A, Loizzo S, et al. 2013. Abnormal NMDA receptor function exacerbates experimental autoimmune encephalomyelitis. *British Journal of Pharmacology* 168: 502-17
- Grunder S, Geissler H, Bassler E, Ruppersberg J. 2000. A new member of acid-sensing ion channels from pituitary gland. *Neuroreport* 11: 1607 - 11
- Haider L, Fischer MT, Frischer JM, Bauer J, Höftberger R, et al. 2011. Oxidative damage in multiple sclerosis lesions. *Brain* 134: 1914-24
- Haines JD, Inglese M, Casaccia P. 2011. Axonal Damage in Multiple Sclerosis. *Mount Sinai Journal of Medicine: A Journal of Translational and Personalized Medicine* 78: 231-43
- Hoagland E, Sherwood T, Lee K, Walker C, Askwith C. 2011. Identification of a calcium permeable human acid-sensing ion channel 1 transcript variant. *J Biol Chem* 285: 41852 - 62
- Holzer P. 2009. Acid-Sensitive Ion Channels and Receptors In Sensory Nerves, ed. BJ Canning, D Spina, pp. 283-332: Springer Berlin Heidelberg
- Jasti J, Furukawa H, Gonzales E, Gouaux E. 2007. Structure of acid-sensing ion channel 1 at 1.9 Å resolution and low pH. *Nature* 449: 316 - 23
- Kaila KaR, B. R. 1998. pH and Brain Function. John Wiley & Sons, Inc., New York
- Kellenberger S, Schild L. 2002. Epithelial Sodium Channel/Degenerin Family of Ion Channels: A Variety of Functions for a Shared Structure. *Physiological Reviews* 82: 735-67
- Koch-Henriksen N, Sørensen PS. 2010. The changing demographic pattern of multiple sclerosis epidemiology. *The Lancet Neurology* 9: 520-32
- Lai AY, Swayze RD, El-Husseini A, Song C. 2006. Interleukin-1 beta modulates AMPA receptor expression and phosphorylation in hippocampal neurons. *Journal of Neuroimmunology* 175: 97-106

- Lassmann H. 2012. Cortical lesions in multiple sclerosis: inflammation versus neurodegeneration. *Brain* 135: 2904-05
- Lebar R LC, Vincent C, Lombrail P, Boutry JM. 1986. The M2 autoantigen of central nervous system myelin, a glycoprotein present in oligodendrocyte membrane. *Clin Exp Immunol.* 66: 423-34
- Li T, Yang Y, Canessa CM. 2011. Outlines of the pore in open and closed conformations describe the gating mechanism of ASIC1. *Nature Communications* 2: 399
- Libbey J, Fujinami R. 2010. Potential Triggers of MS In *Molecular Basis of Multiple Sclerosis*, ed. R Martin, A Lutterotti, pp. 21-42: Springer Berlin Heidelberg
- Liu YE, Robert H. 1997. THE ROLE OF VESICULAR TRANSPORT PROTEINS IN SYNAPTIC TRANSMISSION AND NEURAL DEGENERATION. *Annual Review of Neuroscience* 20: 125-56
- Mandolesi G, Grasselli G, Musella A, Gentile A, Musumeci G, et al. 2012. GABAergic signaling and connectivity on Purkinje cells are impaired in experimental autoimmune encephalomyelitis. *Neurobiology of Disease* 46: 414-24
- Mao J, Li L, McManus M, Wu J, Cui N, Jiang C. 2002. Molecular Determinants for Activation of G-protein-coupled Inward Rectifier K⁺ (GIRK) Channels by Extracellular Acidosis. *Journal of Biological Chemistry* 277: 46166-71
- Martino G, Franklin RJM, Van Evercooren AB, Kerr DA. 2010. Stem cell transplantation in multiple sclerosis: current status and future prospects. *Nat Rev Neurol* 6: 247-55
- Miesenbock G, De Angelis DA, Rothman JE. 1998. Visualizing secretion and synaptic transmission with pH-sensitive green fluorescent proteins. *Nature* 394: 192-95
- Miller D, Barkhof F, Montalban X, Thompson A, Filippi M. 2005. Clinically isolated syndromes suggestive of multiple sclerosis, part I: natural history, pathogenesis, diagnosis, and prognosis. *The Lancet Neurology* 4: 281-88
- Mizuno T, Zhang G, Takeuchi H, Kawanokuchi J, Wang J, et al. 2008. Interferon- γ directly induces neurotoxicity through a neuron specific, calcium-permeable complex of IFN- γ receptor and AMPA GluR1 receptor. *The FASEB Journal* 22: 1797-806
- Muzio L, Martino G, Furlan R. 2007. Multifaceted aspects of inflammation in multiple sclerosis: The role of microglia. *Journal of Neuroimmunology* 191: 39-44
- Nave KA, Trapp BD. 2008. Axon-glial signaling and the glial support of axon function In *Annual Review of Neuroscience*, pp. 535-61. Palo Alto: Annual Reviews

- Newcombe J, Uddin A, Dove R, Patel B, Turski L, et al. 2008. Glutamate Receptor Expression in Multiple Sclerosis Lesions. *Brain Pathology* 18: 52-61
- Nuyts A, Lee W, Bashir-Dar R, Berneman Z, Cools N. 2013. Dendritic cells in multiple sclerosis: key players in the immunopathogenesis, key players for new cellular immunotherapies? *Multiple Sclerosis Journal*
- Ohgoh M, Hanada T, Smith T, Hashimoto T, Ueno M, et al. 2002. Altered expression of glutamate transporters in experimental autoimmune encephalomyelitis. *Journal of Neuroimmunology* 125: 170-78
- Patrikios P, Stadelmann C, Kutzelnigg A, Rauschka H, Schmidbauer M, et al. 2006. Remyelination is extensive in a subset of multiple sclerosis patients. *Brain* 129: 3165-72
- Phillips JT, Fox RJ. 2013. BG-12 in Multiple Sclerosis. *Semin Neurol* 33: 056-65
- Pitt D, Werner P, Raine CS. 2000. Glutamate excitotoxicity in a model of multiple sclerosis. *Nature Medicine* 6: 67-70
- Pluchino S, Gritti A, Blezer E, Amadio S, Brambilla E, et al. 2009. Human neural stem cells ameliorate autoimmune encephalomyelitis in non-human primates. *Annals of Neurology* 66: 343-54
- Ramagopalan SV, Dobson R, Meier UC, Giovannoni G. 2010. Multiple sclerosis: risk factors, prodromes, and potential causal pathways. *The Lancet Neurology* 9: 727-39
- Ransohoff RM. 2012. Animal models of multiple sclerosis: the good, the bad and the bottom line. *Nature Neuroscience* 15: 1074-77
- Reindl M, Linington C, Brehm U, Egg R, Dilitz E, et al. 1999. Antibodies against the myelin oligodendrocyte glycoprotein and the myelin basic protein in multiple sclerosis and other neurological diseases: a comparative study. *Brain* 122: 2047-56
- Rossi S, Muzio L, De Chiara V, Grasselli G, Musella A, et al. 2011. Impaired striatal GABA transmission in experimental autoimmune encephalomyelitis. *Brain, Behavior, and Immunity* 25: 947-56
- Rovaris M, Barnes D, Woodrofe N, du Boulay GH, Thorpe JW, et al. 1996. Patterns of disease activity in multiple sclerosis patients: a study with quantitative gadolinium-enhanced brain MRI and cytokine measurement in different clinical subgroups. *Journal of Neurology* 243: 536-42
- Ruffini F, Rossi S, Bergamaschi A, Brambilla E, Finardi A, et al. 2013. Laquinimod prevents inflammation-induced synaptic alterations occurring in experimental autoimmune encephalomyelitis. *Multiple Sclerosis Journal* 19: 1084-94

- Sethi A, Kulkarni N, Sonar S, Lal G. 2013. Role of miRNAs in CD4 T cell plasticity during inflammation and tolerance. *Frontiers in Genetics* 4
- Sherwood T, Lee K, Gormley M, Askwith C. 2011. Heteromeric acid-sensing ion channels (ASICs) composed of ASIC2b and ASIC1a display novel channel properties and contribute to acidosis-induced neuronal death. *J Neurosci* 31: 9723 - 34
- Shields SD, Cheng X, Gasser A, Saab CY, Tyrrell L, et al. 2012. A channelopathy contributes to cerebellar dysfunction in a model of multiple sclerosis. *Annals of Neurology* 71: 186-94
- Smith KJ, Lassmann H. 2002. The role of nitric oxide in multiple sclerosis. *The Lancet Neurology* 1: 232-41
- Soudré A, Ouédraogo-Koné S, Wurzinger M, Müller S, Hanotte O, et al. 2013. Trypanosomiasis: a priority disease in tsetse-challenged areas of Burkina Faso. *Trop Anim Health Prod* 45: 497-503
- Srinivasan R, Sailasuta N, Hurd R, Nelson S, Pelletier D. 2005. Evidence of elevated glutamate in multiple sclerosis using magnetic resonance spectroscopy at 3 T. *Brain* 128: 1016-25
- Stellwagen D, Beattie EC, Seo JY, Malenka RC. 2005. Differential Regulation of AMPA Receptor and GABA Receptor Trafficking by Tumor Necrosis Factor- α . *The Journal of Neuroscience* 25: 3219-28
- Stys PK, Zamponi GW, van Minnen J, Geurts JGG. 2012. Will the real multiple sclerosis please stand up? *Nature Reviews Neuroscience* 13: 507-14
- Thompson RHS. 1955. MULTIPLE SCLEROSIS. By Douglas McAlpine, Nigel D. Compston and Charles E. Lumsden. Edinburgh and London: E. & S. Livingstone, Ltd. Pp. viii + 304. 35s. *Experimental Physiology* 40: 393-94
- Trapp BD, Nave KA. 2008. Multiple sclerosis: An immune or neurodegenerative disorder? In *Annual Review of Neuroscience*, pp. 247-69. Palo Alto: Annual Reviews
- Trojano M, Lucchese G, Graziano G, Taylor BV, Simpson S, Jr., et al. 2012. Geographical Variations in Sex Ratio Trends over Time in Multiple Sclerosis. *PLoS ONE* 7: e48078
- Ugawa S, Ishida Y, Ueda T, Inoue K, Nagao M, Shimada S. 2007. Nafamostat mesilate reversibly blocks acid-sensing ion channel currents. *Biochemical and Biophysical Research Communications* 363: 203-08
- van der Valk P, Amor S. 2009. Preactive lesions in multiple sclerosis. *Current Opinion in Neurology*: 1
- Vercellino MMD, Merola AMD, Piacentino CMD, Votta BB, Capello EMD, et al. 2007. Altered Glutamate Reuptake in Relapsing-Remitting and Secondary Progressive Multiple Sclerosis Cortex: Correlation With Microglia Infiltration, Demyelination, and Neuronal and Synaptic

- Damage. *Journal of Neuropathology & Experimental Neurology* 66: 732-39
- Vergo S, Craner MJ, Etzensperger R, Attfield K, Friesse MA, et al. 2011. Acid-sensing ion channel 1 is involved in both axonal injury and demyelination in multiple sclerosis and its animal model. *Brain* 134: 571-84
- Voilley N, de Weille J, Mamet J, Lazdunski M. 2001. Nonsteroid Anti-Inflammatory Drugs Inhibit Both the Activity and the Inflammation-Induced Expression of Acid-Sensing Ion Channels in Nociceptors. *The Journal of Neuroscience* 21: 8026-33
- Waldmann R, Champigny G, Bassilana F, Heurteaux C, Lazdunski M. 1997. A proton-gated cation channel involved in acid-sensing. *Nature* 386: 173 - 77
- Wang Y-Z, Xu T-L. 2011. Acidosis, Acid-Sensing Ion Channels, and Neuronal Cell Death. *Molecular Neurobiology* 44: 350-58
- Waxman SG. 2001. Transcriptional channelopathies: An emerging class of disorders. *Nat Rev Neurosci* 2: 652-59
- Waxman SG. 2005. Cerebellar dysfunction in multiple sclerosis: evidence for an acquired channelopathy In *Progress in Brain Research*, ed. Z De, Cicirata, pp. 353-65: Elsevier
- Wegner C, Stadelmann C, Pförtner R, Raymond E, Feigelson S, et al. 2010. Laquinimod interferes with migratory capacity of T cells and reduces IL-17 levels, inflammatory demyelination and acute axonal damage in mice with experimental autoimmune encephalomyelitis. *Journal of Neuroimmunology* 227: 133-43
- Weissert R. 2013. The Immune Pathogenesis of Multiple Sclerosis. *Journal of Neuroimmune Pharmacology*: 1-10
- Wemmie JA, Chen J, Askwith CC, Hruska-Hageman AM, Price MP, et al. 2002. The acid-activated ion channel ASIC contributes to synaptic plasticity, learning, and memory. *Neuron* 34: 463-77
- Wemmie JA, Taugher RJ, Kreple CJ. 2013. Acid-sensing ion channels in pain and disease. *Nat Rev Neurosci* 14: 461-71
- Xiong Z, Zhu X, Chu X, Minami M, Hey J, et al. 2004. Neuroprotection in ischemia: blocking calcium-permeable acid-sensing ion channels. *Cell* 118: 687 - 98
- Yagi J, Wenk H, Naves L, McCleskey E. 2006. Sustained currents through ASIC3 ion channels at the modest pH changes that occur during myocardial ischemia. *Circ Res* 99: 501 - 09
- Zamvil SS, Steinman L. 1990. The T Lymphocyte in Experimental Allergic Encephalomyelitis. *Annual Review of Immunology* 8: 579-621
- Zha X-m. 2013. Acid-sensing ion channels: trafficking and synaptic function. *Molecular Brain* 6: 1

- Zha Xm, Wemmie JA, Green SH, Welsh MJ. 2006. Acid-sensing ion channel 1a is a postsynaptic proton receptor that affects the density of dendritic spines. *Proceedings of the National Academy of Sciences* 103: 16556-61
- Zhang P, Canessa C. 2002. Single channel properties of rat acid-sensitive ion channel-1alpha, -2a, and 3 expressed in *Xenopus* oocytes. *J Gen Physiol* 120: 553 - 66
- Zhou D, Srivastava R, Nessler S, Grummel V, Sommer N, et al. 2006. Identification of a pathogenic antibody response to native myelin oligodendrocyte glycoprotein in multiple sclerosis. *Proc. Natl. Acad. Sci. U. S. A.* 103: 19057-62
- Ziemann A, Schnizler M, Albert G, Severson M, Howard Iii M, et al. 2008. Seizure termination by acidosis depends on ASIC1a. *Nat Neurosci* 11: 816 - 22

CHAPTER 2

CNS acidosis in Experimental Autoimmune Encephalomyelitis; role of ASIC channels

Roberta de Ceglia¹, Linda Chaabane^{1,4,§}, Emilia Biffi^{2,7§}, Andrea Bergamaschi¹, Giancarlo Ferrigno², Stefano Amadio³, Ubaldo Del Carro³, Giancarlo Comi⁴, Veronica Bianchi^{5,6}, Patrizia D'Adamo^{5,6}, Gianvito Martino¹, Andrea D. Menegon^{7, *}, Luca Muzio^{1, *}

* Equally contributing senior authors

§ Equally contributing to the work

¹ Neuroimmunology unit, Institute of Experimental Neurology (INSPE), Division of Neuroscience San Raffaele Scientific Institute

² Neuroengineering and Medical Robotics Laboratory, Department of Electronics, Information and Bioengineering, Politecnico di Milano

³ Neurophysiology Unit, Division of Neuroscience San Raffaele Scientific Institute

⁴ Department of Neurology, Institute of Experimental Neurology (INSPE), Vita Salute San Raffaele University, Milan, Italy.

⁵ Dulbecco Telethon Institute at San Raffaele Scientific Institute, Division of Neuroscience, 20132 Milan, Italy

⁶ Vita-Salute San Raffaele University, 20132 Milan, Italy

⁷ Advanced Light and Electron Microscopy Bio-Imaging Centre, Experimental Imaging Centre, San Raffaele Scientific Institute, 20132 Milan, Italy

Corresponding author: Gianvito Martino

San Raffaele Scientific Institute, Via Olgettina 58, 20132 Milan, Italy. Phone +39 02 2643 4958; Fax +39 02 2643 4855. e-mail: martino.gianvito@hsr.it

Keywords: ASICs, Acidosis, EAE, Multiple Sclerosis, MR-Spectroscopy, Diminazene Aceturate, MEA

Submitted

Abstract

Multiple Sclerosis (MS) is an inflammatory demyelinating disease of the Central Nervous System (CNS) featuring severe neuronal degenerative processes. Emerging findings indicate that several injurious molecular and cellular cascades are contributing to neurodegeneration. Among them, CNS acidosis has been recently demonstrated to have a detrimental role in Experimental Autoimmune Encephalomyelitis (EAE). Good candidates to trigger acidosis-mediated neurodegeneration are represented by Acid Sensing Ion Channels (ASICs) which are H^+ -gated cation channels of the CNS. We measured CNS acidosis in EAE mice by a non-invasive magnetic resonance spectroscopy (MRS), establishing the presence of a substantial extracellular acidification in the Cerebellum (CB). We next examined the ability of Diminazene Aceturate (DA), a new specific ASICs inhibitor, to promote neuroprotective effects in chronic EAE mice. Behavioral and histological evaluations indicated that DA significantly improved walking performances in EAE mice, ameliorated their neurological deficits, as well as, reduced myelin and axonal loss in both CB and Spinal Cord. Additionally, we model *in vitro* the harmful electrophysiological alterations elicited by acidosis using primary neuronal cultures coupled with Micro Electrode Array (MEA) devices. While an acute acidic treatment caused a rapid and transient reduction of firing activity, long term acidosis caused the chronic impairment of synchronized neuronal electrophysiological activity, and a significant loss of pre-synaptic boutons. DA efficiently

compensated the loss of firing activity derived from acute acidosis, as well as protected neurons from injurious effects elicited by chronic acidosis. In conclusion our data suggest that ASICs activation is involved in mediating neuronal derangement during acute neuroinflammation and that the early intervention with specific ASICs antagonists may attenuate these detrimental effects.

Introduction

Multiple Sclerosis (MS) is generally regarded as a neuroinflammatory disease in which infiltrating immune cells participate in myelin disruption and induce axonal damage. Although this scenario depicts a well known cascade of events occurring during acute inflammation of the Central Nervous System (CNS), the characteristic accumulation of neurological defects, and the fact that a large number of patients suffer of a severe cognitive impairment at early stage of the disease (Rocca et al 2009), cannot solely be explained by demyelination of axonal traits.

A large body of experimental evidence indicates that functional mistuning of ion channels might contribute to neuronal deficits occurring in MS patients. Prominent examples, are changes of Nav 1.2 and Nav 1.6 channels expression levels (Black et al 2006), along with alterations of some voltage-gated calcium channel subunits (Kornek et al 2000) and Kv1.1/Kv 1.2 channels, that are significantly increased in demyelinated plaques (Beraud et al 2006). This evidence strongly indicates that abnormalities in the transmembrane flow of Na^+ and Ca^{2+} ions sustains the establishment of neurodegeneration (Stys et al 1998, Stys & Lopachin 1998). The pathogenetic scenario of MS is further complicated by recent findings indicating that mitochondrial failure, and the subsequent energy deficiency, is occurring in neurons and is featuring early neuroinflammation (Mahad et al 2008). Accordingly, immunohistochemistry, biochemical analysis and electron microscopy imaging confirmed the presence of

a substantial impairment of mitochondria in active lesions of mice affected by Experimental Automune Encephalomyelitis (EAE), as well as in CNS lesions of MS patients (Dutta et al 2006). The consequence of mitochondrial dysfunction can culminate in the disruption of the energy metabolism that, in turn, causes a subsequent lactate acidosis of the CNS. Accordingly, increased lactate levels have been correlated with the degree of inflammation occurring in MS lesions, by using magnetic resonance spectroscopy (MRS) (Aboul-Enein et al 2003). Because the extracellular pH is significantly decreased during CNS inflammation (Friese et al 2007a), the selective activation of H⁺-gated Na⁺ and Ca²⁺ channels might compromise neuronal network functionality, thus causing neuronal injury. Acid Sensing Ion channels (ASICs) belong to the Nac/Deg channel super-family that includes epithelial Na⁺ channels subunits (ENaC) and a family of proteins called Degenerins (Deg) (Canessa et al 1993, Canessa et al 1994). Four *Asic* genes (*Asic1-4*) and specific splice variants (a and b) for *Asic1* and *Asic2* have been described in mammals (Bianchi & Driscoll 2002). These proteins are broadly expressed in several tissues and organs, although CNS neurons preferentially express *Asic1a* and *Asic2a/2b* (Wemmie et al 2002). While the activation of Deg channels occurs at extremely low pH, the activation of ASICs occurs in a wide spectrum of pH sensitivity, which is largely dependent on subunit compositions, and can be closer to physiological levels. This implies that ASICs could be activated by subtle changes of pH that might occur during CNS inflammation (Friese et al 2007). The sub-cellular localization of ASICs is still controversial, but recent findings indicate

that these channels operate as a postsynaptic proton receptor. Interestingly, spinal cord neurons express ASIC1 channels at low levels, although they are rapidly upregulated upon neuroinflammation-mediated injuries (Vergo et al 2010). Furthermore, an extensive stimulation with low pH levels caused a constitutive activation of ASIC1 and promoted neuronal cell death (Basilana et al 1997). The pharmacological inhibition of ASICs mediated by Amiloride—an aspecific ASICs channel blocker—ameliorates clinical severity and induces axonal preservation in the CNS of EAE mice (Friese et al 2007, Vergo et al). In keeping with these experiments, a recent study conducted in patients with MS supports the notion that Amiloride-mediated ASIC1 blockage is neuroprotective in the progressive form of MS, possibly reducing rates of brain atrophy (Arun et al). However, it remains unclear whether the positive effects of Amiloride are solely due to inactivation of ASICs in the CNS, considering that this diuretic drug shows a broad spectrum of action including the ability to block ENaCs, voltage-gated Ca^{2+} channels and $\text{Na}^+/\text{Ca}^{2+}$ exchanger, which are critical for normal neuronal function and survival because of their role in maintaining the stable homeostasis of intracellular Ca^{2+} concentrations (Xiong et al 2008) (Kleyman & Cragoe 1988). Beside Amiloride, a new class of anti-protozoan diarylamidines that include Diminazene Aceturate (DA), DAPI, HSB, and Pentamidine, has been recently described as specific and potent ASICs inhibitors (Chen et al). Among them, DA is the most potent small-molecular inhibitor of ASICs channels, being able to inhibit ASIC1a/b, ASIC2b and ASIC3 and

facilitating the desensitization rates of ASIC-mediated currents. Herein we assessed pH fluctuations in the CNS of EAE mice during acute inflammation by an innovative *in vivo* experimental approach based on proton-sensitive MRS. We demonstrated the protective effects of the specific ASICs blocker DA (Chen et al) in chronic EAE mice and *in vitro* on networks of neurons coupled with Micro Electrode Array (MEA) devices. Finally we demonstrated that acidosis can alter synaptic homeostasis by reducing the number of pre-synaptic terminals.

Results

Monitoring CNS acidosis in EAE mice by MR-Spectroscopy.

We used a non invasive MRS-based approach to measure pH fluctuations in the CNS of a chronic EAE mouse model –i.e. obtained by immunizing C57/BL6 females with MOG₃₅₋₅₅ peptide- by using the exogenous probe (\pm) 2-imidazole-1-yl-3-ethoxycarbonyl propionic acid (IEPA) (Garcia-Martin et al 2001). Upon calibration (Fig 1 A, B), the IEPA probe was administrated to EAE mice during acute inflammation –i.e. at 17 days post immunization (d.p.i.)- and successively the relative peak of IEPA (H₂) was detected on MR-spectrums acquired in the CNS (Fig. 1D-F).

Since Cerebellar (CB) lesions are frequently occurring in EAE mice (Brown & Sawchenko 2007), MR-Spectroscopy-mediated analysis was specifically done in this region of the brain (Fig 1D). Furthermore, tissue acidosis was also evaluated into the Thalamus (TH), a region

with less inflammatory processes compared to CB (Brown & Sawchenko 2007)(Fig 1 E). In addition, a gadolinium (Gd) based contrast agent was used to define areas of blood-brain barrier (BBB) leakage by MRI (Fig. 1 C). BBB leakage was easily visualized into CB, as shown by MRI with Gd contrast, while TH showed less BBB permeability to Gd (Fig 1C). IEPA recording into the CB demonstrated the presence of a prominent acidosis, featured by pH levels that dropped around 6.6, while pH levels measured in TH appeared less affected (Fig 1 G).

Upon MRS, we performed the histo-pathological analysis of EAE's brains, that revealed intense inflammation into the CB. Infiltrates were featured by accumulation of CD45⁺ cells (Fig 1H) that covered areas of the CB characterized by intense Gd uptake (Fig 1C and H). Clusters of CD45⁺ cells were forming perivascular cuffs around vessels of the white matter (Fig. 1H). On the other hand, TH regions, showing less acidification and Gd uptake, were characterized by less CD45⁺ infiltration (Fig 1I). These results indicate that pH levels measured into CB are sufficient to activate either ASIC1 homotrimers or heterotrimers also containing the ASIC2 subunit, that display a pH₅₀ of 6.2-6.8 (Waldmann et al 1997a, Zha).

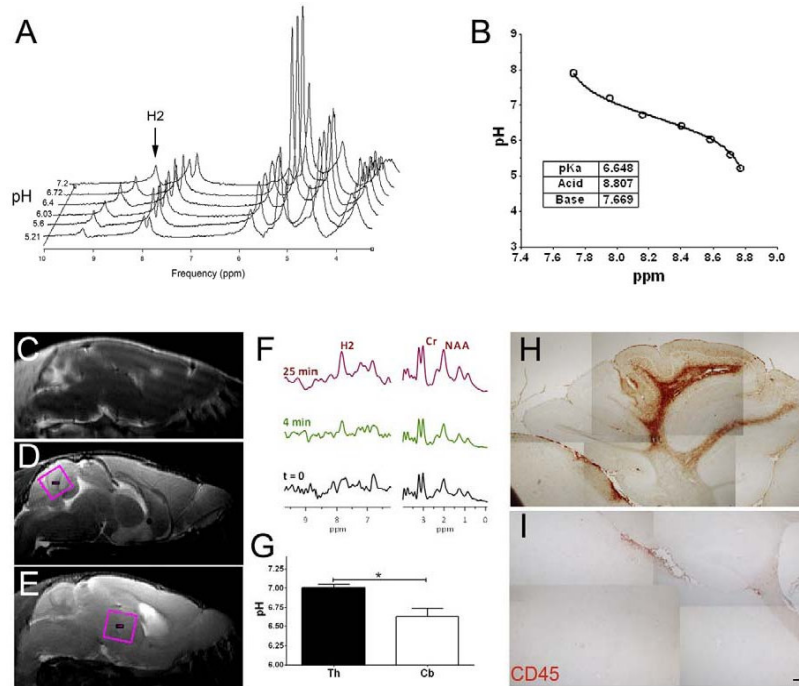


Fig. 1. In vivo MR-spectroscopy mediated detection of pH levels

Panel A shows ^1H spectrums from IEPA in saline solution at different pH values acquired at 24°C . Arrow is showing the H2 peak for which the chemical shift changes with pH. Panel B shows the calibration curve established on IEPA samples (0.3M) at pH ranging from 5 to 7.2 ($n = 7$) and the relative parameters of the linear regression. Panel C-E shows a representative sagittal MRI views from an EAE mouse (17dpi): T1 weighted image (C) with gadolinium contrast to detect BBB leakage (hyperintensity), T2 weighted images (D and E) used to define the voxel (4-12 μL) for ^1H -NMR spectrums within the Cerebellum (CB) and the Thalamus (TH), respectively. Panel F shows spectrums acquired in the CB of an EAE before ($t = 0$) and post infusion of IEPA ($t = 4$ and 24 min) in which the H2-IEPA peak is clearly detected and the metabolic components as NAA and Cr remain unchanged during infusion. From these spectrums, pH value was measured into the CB and TH (G, mean \pm SEM, $n=7$). Following MRI, mice were immediately sacrificed and sagittal sections were used to estimate infiltrating blood-derived cells by labeling for CD45 (G and H). Scale Bar 100 μm . A two-tailed t test was used to assess statistical significance * $p < 0.05$, ** $p < 0.01$, *** $p < 0.001$. NAA: N-acetylaspartate, Cr: Creatine.

DA treatment ameliorates EAE severity

We next tested whether DA-mediated ASICs blockage has beneficial effects on the clinical course of MOG-induced EAE. Because DA has a limited ability in crossing BBB (Odika et al 1995), we injected the compound into the cisterna magna of the forth ventricle one day after the onset of clinical signs of the disease. EAE mice received single injections of DA at the concentration of either 5µg/Kg or 30µg/Kg. Control EAE mice received the injection of saline. We also included a group of EAE mice that were injected with the homomeric ASIC1a inhibitor (Escoubas et al 2000b, Mazzuca et al 2007) Psalmotoxin 1 (Escoubas et al 2000b) (PcTx-1) at the concentration of 2.2µg/Kg. Mice affected by EAE usually develop a chronic disease that is clearly detectable at 10-14 d.p.i.. Starting from this time point, they show an increase of the clinical score that is associated to motor deficits and it is peaking during the acute phase of the disease -i.e. around 20 d.p.i.-. Neuropathology is further accompanied by a progressive decline in body weight. Indeed, during the acute phase, EAE mice receiving saline injections experienced about 10-20% of body weight loss and the mean clinical score was around 2.6 (Fig 2 A and C). However, mean daily clinical scores of mice receiving DA (both 5µg/Kg and 30µg/Kg treatments) became significantly lower than of the saline-injected group and remained so until the end of the experiment at 39 d.p.i. (Fig. 2 A and C). The reduced disease severity observed in DA treated groups was also reflected in the lower maximum score, as well as in reduced cumulative scores (table I). Furthermore, the administration of DA was accompanied by

weight gain and at 39 d.p.i. mice receiving DA treatments showed higher means body weight than controls (Fig 2 B and D). A partial recovery of clinical scores was also seen in EAE mice receiving the PcTx-1 treatment, however, the gain of body weight as well as of the decreased cumulative score detectable in these mice were only trends, not reaching the statistical significance (Fig 2A, B and table I), suggesting that homomeric ASIC1a channels are partially involved in mediating the EAE neuronal derangement.

We next tracked locomotion, as a parameter indicating the healthy status of mice, by using an unbiased open field approach. EAE mice receiving DA, PcTx-1 and saline treatments along with age and sex matched healthy controls were placed in the open field arena and recorded for 30 minutes (Fig 2 E-H). EAE mice receiving DA showed significantly increased locomotor activity compared with saline or PcTx-1 treated mice. Indeed, the distance travelled was 50% more than saline and PcTx-1 treated mice (ANOVA treatment effect, DA vs saline $F[1,30]=7.6$, $p\text{-value}=0.009$ and DA vs PcTx-1 $F[1,22]=12.9$, $p\text{-value}=0.002$; Fig 2 E), even if they did not reach the control animals (ANOVA treatment effect, DA vs HC $F[1,26]=49.2$, $p\text{-value}<0.0001$). Moreover, DA mice moved faster than saline and PcTx-1 treated mice, as indicated by a significant difference in velocity (ANOVA treatment effect, DA vs saline $F[1,30]=17.2$, $p\text{-value}=0.0003$ and DA vs PcTx-1 $F[1,22]=6.6$, $p\text{-value}=0.017$; Fig 2 F), reaching control mice levels (ANOVA treatment effect, DA vs HC $F[1,26]=0.2$, $p\text{-value}=0.6$). The statistical analysis of zone preference during the 30 minutes test revealed a significant increase on the exploration index in DA treated

mice (ANOVA treatment effect, DA vs saline $F[1,30]=9.0$, p -value=0.005 and DA vs PcTx-1 $F[1,22]=8.5$, p -value=0.008; Fig 2 F, H). Interestingly, the two DA dosages that we administered to EAE mice, resulted in the same amelioration and all DA-treated EAE mice were pooled in the analysis. All these results confirmed that beside a significant reduction of disease severity, EAE mice receiving the DA treatment also showed a substantial amelioration of their locomotor performances.

We next assessed whether DA treatment can also improve neurophysiological parameters that are typically affected in EAE mice (Amadio et al 2006). As expected, we found a significant increase of both the latency of Motor Evoked Potentials (MEPs) and the Central Conduction Time (CCT) in saline treated EAE mice, demonstrating a slowing of conduction of descending cortico-spinal volleys, in keeping with worsening clinical motor scores and with pathological features of demyelination and axonal damage as well. We found that mice receiving DA (5 μ g/Kg) showed a partial, but significant recovery of these variables (Supplementary Fig 1A and 1B), suggesting that DA was exerting neuro-protective effects during neuroinflammation.

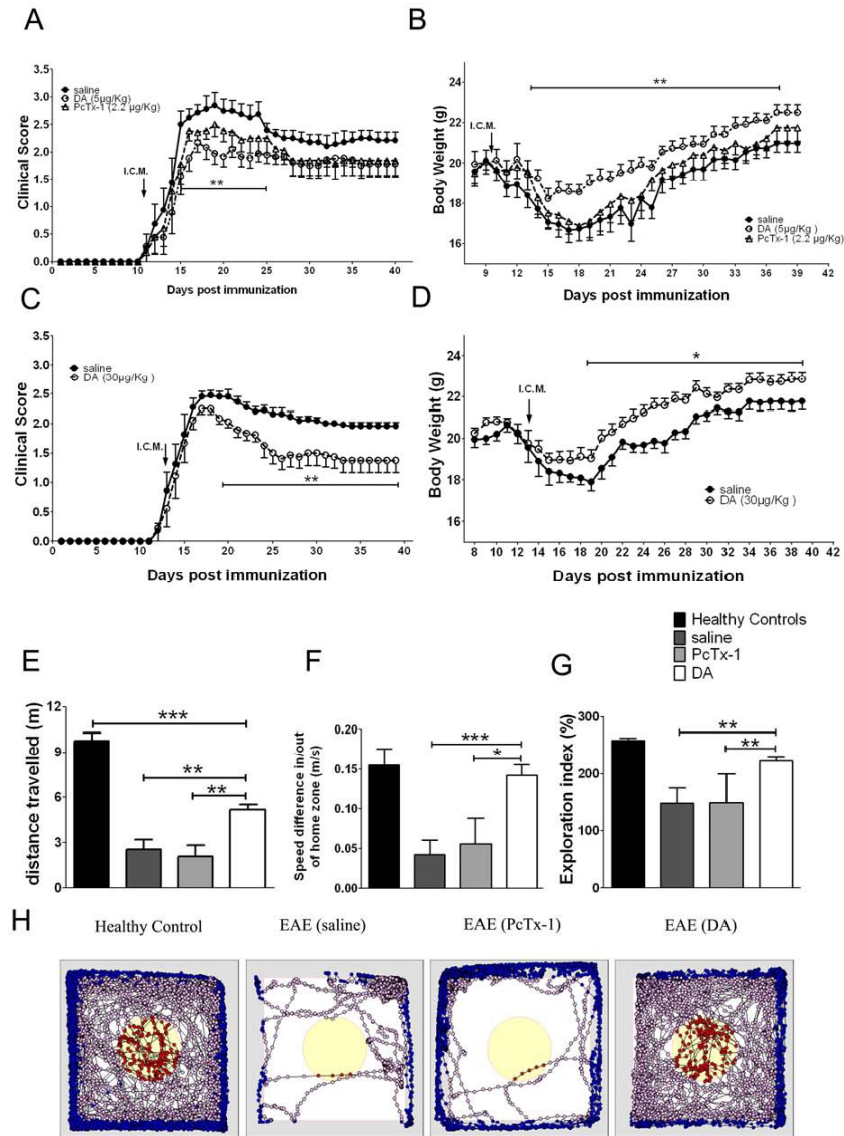


Fig. 2. Development of EAE was reduced in DA treated mice

EAE was induced in mice by immunization with MOG/CFA co-injected with PTx. Panels A and C show clinical scores of diseased mice receiving a single injection of: saline, DA (5 and 30 µg/Kg, respectively) and PcTx-1 (2.2 µg/Kg) , one day after the onset of the disease (arrow in the panel, n=9 for each group). (continue on pg.66)

(continue from pg.65) Data are shown as an average \pm S.E.M. in each group. Weight (mean \pm S.E.M.) of mice with EAE receiving drugs are provided in panels B and D. EAE mice (17 d.p.i, n=8 for each group) were video recorded using EthoVision 2.3 system. Data derived from 30 minutes of measurement were used to express: the travelled distance, (E), speed difference in/out of home zone, (F) and the exploration index (G). Recording tracks, provided in panel H, show a representative tracking from an untreated single mouse (left in the panel) and from single EAE mice receiving saline, PcTx-1 or DA treatments. One way ANOVA tests and a two-tailed t test were used to assess statistical significance * $p < 0.05$, ** $p < 0.01$, *** $p < 0.001$.

Effects of DA treatment on neuropathological markers of EAE mice

Demyelination and axonal loss were quantified at 40 d.p.i. in both CB and Spinal cord (SC), which are the most commonly affected regions of the CNS in MOG-EAE mice (Brown & Sawchenko 2007) We compared saline-treated EAE mice with mice receiving DA at low dosage (5 μ g/Kg) and with mice receiving PcTx-1 (2.2 μ g/Kg).

One CB sagittal section every 180 μ m (Fig 3 A, C and E) and one SC coronal section every 500 μ m (Fig 3 G, H and I) were labeled for MBP and luxol fast blue (LFB), respectively, for studying myelin loss. Both DA and PcTx-1 treatments significantly reduced the number of demyelinated lesions in CB and SC, when compared with EAE mice receiving saline (Fig 3 J and L).

We labeled adjacent sections for Bielschowsky staining to evaluate the presence of axonal damage (Fig 3 B, D, F and Supplementary Fig 2A-C). Accordingly to myelin preservation, DA treated EAE mice showed less axonal damage than saline treated EAE mice in both CB and SC (Fig 3K and Supplementary Fig 2D). EAE mice receiving PcTx-1

displayed a general reduction of the axonal loss in the CB, although this decrease was only a trend not reaching statistical significance ($p < 0.08$, Fig 3K). However, PcTx-1 treatment was able to significantly diminish axonal loss in the SC (Supplementary Fig 2D). Thus, in agreement with other studies (Frieze et al 2007a, Vergo et al), we demonstrated that a general inhibition of ASICs during neuroinflammatory episodes, exerts protective effects on myelin and reduces the axonal loss. However, PcTx-1 was less effective than DA in reducing axonal derangement, suggesting that beside ASIC1, the blockage of both ASIC2 and ASIC3 is critical to reduce neurodegenerative processes linked to neuroinflammation. Given the fact that *Asics* are broadly expressed in several tissues and organs (Waldmann et al 1997a), including bone marrow-derived macrophages (Kong et al) and that the immune response, in terms of activation and production pro-inflammatory cytokines, is largely dependent on ion channels (Ehling et al), it is possible that DA had exerted protective effects by blocking ASICs in CNS-infiltrating immune cells. Therefore, we compared the expression levels of *Asic1*, *Asic2* and *Asic3* mRNAs in primary cultures of neurons, astrocytes, microglia (MG) cells and, above all, in infiltrating mononuclear cells derived from acute EAE mice –i.e. 17 d.p.i.-

Asic1 and *Asic2* were expressed at higher levels in neuronal cultures, than in Astrocytes, MG and infiltrating mononuclear cells from EAE mice, while the expression levels of *Asic3* were extremely low in all samples we examined (Supplementary Fig 3A). Furthermore, *Asic3* expression levels in astrocytes, MG and infiltrating mononuclear cells

from EAE mice were approximately 50% less than in neurons, suggesting that *Asics* are prevalently confined in neuronal cells (Supplementary Fig 3B).

Accordingly, when we examined inflammatory infiltrates in EAE mice treated with saline, PcTx-1 and DA at 40 d.p.i., we did not find significant differences in the number of inflammatory lesions containing CD45⁺ cells in both the CB and the SC of DA treated mice respect to saline controls (Supplementary Fig 3C-F, and not shown).

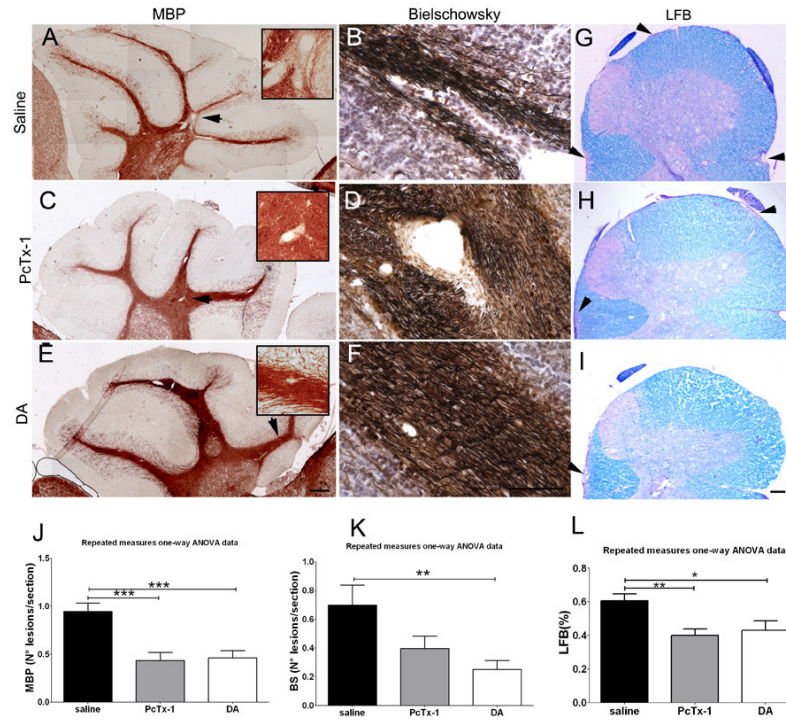


Fig. 3. DA reduces demyelization and axonal loss in CB of EAE mice

Panels A, C and E show immunocytochemical staining for MBP in CB of EAE mice (40 d.p.i, n= 4 for each group) receiving saline (A), PcTx-1 (2.2 µg/Kg, C) and DA (5µg/Kg, E). Representative high magnification of a demyelinating lesion by loss of MBP is shown in inset of panel A. Inset in C shows demyelination around a vessel, while inset in E shows intact myelin. Quantification of MBP lesions per section (mean± S.E.M.) are provided in panel J. Panels B, D and F show high power magnifications of Bielschowsky silver impregnation in CB cross-sections from EAE mice (n= 4 for each group), receiving saline (B), PcTx-1 (D) and DA (F). Axonal damage is predominant in mice receiving saline, as compared to DA and PcTx-1 treated mice, although the reduction obtained upon PcTx-1 treatment did not reached statistical significance ($p < 0.08$), as shown in quantification (mean± S.E.M.) provided in panel K. Panels G, H and I show LFB staining on SC sections from EAE mice receiving saline (G), PcTx-1 (H) and DA (I). Quantification is shown in panel L. Scale bar 100µm. One way ANOVA tests with Bonferroni post test was used to assess statistical significance * $p < 0.05$, ** $p < 0.01$, *** $p < 0.001$.

Study of the effect of acidosis and DA protection on neuronal network activity in vitro

We next investigated low pH on networks of neurons coupled with MEA devices, which represent a well-established method for electrophysiological studies, allowing the detection of synchronized firing activity of assembled neurons (Biffi et al , Biffi et al , Chiappalone et al 2003, Rossi et al). After plating, cortical neurons from embryonic (E) day 17.5, were kept in vitro for 10/14 days until they had developed rich functional networks, featured by intense spontaneous electrophysiological activity (Chiappalone et al 2007). At the neuronal density that we adopted in our experiments (3×10^5 cells/MEA chip), networks displayed a well synchronized activity which was organized in short spike trains (bursts) and very few single spikes arising between bursts. We measured the basal spontaneous activity at physiological pH (7.4) for 10', neurons were then exposed to pH 6.6 for 40', thus mimicking the acidosis that we detected in EAE mice (Fig 1 F, pH 6.6). Finally, neurons returned to pH 7.4 and were further recorded for 60', as shown in figure 4A. While control neuronal networks -i.e. exposed to pH 7.4 - were stable for all parameters we scored in the analysis (Fig 4B, E, H and K), networks exposed to low pH displayed a dramatic and stable reduction of the overall firing activity (Fig 4C, F, I and L).

Interestingly, the spike number was more affected by acidosis than other parameters that we included in the analysis (Fig. 4C, D), possibly because low pH was acting on the proper firing activities of GABAergic neurons, which are involved in the regulation of an entire

network (Li et al , Ziemann et al 2008b). However, the electrophysiological activity was promptly recovered upon the restoring of the physiological pH, suggesting that short acidosis is a reversible phenomenon (Fig 4C, D). Of note, the intra burst frequency (IB) and percentages of spikes organized in bursts –i.e. two parameters linked to the functional connectivity and integration of the network- displayed a trend to recover even in the presence of acidosis, although they remained largely below baseline values (Fig. 4 I, L). The reduction of spike numbers elicited by the low pH treatment was partially restored by applying PcTx-1 to the acidic bath, suggesting that ASIC1 was involved in mediating part of this phenotype (Fig 4C). DA treatments were even more efficient in restoring the spike number during acidosis (Fig 4 D). Low pH significantly affected the number of bursts and the administration of PcTx-1 partially reverted this phenotype (Fig 4F). Accordingly, DA efficiently induced a recovery of number of bursts in neurons exposed to pH 6.6 (Fig 4G). However, functional recovers elicited by both drugs were partial, indicating that further mechanisms other than ASICs activation, are involved in their regulation. It is important to note, that the frequency of firing recorded in each burst (i.e. IB-frequency) and percentages of spikes organized in bursts, both affected by acidosis (Fig. 4 L, M), were totally recovered by PcTx-1 (Fig. 4I, L) and DA treatments (Fig 4J, M), implying that ASICs are critically contributing to the regulation of the coordinated distribution of spikes within bursts. In line with this concept, networks of neurons receiving the physiological pH and DA (3 μ M)

showed slight, but not significant, alterations of spike and burst numbers (Supplementary Fig 4 A, B), while intra-burst frequency and spikes distribution in bursts were unchanged (Supplementary Fig 4 C, D), suggesting that ASICs are implicated in the maintenance of network homeostasis and their inhibitions, even at physiological pH, influences firing activity. Furthermore, amplitudes (peak to peak) of recorded signals were significantly reduced during acidosis (Supplementary Fig 5A, B, C), reflecting the inhibition of firing activity mediated by the acidic pH. However, PcTx-1 as well as DA treatments (high dosage) reverted this phenotype (Supplementary Fig. 5B, C). These data demonstrate that a short acidic treatment was sufficient to alter the homeostasis of neuronal networks, although in reversible way, and that ASICs are rapidly activated during acidosis and are partially involved in mediating these alterations.

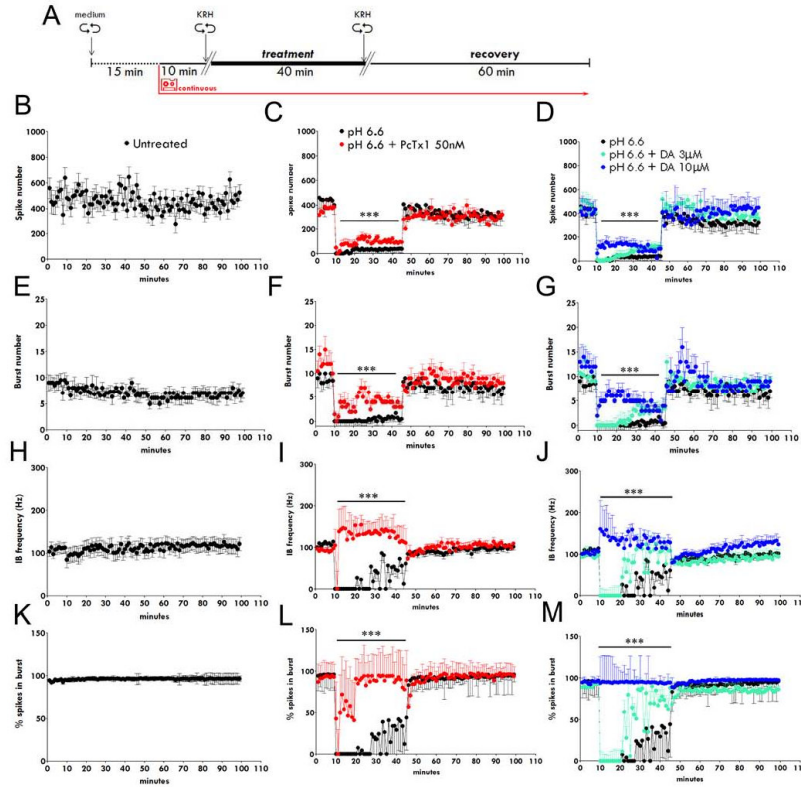


Fig. 4. Effects of acidosis on spontaneous activity of a cortical neuronal culture.

Sketch of the experimental paradigm is shown in panel A. Neurons (12/14 div) coupled with MEA were incubated with KRH (pH 7.4) for 15', then spontaneous electrophysiological activity was continuously recorded for 10' to establish the baseline. Neurons received the change of the bath (KRH, pH 6.6) and were further recorded for 40'. Finally, neurons received the KRH at pH 7.4 (recovery phase) and were recorded for 60'. Spontaneous firing activities of controls neuronal networks, receiving KRH at pH 7.4, are provided in panels B, E, H and K (black dots n=15). Mean firing rates (i.e. number of spikes in single active electrode per minute) are significantly reduced during acidosis (black dots in C and D, n=18). Networks receiving KRH pH6.6 and PcTx1 (red dots in C, n=3) or DA (blue dots in D, 3μM n=10, 10μM n=3) increased the number of recorded spikes. (continued on pg.74)

(continue from pg. 73)

Mean bursting rates (i.e. number of bursts per minute) are reduced during acidosis (black dots in F and G), while PcTx-1 (red dots in F) or DA (blue dots in G) increased burst numbers. Frequencies of spikes during bursting activity are provided in panels H, I and J. While acidosis dramatically reduced the firing frequency (black dots in I and J), the administration of PcTx-1 (red dots in I) or DA (blue dots in J) substantially rescued the loss of frequency. Random activity was evaluated by calculating percentages of spikes organized in bursts (K, L and M). While controls exhibited highly synchronized activity (K), acidosis depleted the number of spikes in bursts (black dots in L and M). In contrast, PcTx-1 (red dots in L) and DA (blue dots in M) reverted this phenotype. Error bars indicate S.E.M. A two-tailed t test were used to assess statistical significance, *** $p < 0.001$.

Long term acidosis alters synaptic connectivity.

We next studied the influence of acidosis on the stability and the homeostasis of pre- and post-synaptic neuronal compartments. We speculated that, during acute EAE, either inflammatory processes or the acidosis might persist into the CNS for hours or even days (Morrissey et al 1996), thus dictating a sustained activation of ASICs channels. Primary neuronal cultures were infected with lentiviruses expressing PSD-95-GFP and Synapsin I-Cherry chimeric proteins to label both post- and pre-synaptic compartments, respectively. Cultures were left to develop until robust expression levels of both reporters were effectively detectable. Long term acidosis was obtained by exposing neurons at pH 6.6 for 12 hours. Imaging was done by acquiring one image of the same field every hour for the entire duration of the treatment (Fig. 5A). The number of pre-and post-synaptic spines was calculated at each time point in both

controls –i.e. neurons receiving the physiological pH- (Fig 5B) and in neurons receiving pH 6.6 (Fig. 5C). Results showed that acidosis significantly affected the pre-synaptic compartment reducing the number of Syn1-Cherry⁺ spines of about 20%. Interestingly, the reduction of pre-synaptic spines rapidly occurred upon acidic pH administration and persisted along the treatment. On the other hand, low pH treatment did not affect the number of Psd-95-GFP⁺ spines. These results demonstrate that long lasting acidification alters network connectivity thus influencing network functional characteristics.

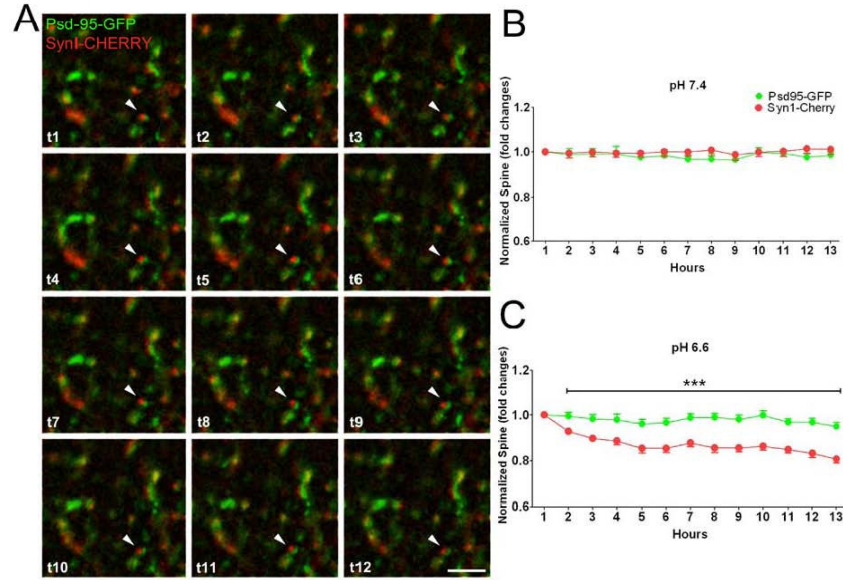


Fig. 5. Pre-synaptic alterations of neurons exposed to acidosis

Panel A shows the time lapse image sequences of pre- and post-synaptic compartments in Syn1-Cherry and PSD95-GFP co-infected primary neuronal cultures (DIV 15-17). Samples receiving pH 7.4 or 6.6 were imaged every hour for 12h using a microscope with a temperature and pH controlled environments (DeltaVision, Olympus equipped with a weather station precision-control chamber). Z stack images were taken each 500 nm for $\pm 4 \mu$ m from the focal plane selected at t0. The number of Syn-1 and PSD95 positive spots was counted in all the images taken during the 12h of treatment. The mean of the counts normalized on t0 count and the relative S.E.M. of the control (pH 7.4) and pH 6.6 treated samples were shown in panel B and C, respectively. n=3 experiments for each group from 3 different preparation. 8 fields per experiment were analyzed and an average of 964 ± 568 and 1053 ± 605 per field of pre- and post- synaptic terminals respectively were detected. Scale Bar 5 μ m.

Long term effects of acidosis on neuronal networks electrophysiology.

Because alterations of pre-synaptic spines may negatively influence neuronal firing activity, we investigated whether prolonged acidosis can induce permanent electrophysiological alterations in networks of neurons. We firstly established baseline electrophysiological activities by recording neurons at physiological pH. Neurons were then exposed to pH 6.6 for 12 hours and recorded at the end of the acidic treatment. Networks were returned to the physiological pH and further recorded one hour and 12 hours after the exchange of the bath (Fig 6A). Some of the parameters that we analyzed (i.e. total spikes and bursts numbers) showed a slight reduction after 12 hours of incubation, even in the presence of the physiological pH (Fig 6 B, C). These small fluctuations, however, might derive from procedures required for bath exchange, while other parameters, such as: the number of spikes in bursts and the number of active electrodes, were much more stable and tended to be rapidly restored after physical and mechanical perturbations (Fig 6 D, E). Long term acidification, however, significantly affected both the former and the latter parameters, although with different intensity. Indeed, numbers of recorded spikes and bursts were dramatically reduced in neurons exposed to low pH (Fig 6 B, C), while numbers of spikes in burst and the number of active electrodes were less affected (Fig 6D, E). However, all these parameters returned to values closer to the baseline soon after we exchanged the acidic bath with the bath at pH 7.4, suggesting that neurons are able to recover firing activity upon

the restoring of the physiological pH. Despite this rapid functional recovery, occurring in the first hour from bath exchange, the evaluation of firing activity 12 hours later showed that these electrophysiological parameters displayed a further significant reduction. In fact, both the total numbers of recorded spikes and burst numbers were significantly affected in neurons that were transiently exposed to pH 6.6 (Fig 6 B, C), while the number of spikes organized in burst as well as the number of active electrodes were somehow preserved. Interestingly, the administration of DA during low pH treatment exerted protective effects, preserving neurons from reducing spikes and bursts in the recovery phase- i.e. 12 hours after the bath exchange-.

It is interesting to note that, DA-treated neurons increased all electrophysiological parameters we scored, soon after they received the change of bath from the acidic pH to the physiological one (Fig 6 B-E). We speculated that the increased activity, sustained by DA in the first hours from pH recovery, can be beneficial and protective for long term recovery of the network physiology. Because a general reduction of neuronal network firing activity might be due to increase rates of neuronal cell death, we scored the number of dying neurons receiving acidosis by adding Sytox and Hoechst tracers to cultures (Supplementary Fig. 6, B). However, cell death rates measured in neurons receiving pH 6.6 and neurons receiving the bath at physiological pH were similar, suggesting that cell death was not involved in modulating electrophysiological alterations induced by low pH treatment (Supplementary Fig. 6C).

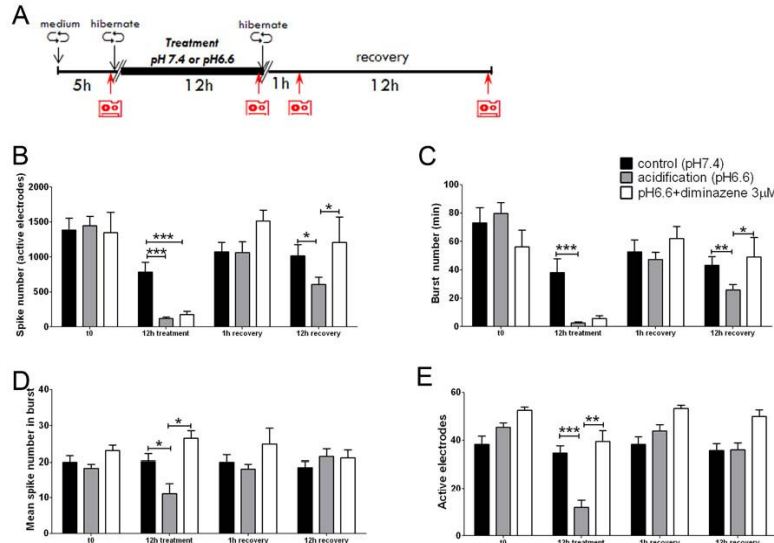


Fig. 6. Long term effects of acidosis on neuronal network activity

Panel A shows the schematic representation of the experimental paradigm. Black bars in panels B, C, D and E show control neurons (12 div) receiving Hibernate medium at pH 7.4 (n=13). Grey bars show neurons only receiving Hibernate medium at pH 6.6 (n=20), while neurons receiving Hibernate pH6.6 and DA (3μM, n=4) are indicated with white bars. The reduction of firing activity (i.e. number of spikes in single active electrode per minute) experienced by neurons during the 12 hours long acidosis treatment induced a substantial reduction of spike numbers when neurons returned to pH 7.4 (B). DA increased the number of spikes recorded in the recovery phase at pH 7.4 (B). Accordingly, acidosis induced a significant reduction the number of bursts (C). This number was also reduced when neurons returned to pH 7.4. DA counteracted this phenotype increasing the number of bursts in the recovery phase, as shown in panel B. Mean spike numbers organized in burst activity are shown in panel D. Acidosis significantly reduced this number as compare to the control (black bars), while this number did not change in neurons receiving acidosis and DA (D). Because acidosis dramatically impaired firing activity, also the number of active channels were significantly depleted by acidosis as compared with controls (E). This reduction, however, was prevented by DA administration (E). Error bars indicate S.E.M. *p <0.05, ** p<0.01, *** p<0.001

Discussion

Although inflammation and demyelization are featuring the CNS of MS patients, the presence of cognitive deficit in a relevant percentage of MS patients already at the first episode of the disease (Rocca et al 2009), suggests that other mechanisms might concur to the establishment of functional neuronal alterations. These molecular cascades are likely to be complex and are possibly involving combinations of harmful cues that include inflammatory mediators and changes in neuronal ion channels expression and functioning. In line with this concept, the presence of mitochondrial dysfunctions in neurons and the consequent alterations of ion-exchange mechanisms have been recently described in lesions of MS patients and animal models. The failure of the mitochondrial functioning results in the overproduction of lactic acid, causing a reduction of the extracellular pH that, in turn, is inducing an aberrant activation of ASICs channels (Friese et al 2007). In this work, we have focused our attention on the relationship between inflammation and acidification occurring in CNS lesions of mice affected by chronic EAE, posing the question on a possible role of pH sensitive channels in the initial phases of the CNS pathogenesis and proposing these channels as reliable therapeutic targets.

We firstly established whether acidosis is really affecting EAE mice by using a new technique based on MR-Spectroscopy. Indeed, the presence of sustained CNS acidification in chronic EAE has been recently described by introducing a micro-pH meter into the CNS that

allowed pH recording at the peak of the inflammation (Frieze et al 2007). The pH reduction documented by Frieze and coworkers was ranged around pH 6.6, a value that is compatible with the activation of ASICs (Benson et al 2002). However, the introduction of a micro-pH meter does not allow the precise detection of pH levels featuring different CNS regions, as well as the surgical procedure used for the introduction of the probe may, *per se*, generate bleeding and a subsequent general acidosis of tissues. We used a non invasive method to measure the extracellular pH fluctuations *in vivo*, based on the specific responsivity of IEPA probe (Garcia-Martin et al 2001) to pH detectable by MR-Spectroscopy. Our *in vivo* MRS results indicate the existence of a tight correlation between Gd accumulation into the CNS and the presence of a persistent acidosis. Accordingly, measurements in CNS areas featured by intense accumulation of CD45⁺ inflammatory cells showed pH values around 6.6, in agreement with previous results (Frieze et al 2007). However, pH levels were only partially affected in CNS regions displaying less blood-derived cell infiltrates and Gd uptake, suggesting that the acidification of the CNS is a dynamic process possibly driven by inflammatory episodes. These findings, however, need further investigations and possibly dedicated preclinical studies to establish the dynamic of acidosis during neuroinflammatory processes occurring in EAE.

We next attempted to selectively inhibit ASICs in chronic EAE mice. Among ASICs inhibitor, Amiloride mediates beneficial effects in EAE mice, inducing myelin and axonal preservation (Frieze et al 2007,

Vergo et al), as well as exerting protective effects in progressive MS patients (Arun et al). However, Amiloride displays a broad spectrum of action, being able to block epithelial sodium channels (ENaC), the Sodium-hydrogen antiporter 1 in the heart, $\text{Na}^+/\text{Ca}^{2+}$ exchanger and voltage-gated Ca^{2+} channels (Kleyman & Cragoe 1988), in addition to ASICs inhibition, thus posing questions about its specificity and suggesting additional studies. Our pharmacological approach was based on DA, which is a member of diarylamidines/pentamidine family, that has been successfully used in the treatment of second stage human trypanosomiasis in several countries (Atouguia & Costa 1999, Bacchi 2009). In particular, DA can exert the blockage of ASIC1a, -1b -2a, and -3 currents in transfected CHO cells, with the following efficiency $1b > 3 > 2a > 1a$ (Chen et al), thus providing the opportunity for a selective inactivation of ASICs in EAE .

It is important to note, that under physiological conditions, ASICs mediated H^+ evoked currents are involved in synaptic transmission and contribute to the synaptic plasticity, thus suggesting that the proper activation of these channels is necessary for the homeostasis of the CNS. In line with this concept, the constitutive knockout mice for *Asic1a* display reduced long-term potentiation (LTP), reduced acid-evoked Ca^{2+} entry at dendritic spines as well as a general reduction of dendritic spine numbers (Basilana et al 1997, Jasti et al 2007b). Nevertheless, during pathological conditions, such as during neuroinflammation, the excessive activation of ASICs caused CNS damage, as demonstrated in constitutive knockout mice for ASIC1a which are partially protected in the EAE experimental paradigm

(Friese et al 2007, Vergo et al). Furthermore, the fact that ASIC1a is increased in damaged axons of EAE mice and in MS patients, possibly suggests that inflammatory cues might trigger ASICs activation in neurons (Vergo et al).

Interestingly, DA-mediated ASICs inhibition produced beneficial clinical effects in EAE mice even if we administered the compound in mice by a single intra cisterna magna injection, suggesting that DA levels into the CNS are quite stable for protracted time. When we compared DA with the specific ASIC1a blocker PcTx-1, we found that the inhibition of homomeric ASIC1a channels was partially effective in protecting mice from EAE. We raised two hypotheses to explain these results. On one side, it is possible that PcTx-1 displays a low diffusivity into the CNS parenchyma, hampering its ability to reach deep CNS lesions, such as lesions of CB. On the other, it is possible that ASIC2a/b and ASIC3 are participating to the establishment of the CNS damage. In this framework, the ability of DA to block both channels, in addition to ASIC1, might provide a comprehensive inhibition of ASICs activity during CNS acidosis. Furthermore, the administration of DA did not cause any side effects in mice, in agreement with the attributed major role of ASIC1 in sustaining neuro-physiological processes, and suggesting ASIC2 and ASIC3 as therapeutic targets for the treatment of acidosis in neuroinflammatory disorders.

We also documented that EAE mice injected with DA were featured by a substantial amelioration of their walking performances, witnessing the general beneficial effect of DA treatment. These

results were further supported by improvement of motor cortex output that was demonstrated by significant reduction of CCT in treated animals. However, ASIC2 and ASIC3 are expressed in CNS areas that are involved in pain processing, thus the amelioration of locomotion that we observed in DA-treated mice might also be due to a reduction of pain perception (Deval et al). In this framework, PcTx-1 did not ameliorate locomotion performances of EAE mice, suggesting that ASIC2 and ASIC3 are critically involved in mediating EAE pathophysiology. However, the contribution of ASICs in the inflammatory- and neuropathic-mediated pain perception needs further investigation to be completely elucidated.

CNS acidosis and ASICs activation are involved in a large number of neurodegenerative diseases including ischemia, Parkinson's disease and MS. The general concept emerging from these studies suggests that extreme and/or prolonged acidosis kills neurons and ASICs activation is largely taking part to acidosis-induced neuronal cell death. For example, the inhibition of ASICs in a classic model of ischemia, the middle cerebral artery occlusion (MCAO), substantially reduces the infarct volume (Xiong et al 2004b), supporting the idea that the acidosis associated to the ischemia, affects neurons located at the penumbra. In line with these concepts, a recent study demonstrated a protective effects mediated by Amiloride in patients affected by progressive MS (Arun et al), extending experimental evidence linking ASICs with the neurodegeneration.

We attempted to reproduce *in vitro* the effects of acidosis and the protective features mediated by the blockage of ASICs, by

investigating neuronal networks electrophysiology on MEAs. The most evident effect of acidosis on neuronal network activity was represented by the almost complete block of firing. This phenomenon is complex and influences a variety of membrane receptors and ion channels also involving long term potentiation events (Hsu et al 2000). In addition, it has been demonstrated that increasing concentrations of H^+ negatively modulate N-methyl-D-aspartate (NMDA) channels (Tang et al 1990, Traynelis & Cull-Candy 1990), as well as induce alterations on GABAergic neurons that are affecting voltage gated sodium channels and Glu-R channels (Li et al). The administration of both PcTx-1 and DA sustained the electrophysiological activity of networks of neurons, thus counteracting negative effects elicited by acidosis. However, a restricted number of parameters were only partially restored by both PcTx-1 and DA, confirming that acidosis induces remarkable electrophysiological alterations that are ASICs independent. Since acidosis *in vivo* is likely to have a long lasting duration, we exposed cultures for 12 hours to low pH. Networks of neurons treated with acid bath for 12 hours were able to recover their activity after physiological pH restoration, but tended to reduce their firing activity 12 hours after this recovery. These results indicate that long term acidification was mediating chronic functional alterations of neuronal firing. Interestingly, the administration of DA was sufficient to compensate this reduction, thus protecting networks from long lasting detrimental effects.

We also found that long lasting acidification was able to induce a structural alteration of the pre-synaptic compartment, causing a 20% reduction of pre-synaptic terminals, probably caused by the chronic alteration of the electrical network activity. Accordingly, the stability/homeostasis of the synaptic apparatus has been reported to be largely influenced by the activity (Kossel et al 1997). On the other hand, we did not observed any postsynaptic alterations, possibly for the shorter time of activity inhibition.

Despite several reports indicate that acidosis trigger extensive neuronal cell death (Schonfeld-Dado & Segal 2009) (Wang & Xu), we did not observe this effect even in neurons receiving pH 6.6 for 12 hours, suggesting that alterations of network physiology and synaptic connections, were not the consequence of neuronal suffering and delayed neuronal cell death. This discrepancy with other reports can be explained by the fact that we exposed neurons to low pH for a relative shorter period of time and, above all, by applying milder acidification.

In conclusion, our study supports the notion that ASIC channels are mediating CNS detrimental effects and that their blocking can attenuate part of these effects.

Material and Methods

EAE induction and drug administration

All procedures involving animals were performed according to the guidelines of the Animal Ethical Committee of San Raffaele Scientific Institute (IACUC protocol number 427). Naive C57Bl/6 female of 6 weeks of age (Charles Rivers laboratory) were used for EAE induction. Briefly, mice were subcutaneously injected (in both flanks and at the base of the tail) with an emulsion containing 200 µg of Myelin Oligodendrocyte Glycoprotein (MOG) peptide 35-55 (Espinkem) and 8 mg/ml of Mycobacterium tuberculosis (strain H37Ra, DIFCO) dissolved in incomplete Freund's adjuvant (SIGMA). In addition, 500ng of Pertussis Toxin (SIGMA) was injected intravenously on days 0 and 2 after immunization. Body weight and clinical score (0= healthy; 1= limp tail; 2= ataxia and/or paresis of hind limbs; 3= paralysis of hind limbs and/or paresis of forelimbs; 4= tetraparalysis; 5= moribund or death) were daily and blindly recorded until the day of the sacrifice. The day after the onset of clinical outcomes, mice were randomized and divided in three groups that received pharmacological treatments. Drugs were administered by a single stereotaxic injection into the cisterna magna of the fourth ventricle (i.c.m) at the following coordinates: lambda -7, 4.5° syringe inclination angle, and depth -3.5. DA and pcTx-1 were dissolved in sterile saline at appropriate concentration and injected in a volume of 4µl, controls received saline injections. At the day of the sacrifice, mice were anesthetized and then perfused with 4%

paraformaldehyde (PFA) in PBS 1X. Brains and spinal cord were carefully removed and post-fixed in the same solution at 4°C for 12h. Tissues were cryoprotected in 30% Sucrose (Sigma) in PBS 1X at +4 °C for 24h , embedded in OCT and stored at -80°C.

MR-spectroscopy of IEPA

Calibration of the pH dependence of the chemical shift of the H2 resonance were performed in 7 samples of saline water containing IEPA ((±) 2-imidazole-1-yl-3-ethoxycarbonyl propionic acid, at 0.3M, SOIREM Research, S.L., Spain) with pH ranging from 5 to 8. ¹H-NMR spectra were acquired on a 7T-MRI scanner (Biospec, Bruker Biospin, Germany) with a PRESS sequence (TR/TE=2500/10ms, average=1, water suppression). The chemical shift of H2-IEPA peak was measured on spectrum acquired on each sample using Mnova tool (Mestrelab Research SL). The curve of pH as function of chemical shift (ppm) was fitted using a non linear regression with the Henderson-Hasselbalch equation ($\text{pH} = \text{pKa} + \text{Log}((\text{ppm-Acid})/(\text{Base-ppm}))$), pKa, Acid and Base are constant) using Prism (GraphPad software). In vivo analysis of pH was done by MRS on EAE mice at 17 d.p.i (n=7). During MRS, animals were maintained under anesthesia with a mixture of 1-2% of flurane in oxygen, respiration rate was constantly monitored and body temperature maintained (36-37°C) by warm water heating system. MR-Spectrums were acquired in a voxel selected the anatomic T2-MR images in Cb and Th regions of the brain with the PRESS sequence (TR/TE=1850/14ms, average=256, water suppression and voxel=2×3×2 or 1.3×1.5×2.2 mm³ respectively). Such spectrums were acquired before and after the slow infusion of IEPA (20

mmol/kg at 0.4 mL/hrs) through a catheter placed on the tail vein. Successively, BBB leakage was evaluated with T1 weighted images acquired post administration of gadolinium contrast (1.2mmol/kg of MultiHance, Bracco Imaging Spa). All spectrums were processed using Mnova program to determine the H₂-IEPA chemical shift (between 8.8 and 7.67ppm) using the Creatine peak (Cr) as reference (3.02ppm).

Primary neuronal cultures & MEA recording

Primary neuronal cell cultures were obtained from E17.5 embryos collected from C57Bl/6/CD1 mice sacrificed by inhalation of CO₂. Brains were dissected in cold HBSS (Gibco) supplemented with Glucose 0.6% and 5 mM Hepes pH 7.4 (Sigma). Cerebral cortices were mechanically dissociated in single cells and re-suspended in culture medium containing: 50% D-MEM (LONZA); 50% Ham's -F12 (GIBCO); 5 mM HEPES pH 7.4 (SIGMA); 0.6% glucose (SIGMA); 0.5% Glutamine(GIBCO); 30 nM Na-Selenite (SIGMA); 20 nM Progesterone(SIGMA); 60 nM Putrescine(SIGMA) ; 100 µg/ml Apo-Transferrin (SIGMA); 0.025 mg/ml of bovine Insulin (TEBU-BIO) and 5% of FBS (EUROCLONE) in absence of antimitotic and antibiotic drugs. After 5 hours, medium was replaced completely with fresh culture medium without FBS. Cells were seeded onto coated MEA chip at the final density of 3x10⁵ cells/MEA. For synapses analysis, neurons were plated onto 1mg/ml poly-L-lysine (P2636 Sigma) coated glass coverslips at the density of 100 cells/mm². Neurons were maintained in culture for 12-16 days in standard culture medium in a humidified 5% CO₂ atmosphere at 37°C. Standard 60

electrode Multi Electrodes Array (MEA) biochips with 200 μ m electrode spacing and 30 μ m electrodes diameter with an integrated reference electrode (Multichannel Systems GmbH, Reutlingen, Germany) were employed for the study of electrophysiology. Before plating the cells, MEAs were coated with poly-L-lysine (2 mg/ml; P2636 Sigma) and laminin (10 μ g/ml; L2020 Sigma). Upon plating, neurons were kept in vitro for 12/13 days and their electrical activity was recorded by using a commercial setup by MultiChannels Systems. This is made of a pre-amplifier stage (MEA-1060-Inv-BC-Standard, gain: 55, bandwidth: 0.02 Hz–8.5 kHz, MCS GmbH), an amplification and filtering stage (FA64, gain 20, bandwidth: 10Hz–3kHz, MCS GmbH) and a data acquisition system. Raw data were detected using a sampling frequency equal to 25kHz.

Off-line Signal Processing: raw data were analyzed by MC_Rack Software (MCS GmbH). Spike detection and peak to peak amplitudes were calculated by fixing in each channel, a threshold equal to 5 folds the standard deviation of the average noise amplitude recorded in the first 500 ms. Analysis was implemented in Matlab (The Mathworks, Natick, USA) as previously described (Rossi et al). For each MEA culture we extracted parameters describing both the spiking activity, such as the median number of active channels firing with a mean frequency > 0.03Hz (Eytan & Marom 2006) and the total number of spikes (Chiappalone et al 2006), and the burst activity. Bursts were included in our study if they displayed a minimum number of spike equal to 10/burst and the maximum Inter Spike Interval (ISI) of 100 ms (Martinoia et al 2005). The median number of

bursts, the Intra Burst Frequency, the spike number in burst and the percentage of spikes in burst were evaluated.

For short term recordings we kept neurons in standard medium until day 12, then the medium was replaced with Krebs–Ringer-Hepes buffer (KRH, 130 mM NaCl, 5mM KCl, 1.2 mM KH₂PO₄, 1.2 mM MgSO₄, 2mM CaCl₂, 25 mM Hepes, 0.6% glucose, 1% glutamine). Appropriate adjustment of the pH of the KRH was done by using HCl. Cultures were left to equilibrate in KRH pH 7.4 for 15 minutes, then recorded for 10 minutes. Acidification was established by replacing the bath with KRH at pH 6.6 and neurons were continuously recorded for 40'. During acidic treatment, neurons also received DA (3-10 μ M, SIGMA) or PcTx-1 (50nM, Peptide International). We next changed the bath (KRH pH 7.4) and neurons were further recorded for 60 minutes (recovery phase). For long term recordings of MEAs, we incubated neurons (12 div) in Hibernate A (GIBCO) supplemented with 10 mM HEPES (SIGMA); 0.6% glucose (SIGMA); 1% Glutamine(GIBCO); 30 nM Na-Selenite(SIGMA); 20 nM Progesterone(SIGMA); 60 nM Putrescine (SIGMA); 100 μ g/ml Apo-Transferrin (SIGMA), 0.025 mg/ml of Insulin (TEBU-BIO) at pH 7.4 the day of the recording. Neurons were recorded for 10' to establish the baseline activity, then they received Hibernate medium at pH 6.6. Recording were done after 12 hours of incubation. During acidosis, neurons also received Diminazene (3 μ M). After 12 hours of treatment, we replaced the acid bath with fresh Hibernate A medium (pH 7.4) and neurons were further recorded after 1 hour and 12 hours from medium exchange.

Motor evoked potentials (MEP) analysis

MEP were already recorded in EAE mouse as described elsewhere (Amadio et al 2007). Briefly, MEP are muscle potentials evoked in hind limb footpad muscles by transcranial electrical stimulation of anesthetized mouse subcortical white matter, which generates volleys descending along fast-conducting cortico-spinal pathways and peripheral nerves through the trans-synaptic depolarization of spinal α -motor neurons. Thus, the latency of cortical MEP measures the cortico-muscular time of propagation: we can also measure the central conduction time (CCT) by subtracting the latency of the spinal MEP, obtained by lumbar roots stimulation. CCT proved to be a reliable functional marker of descending cortical projections to lumbar spinal enlargement α -motoneurons (Amadio et al, 2007).

Neuropathological analysis of EAE mice

Luxol Fast Blue staining was used to reveal demyelinated areas, and Bielshowsky staining was used to detect axonal loss accordingly to a previously published method (Furlan et al 2001). Immunohistochemistry was done on sagittal brain cryosections (12 μ m) that were rinsed in PBS 1X 3x5' and then incubated in 3% H₂O₂ for 20'. Then sections were incubated in blocking buffer (PBS 1x, FBS 10%, BSA 1 mg/ml and Triton X-100 0.1%) for 1 hour at room temperature. Primary antibodies were diluted in blocking mix accordingly manufacturer' instructions and incubated at 4°C overnight. The following day, sections were rinsed in PBS 3x 5', and the secondary antibody (biotin-conjugated, Vector labs, Milan, Italy) was applied for 2 h. Then sections were washed 3x5' in PBS 1x before

adding the avidin-HRP reagent (Vector). Signals were revealed by incubating slices with 3-amino-9-ethylcarbazole (AEC, Sigma) solution. The following antibodies were used: rat- α -MBP (1:200 millipore), rat- α -CD45 (1:100 BD, Pharmingen) .

Behavioural test-Open field test

EAE mice receiving Saline, Pctx-1, DA, as well as age and sex matched healthy controls were maintained on a reversed 12 h light/darkness cycle at 22-25°C (lights ON: 7:30 am to 7:30 pm). Food and water were available *ab libitum*. Behavioural experiments were done according to the animal protocols approved by the Institutional Animal Care and Use Committee San Raffaele (IACUC) (San Raffaele, Milan, Italy) and were approved by the National Ministry of Health, IACUC ID 470. Frames of non-reflective black Perspex walls (37 cm high) were used to partition a round open field arena (diameter of 150 cm and 35-cm high walls) into four squares 50 × 50-cm arenas, allowing for concurrent tracking of four animals at one time. Illumination in the room was provided by indirect diffuse light (4 x 40-W bulbs, 12 lx). Each animal was tracked for 30 minutes. We defined three zones in each test arena that allow quantifying exploration activity or fear-related behaviour: *exploration*, *home* and *intermediate* zone (Madani et al 2003). The exploration zone corresponds to the more aversive area of the arena, like the centre zone. The home zone is the preferred part of the arena, corresponding to the wall zone. The remaining areas are defined as intermediate zone. With the aid of the program WINTRACK (<http://www.dpwolfer.ch>), digitally stored XY coordinates of the

animal tracking (4.2/sec) were used to extract a set of parameters assessing exploration activity such as the total path length and velocity in different zones of the arena. During all the tests, animals were video-tracked using the EthoVision 2.3 system (Noldus Information Technology, Wageningen, the Netherlands, <http://www.noldus.com>) using an image frequency of 4.2/s. Raw data were transferred to Wintrack 2.4 (<http://www.dpwolfer.ch/wintrack>) for off-line analysis. Statistical computations were done using Statview 5.0 (SAS Institute, Cary, NC, USA).

Real time PCR

Total RNA was extracted from tissues and cell cultures, by using RNeasy Mini Kit (Qiagen) according to manufacturer's recommendations, including DNase digestion. cDNA synthesis was performed by using ThermoScript™ RT-PCR System (Invitrogen) and Random Hexamer (Invitrogen) according the manufacturer's instructions. Gene expression analysis was performed by using the LightCycler R 480 System (Roche) and SYBR Green JumpStart™ Taq ReadyMix™ for High Throughput QPCR (Sigma). Total RNA from mononuclear infiltrating cells was obtained from cells purification of EAE 17 d.p.i. brains and the SCs by using Neural tissue Dissociation kit (Miltenyi Biotec). Briefly, upon tissue dissociation, cells were centrifuged at 300g and then resuspended in 37% Percoll in HBSS for stratification. Upon centrifugation of the gradient the interphase containing mononuclear cells was collected and used for RNA extraction.

Real time PCR was performed by using following primers:

H3 F: GGTGAAGAAACCTCATCGTTACAGGCCTGGTAC

H3 R: CTGCAAAGCACCAATAGCTGCACTCTGGAAGC

ASIC1 F: ATGCGTGAGTTCTACGACAGAGC

ASIC1 R: CACAGGCAAGTATTCATCTTGCTG

ASIC2 F: ACACCCTGCAACCTGACCCGC

ASIC2 R: AGCAACTTCATACGCCTTCTTCTG

ASIC3 F: CTCCAGCCCTCCTTATAGCTTA

ASIC3 R: ACAAGTGTCTTTCGCAGCATA

Lentiviral production

Vesicular stomatitis virus-pseudotyped lentivirus (LV) encoding PSD-95-GFP and hSyn1-Cherry (provided by Dr. C. Sala, CNR Institute of Neuroscience, Milan and Dr. F. Valtorta, San Raffaele Hospital, Milan, Italy) were produced accordingly as previously described (Muzio et al 2009). Neurons (7 div) were infected at the M.O.I. of 25, then were left to develop in vitro for further 7 days before the imaging analysis.

Live imaging of the synaptic compartments

Primary neuronal cultures (9 div) were infected with lentiviral vectors carrying chimeric proteins that label pre (Syn1-Cherry protein) and post synaptic (Psd95-GFP protein) compartments. Neurons were imaged at 15 div by using an Olympus DeltaVision instrumentation with an objective zeiss 40 x 0.95 air with GFP and Cherry filters in a temperature (37°C) and pH controlled environment. Experiments were performed by incubating neurons in Hibernate A (GIBCO) supplemented with 10 mM HEPES (SIGMA); 0.6% glucose (SIGMA); 1% Glutamine(GIBCO); 30 nM Na-Selenite(SIGMA); 20 nM Progesterone(SIGMA); 60 nM Putrescine (SIGMA);100 µg/ml Apo-

Transferrin (SIGMA), 0.025 mg/ml of Insulin (TEBU-BIO) at pH 6.6 or 7.4. Neurons were imaged every hour for the 12 hours of acidic (pH 6.6) or physiological (pH 7.4) pH exposure. A z stack of images, with the precision of 500 nm for a full thickness of 8µm for both channels, were acquired in order to analyze the precise focus plane during the experiments. The same fields were followed during the experiment. Image processing were performed by using the Image-J software from the NIH institute. In brief: after imaging, the corresponding precise focal plane and the x,y eventual shift, that may occur during long lasting experiments, were corrected using cross-correlation algorithms. The background noise was removed and for the detection of the objects were used a granulometric filter , followed by an automatic particle counting. Pre and post synaptic compartments were counted in the same fields during the experiment.

Live imaging of cell death

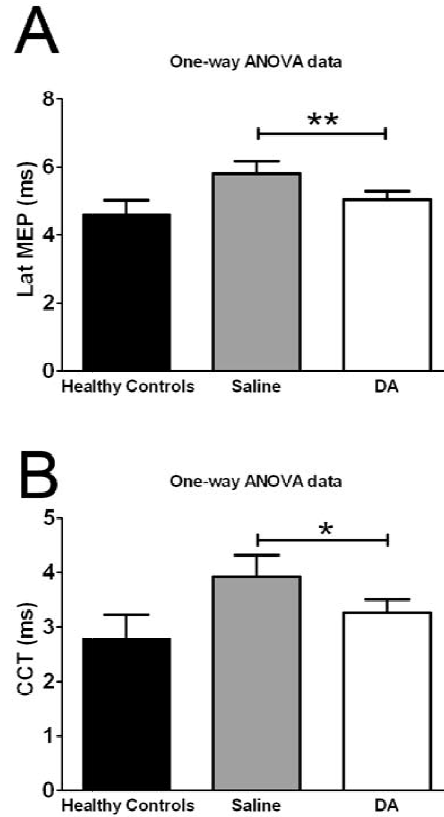
To test cell viability, cortical neurons were cultured for 13 DIV and then subjected to both pH 7.4 and 6.6 for 12 h followed by an additional 12 h of recovery. Neurons weretested for cell death at time 0, 12 h after acidic or physiological pH exposure and 12 h after the recovery at pH 7.4.. Experiments were conducted in Hibernate A (GIBCO) supplemented with 10 mM HEPES (SIGMA); 0.6% glucose (SIGMA); 1% Glutamine(GIBCO); 30 nM Na-Selenite(SIGMA); 20 nM Progesterone(SIGMA); 60 nM Putrescine (SIGMA);100 µg/ml Apo-Transferrin (SIGMA), 0.025 mg/ml of Insulin (TEBU-BIO) at pH 7.4. After treatment, neurons were stained with both Hoechst (Molecular Probes) and Sytox (Invitrogen) in Krebs–Ringer-Hepes buffer (KRH,

130 mM NaCl, 5mM KCl, 1.2 mM KH₂PO₄, 1.2 mM MgSO₄, 2mM CaCl₂, 25 mM Hepes, 0.6% glucose, 1% glutamine) at pH 7.4, staining all the nuclei present in the culture and the fraction of cell death, respectively. Automated imaging were performed with the InCell analyzer (GE) with a 40x air objective. More than 300 fields per conditions were included in the statistic.

Statistics

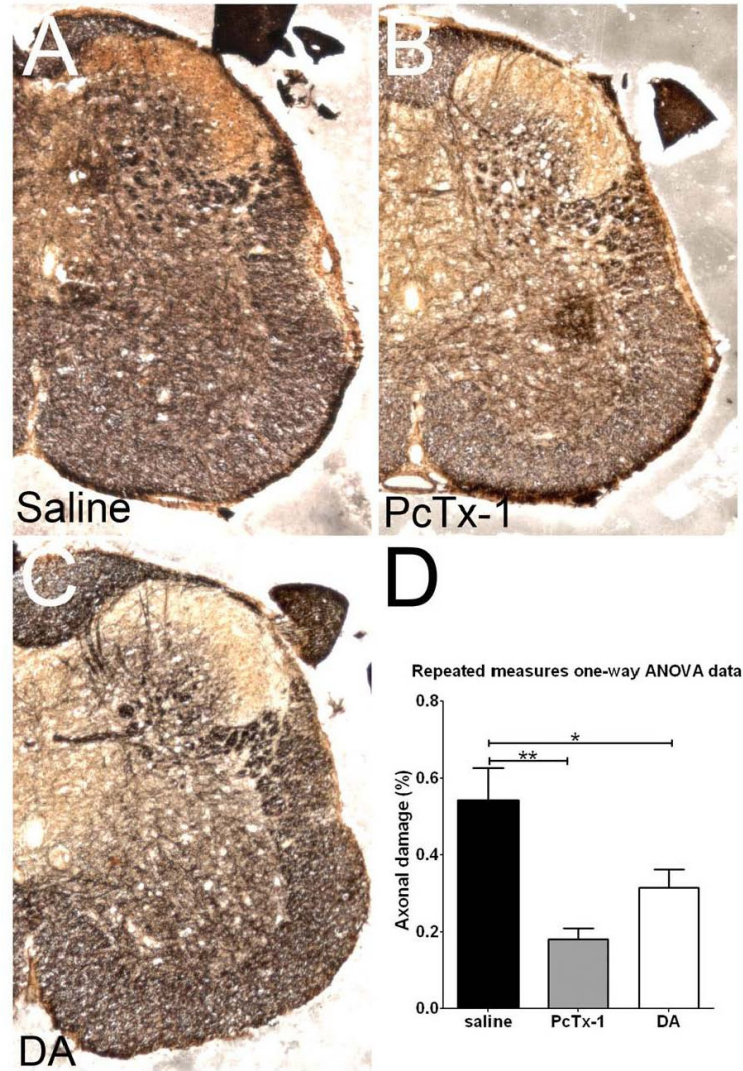
Data are expressed as the mean \pm standard error of the mean (S.E.M.) of independent experiments. Comparisons were made using the unpaired t-test, one-way analysis of variance (ANOVA), followed by Bonferroni post hoc test. Statistical tests were carried out using PRISM5.01 (GraphPad Software, La Jolla, CA). A p-value less than 0.05 was considered statistically significant.

Supplementary figures

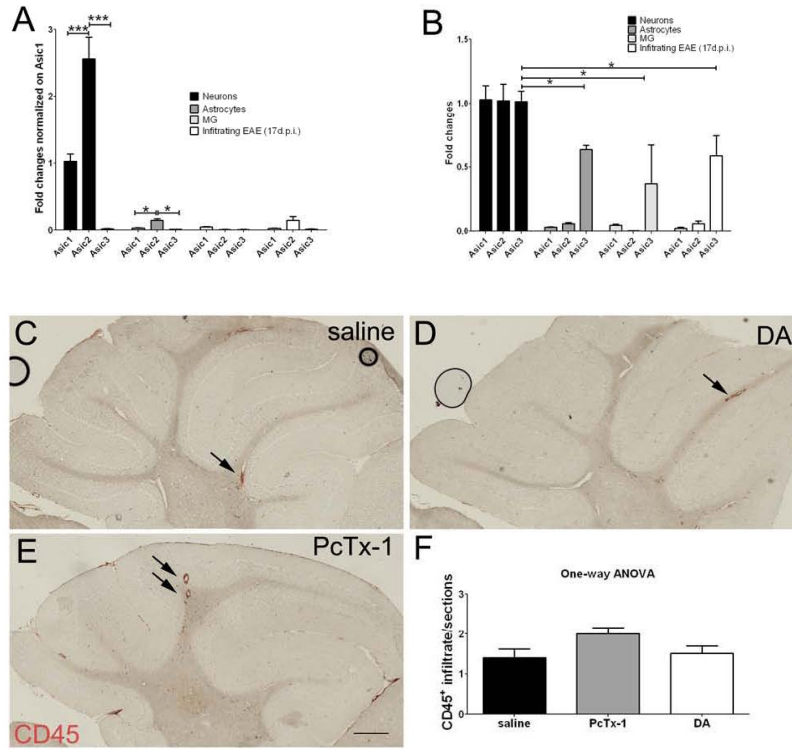


Supplementary Fig. 1. DA restored MEP latency and CCT in EAE mice

Panel A shows latency of MEP (mean \pm S.D.), measured in milliseconds (ms) in healthy naive mice (black bar), and EAE mice at 39 d.i.p. EAE mice received saline (grey bar) or DA (5 μ g/Kg) by single injection the day after the onset of clinical outcomes (n=4 for each group). Restored central conduction time (mean \pm S.D.), expressed as milliseconds (ms) is shown in panel B, confirming that MEP latency recovery is related to an improvement of cortico-spinal conduction. Black bar indicates healthy control, grey bar indicates EAE mice receiving saline, while white bar indicates EAE mice receiving DA. One way ANOVA tests with Bonferroni post test was used to assess statistical significance * p<0.05, ** p<0.01.

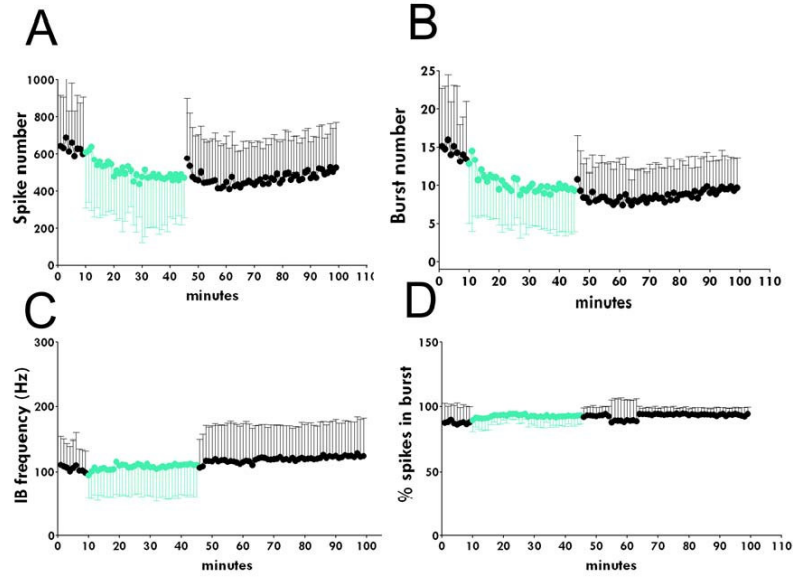


Supplementary Fig 2. DA treatment protects axonal loss in SC of EAE mice. Coronal section of SC from 40 d.p.i. EAE mice receiving saline (A), PcTx-1 (B) and DA (C) were labeled for Bielschowsky silver impregnation to detect axonal loss (n=3 for each group). Quantification is provided in panel D. Scale bar 100 μ m. One way ANOVA tests with Bonferroni post test was used to assess statistical significance * $p < 0.05$, ** $p < 0.01$.



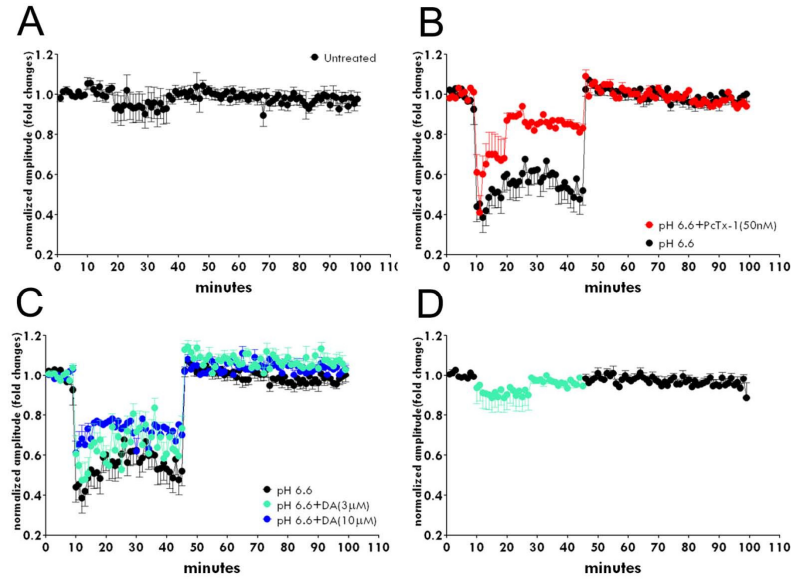
Supplementary Fig 3. Expression of *Asic* mRNAs in primary cell cultures and in EAE infiltrating mononuclear cells

Expression levels of *Asic1*, *Asic2* and *Asic3* mRNAs were measured on: primary neuronal cultures established from E17.5 cerebral cortex and kept in vitro for 12 days (black bar, n=6), astrocytes and MG cultures from the cerebral cortex of P2 brains (10 div, n=3) as well as in purified infiltrating mononuclear cells from brains and spinal cords of EAE 17d.p.i (n=4). Values (mean± S.E.M.) represent the relative amounts of amplified mRNA normalized against the housekeeping gene *HistH3* and expressed as percentages relative to neuronal *Asic1* expression levels are shown in A. Panel B is showing relative expression levels of *Asic1*, *Asic2* and *Asic3* on neurons, astrocytes, MG cells and infiltrating cells from EAE mice. Panels C, D and E show CB sagittal sections from EAE mice (40d.p.i.) labeled for CD45 (n=3 for each group). Quantifications of CD45⁺ foci in mice receiving saline (C), DA 5µg/Kg (D) and PcTx-1 (E) are provided in panel F (mean ± S.E.M.) One way ANOVA tests with Bonferroni post test was used to assess statistical significance *** p<0.001.



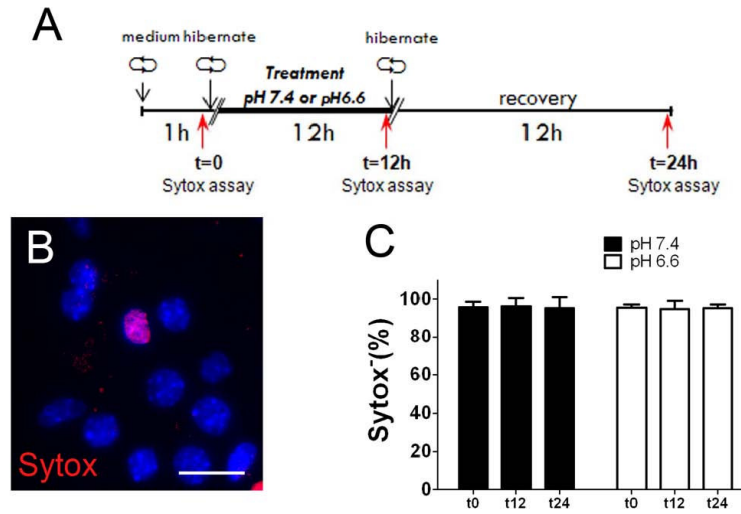
Supplementary Fig 4. Effects of DA on networks on neurons

Neurons (12/14 div) coupled with MEA were incubated with KRH (pH 7.4) for 15', then spontaneous electrophysiological activity was continuously recorded for 10' to establish the baseline. Neurons received the change of the bath (KRH, pH 7.4), supplemented with DA (3 μ M) and were further recorded for 40'. Finally, neurons received the KRH at pH 7.4 (recovery phase) and were recorded for 60'. The spike number is shown in A, burst number in panel B, Intra burst frequency in panel C and percentages of spikes in burst are indicated in panel D (n= 12 for each group). Error bars indicate S.E.M..



Supplementary Fig 5. Acidosis affects peak to peak amplitudes

Neurons (12/14 div) coupled with MEA were incubated with KRH (pH 7.4) for 15', then spontaneous electrophysiological activity was continuously recorded for 10' to establish the baseline. Neurons received the change of the bath (KRH, pH 6.6) and were further recorded for 40'. Finally, neurons received the KRH at pH 7.4 (recovery phase) and were recorded for 60'. Amplitudes (peak to peak) were measured in μV from untreated neurons (A, $n=12$), neurons receiving pH 6.6 ($n=8$, black dots in B and C), neurons receiving acidosis and PcTx-1 (50nM), ($n=3$, red dots in B) and in neurons receiving acidosis and DA (3 and 10 μM , blue dots in C) ($n=12$ and 3 for each group). Controls were done by incubating neurons with physiological pH and DA (3 μM , blue dots in D), ($n=8$).



Supplementary Fig 6. Analysis of cell death rates in neuronal cultures exposed to low pH

Sketch of the experimental paradigm is shown in panel A. Neurons were incubated in Hibernate at pH 7.4 or pH 6.6 for 12 hours followed by 12 hours of recovery. Neurons were stained with both Sytox and Hoechst in order to measure the fractional rate of cell death (B). The experiments were performed using the automatic microscope InCell analyzer, GE. Neurons have been plated and grown in 96 multiwells, 20 wells per condition were used with an average number of neurons of 42 ± 27 per sampled area, 15 areas per well. Results are summarized in C, showing that cell death is neither induced by 12h treatment in pH 6.6 neither during the following 12 hours of recovery.

Acknowledgement

The authors would like to thank Professor Sebastian Cerdan (Instituto de Investigaciones Biomédicas, Madrid) for his great advices for the use of IEPA probe. We acknowledge Roberto Furlan and P. Brown for the helpful discussion and suggestions This project was supported by a FISM grant.

References

- Aboul-Enein F, Rauschka H, Kornek B, Stadelmann C, Stefferl A, et al. 2003. Preferential loss of myelin-associated glycoprotein reflects hypoxia-like white matter damage in stroke and inflammatory brain diseases. *Journal of neuropathology and experimental neurology* 62: 25-33
- Amadio S, Pluchino S, Brini E, Morana P, Guerriero R, et al. 2006. Motor evoked potentials in a mouse model of chronic multiple sclerosis. *Muscle & nerve* 33: 265-73
- Arun T, Tomassini V, Sbardella E, de Ruiter MB, Matthews L, et al. Targeting ASIC1 in primary progressive multiple sclerosis: evidence of neuroprotection with amiloride. *Brain* 136: 106-15
- Atouguia J, Costa J. 1999. Therapy of human African trypanosomiasis: current situation. *Mem Inst Oswaldo Cruz* 94: 221-4
- Bacchi CJ. 2009. Chemotherapy of human african trypanosomiasis. *Interdiscip Perspect Infect Dis* 2009: 195040
- Bassilana F, Champigny G, Waldmann R, de Weille JR, Heurteaux C, Lazdunski M. 1997. The acid-sensitive ionic channel subunit ASIC and the mammalian degenerin MDEG form a heteromultimeric H⁺-gated Na⁺ channel with novel properties. *The Journal of biological chemistry* 272: 28819-22
- Benson CJ, Xie J, Wemmie JA, Price MP, Henss JM, et al. 2002. Heteromultimers of DEG/ENaC subunits form H⁺-gated channels in mouse sensory neurons. *Proceedings of the National Academy of Sciences of the United States of America* 99: 2338-43
- Beraud E, Viola A, Regaya I, Confort-Gouny S, Siau P, et al. 2006. Block of neural Kv1.1 potassium channels for neuroinflammatory disease therapy. *Ann Neurol* 60: 586-96
- Bianchi L, Driscoll M. 2002. Protons at the gate: DEG/ENaC ion channels help us feel and remember. *Neuron* 34: 337-40
- Biffi E, Menegon A, Piraino F, Pedrocchi A, Fiore GB, Rasponi M. Validation of long-term primary neuronal cultures and network activity

- through the integration of reversibly bonded microbioreactors and MEA substrates. *Biotechnol Bioeng* 109: 166-75
- Biffi E, Menegon A, Regalia G, Maida S, Ferrigno G, Pedrocchi A. A new cross-correlation algorithm for the analysis of "in vitro" neuronal network activity aimed at pharmacological studies. *Journal of neuroscience methods* 199: 321-7
- Black JA, Waxman SG, Smith KJ. 2006. Remyelination of dorsal column axons by endogenous Schwann cells restores the normal pattern of Nav1.6 and Kv1.2 at nodes of Ranvier. *Brain* 129: 1319-29
- Brown DA, Sawchenko PE. 2007. Time course and distribution of inflammatory and neurodegenerative events suggest structural bases for the pathogenesis of experimental autoimmune encephalomyelitis. *The Journal of comparative neurology* 502: 236-60
- Canessa CM, Horisberger JD, Rossier BC. 1993. Epithelial sodium channel related to proteins involved in neurodegeneration. *Nature* 361: 467-70
- Canessa CM, Schild L, Buell G, Thorens B, Gautschi I, et al. 1994. Amiloride-sensitive epithelial Na⁺ channel is made of three homologous subunits. *Nature* 367: 463-7
- Chen X, Qiu L, Li M, Durrnagel S, Orser BA, et al. Diarylamidines: high potency inhibitors of acid-sensing ion channels. *Neuropharmacology* 58: 1045-53
- Chiappalone M, Bove M, Vato A, Tedesco M, Martinoia S. 2006. Dissociated cortical networks show spontaneously correlated activity patterns during in vitro development. *Brain Res* 1093: 41-53
- Chiappalone M, Vato A, Berdondini L, Koudelka-Hep M, Martinoia S. 2007. Network dynamics and synchronous activity in cultured cortical neurons. *Int J Neural Syst* 17: 87-103
- Chiappalone M, Vato A, Tedesco MB, Marcoli M, Davide F, Martinoia S. 2003. Networks of neurons coupled to microelectrode arrays: a neuronal sensory system for pharmacological applications. *Biosensors & bioelectronics* 18: 627-34
- Deval E, Gasull X, Noel J, Salinas M, Baron A, et al. Acid-sensing ion channels (ASICs): pharmacology and implication in pain. *Pharmacology & therapeutics* 128: 549-58
- Dutta R, McDonough J, Yin X, Peterson J, Chang A, et al. 2006. Mitochondrial dysfunction as a cause of axonal degeneration in multiple sclerosis patients. *Ann Neurol* 59: 478-89
- Ehling P, Bittner S, Budde T, Wiendl H, Meuth SG. Ion channels in autoimmune neurodegeneration. *FEBS letters* 585: 3836-42

- Escoubas P, De Weille JR, Lecoq A, Diochot S, Waldmann R, et al. 2000. Isolation of a tarantula toxin specific for a class of proton-gated Na⁺ channels. *The Journal of biological chemistry* 275: 25116-21
- Eytan D, Marom S. 2006. Dynamics and effective topology underlying synchronization in networks of cortical neurons. *J Neurosci* 26: 8465-76
- Friesse MA, Craner MJ, Etzensperger R, Vergo S, Wemmie JA, et al. 2007. Acid-sensing ion channel-1 contributes to axonal degeneration in autoimmune inflammation of the central nervous system. *Nature medicine* 13: 1483-9
- Furlan R, Brambilla E, Ruffini F, Poliani PL, Bergami A, et al. 2001. Intrathecal delivery of IFN-gamma protects C57BL/6 mice from chronic-progressive experimental autoimmune encephalomyelitis by increasing apoptosis of central nervous system-infiltrating lymphocytes. *J Immunol* 167: 1821-9
- Garcia-Martin ML, Herigault G, Remy C, Farion R, Ballesteros P, et al. 2001. Mapping extracellular pH in rat brain gliomas in vivo by ¹H magnetic resonance spectroscopic imaging: comparison with maps of metabolites. *Cancer research* 61: 6524-31
- Hsu KS, Liang YC, Huang CC. 2000. Influence of an extracellular acidosis on excitatory synaptic transmission and long-term potentiation in the CA1 region of rat hippocampal slices. *Journal of neuroscience research* 62: 403-15
- Jasti J, Furukawa H, Gonzales EB, Gouaux E. 2007. Structure of acid-sensing ion channel 1 at 1.9 Å resolution and low pH. *Nature* 449: 316-23
- Kleyman TR, Cragoe EJ, Jr. 1988. Amiloride and its analogs as tools in the study of ion transport. *The Journal of membrane biology* 105: 1-21
- Kong X, Tang X, Du W, Tong J, Yan Y, et al. Extracellular acidosis modulates the endocytosis and maturation of macrophages. *Cellular immunology* 281: 44-50
- Kornek B, Storch MK, Weissert R, Wallstroem E, Stefferl A, et al. 2000. Multiple sclerosis and chronic autoimmune encephalomyelitis: a comparative quantitative study of axonal injury in active, inactive, and remyelinated lesions. *The American journal of pathology* 157: 267-76
- Kossel AH, Williams CV, Schweizer M, Kater SB. 1997. Afferent innervation influences the development of dendritic branches and spines via both activity-dependent and non-activity-dependent mechanisms. *J Neurosci* 17: 6314-24
- Li F, Liu X, Su Z, Sun R. Acidosis leads to brain dysfunctions through impairing cortical GABAergic neurons. *Biochemical and biophysical research communications* 410: 775-9

- Madani R, Kozlov S, Akhmedov A, Cinelli P, Kinter J, et al. 2003. Impaired explorative behavior and neophobia in genetically modified mice lacking or overexpressing the extracellular serine protease inhibitor neuroserpin. *Molecular and cellular neurosciences* 23: 473-94
- Mahad D, Ziabreva I, Lassmann H, Turnbull D. 2008. Mitochondrial defects in acute multiple sclerosis lesions. *Brain* 131: 1722-35
- Martinoia S, Bonzano L, Chiappalone M, Tedesco M, Marcoli M, Maura G. 2005. In vitro cortical neuronal networks as a new high-sensitive system for biosensing applications. *Biosensors & bioelectronics* 20: 2071-8
- Mazzuca M, Heurteaux C, Alloui A, Diochot S, Baron A, et al. 2007. A tarantula peptide against pain via ASIC1a channels and opioid mechanisms. *Nature neuroscience* 10: 943-5
- Morrissey SP, Stodal H, Zettl U, Simonis C, Jung S, et al. 1996. In vivo MRI and its histological correlates in acute adoptive transfer experimental allergic encephalomyelitis. Quantification of inflammation and oedema. *Brain* 119 (Pt 1): 239-48
- Muzio L, Cavasinni F, Marinaro C, Bergamaschi A, Bergami A, et al. 2009. Cxcl10 enhances blood cells migration in the sub-ventricular zone of mice affected by experimental autoimmune encephalomyelitis. *Molecular and cellular neurosciences*
- Odika IE, Asuzu IU, Anika SM. 1995. The effects of hyperosmolar agents lithium chloride and sucrose on the brain concentration of diminazene aceturate in rats. *Acta tropica* 60: 119-25
- Rocca MA, Absinta M, Valsasina P, Ciccarelli O, Marino S, et al. 2009. Abnormal connectivity of the sensorimotor network in patients with MS: a multicenter fMRI study. *Human brain mapping* 30: 2412-25
- Rossi S, Muzio L, De Chiara V, Grasselli G, Musella A, et al. Impaired striatal GABA transmission in experimental autoimmune encephalomyelitis. *Brain, behavior, and immunity*
- Schonfeld-Dado E, Segal M. 2009. Activity-dependent survival of neurons in culture: a model of slow neurodegeneration. *Journal of neural transmission* 116: 1363-9
- Stys PK, Hubatsch DA, Leppanen LL. 1998. Effects of K⁺ channel blockers on the anoxic response of CNS myelinated axons. *Neuroreport* 9: 447-53
- Stys PK, Lopachin RM. 1998. Mechanisms of calcium and sodium fluxes in anoxic myelinated central nervous system axons. *Neuroscience* 82: 21-32
- Tang CM, Dichter M, Morad M. 1990. Modulation of the N-methyl-D-aspartate channel by extracellular H⁺. *Proceedings of the National Academy of Sciences of the United States of America* 87: 6445-9

- Traynelis SF, Cull-Candy SG. 1990. Proton inhibition of N-methyl-D-aspartate receptors in cerebellar neurons. *Nature* 345: 347-50
- Vergo S, Craner MJ, Etzensperger R, Attfield K, Friesen MA, et al. Acid-sensing ion channel 1 is involved in both axonal injury and demyelination in multiple sclerosis and its animal model. *Brain* 134: 571-84
- Waldmann R, Bassilana F, de Weille J, Champigny G, Heurteaux C, Lazdunski M. 1997. Molecular cloning of a non-inactivating proton-gated Na⁺ channel specific for sensory neurons. *The Journal of biological chemistry* 272: 20975-8
- Wang YZ, Xu TL. Acidosis, acid-sensing ion channels, and neuronal cell death. *Molecular neurobiology* 44: 350-8
- Wemmie JA, Chen J, Askwith CC, Hruska-Hageman AM, Price MP, et al. 2002. The acid-activated ion channel ASIC contributes to synaptic plasticity, learning, and memory. *Neuron* 34: 463-77
- Xiong ZG, Pignataro G, Li M, Chang SY, Simon RP. 2008. Acid-sensing ion channels (ASICs) as pharmacological targets for neurodegenerative diseases. *Curr Opin Pharmacol* 8: 25-32
- Xiong ZG, Zhu XM, Chu XP, Minami M, Hey J, et al. 2004. Neuroprotection in ischemia: blocking calcium-permeable acid-sensing ion channels. *Cell* 118: 687-98
- Zha XM. Acid-sensing ion channels: trafficking and synaptic function. *Mol Brain* 6: 1
- Ziemann AE, Schnitzler MK, Albert GW, Severson MA, Howard MA, 3rd, et al. 2008. Seizure termination by acidosis depends on ASIC1a. *Nature neuroscience* 11: 816-22

CHAPTER 3

Impaired striatal GABA transmission in experimental autoimmune encephalomyelitis

Silvia Rossi^{a,b,1}, Luca Muzio^{c,1}, Valentina De Chiara^{a,b}, Giorgio Grasselli^{a,b}, Alessandra Musella^{a,b}, Gabriele Musumeci^{a,b}, Georgia Mandolesi^{a,b}, **Roberta De Ceglia^c**, Simona Maida^d, Emilia Biffi^e, Alessandra Pedrocchi^e, Andrea Menegon^d, Giorgio Bernardi^{a,b}, Roberto Furlan^c, Gianvito Martino^{c,†}, Diego Centonze^{a,b}

^a Clinica Neurologica, Dipartimento di Neuroscienze, Università Tor Vergata, Rome, Italy

^b Centro Europeo per la Ricerca sul Cervello (CERC)/Fondazione Santa Lucia, Rome, Italy

^c Neuroimmunology Unit-DIBIT2, INSPE, Department of Neuroscience, San Raffaele Scientific Institute, Milan, Italy

^d Alembic (Advanced Light and Electron Microscopy Bio-Imaging Centre) R&D Laboratory, San Raffaele Scientific Institute, Milan, Italy

^e Neuroengineering and Medical Robotics Laboratory, Bioengineering Department, Politecnico di Milano, Milan, Italy

[†] Corresponding author. Address: Gianvito Martino, Neuroimmunology Unit, Institute of Experimental Neurology (INSPE), San Raffaele Scientific Institute, Via Olgettina 58, 20132 Milan, Italy. Fax: +39 02 2643 4855.
E-mail address: martino.gianvito@hsr.it (G. Martino).

¹ S.R. and L.M. contributed equally to this work.

Keywords: EAE, Excitotoxicity, IPSC, Multiple sclerosis, Neurodegeneration, Parvalbumin, Striatum, MEA

Brain, Behavior, and Immunity Volume 25, Issue 5 (2011) 947 - 956

<http://dx.doi.org/10.1016/j.bbi.2010.10.004>

ABSTRACT

Synaptic dysfunction triggers neuronal damage in experimental autoimmune encephalomyelitis (EAE), a model of multiple sclerosis (MS). While excessive glutamate signaling has been reported in the striatum of EAE, it is still uncertain whether GABA synapses are altered. Electrophysiological recordings showed a reduction of spontaneous GABAergic synaptic currents (sIPSCs) recorded from striatal projection neurons of mice with MOG₍₃₅₋₅₅₎-induced EAE. GABAergic sIPSC deficits started in the acute phase of the disease (20–25 days post immunization, dpi), and were exacerbated at later time-points (35, 50, 70 and 90 dpi). Of note, in slices they were independent of microglial activation and of release of TNF α . Indeed, sIPSC inhibition likely involved synaptic inputs arising from GABAergic interneurons, because EAE preferentially reduced sIPSCs of high amplitude, and was associated with a selective loss of striatal parvalbumin (PV)-positive GABAergic interneurons, which contact striatal projection neurons in their somatic region, giving rise to more efficient synaptic inhibition. Furthermore, we found also that the chronic persistence of pro-inflammatory cytokines were able, per se, to produce profound alterations of electrophysiological network properties, that were reverted by GABA administration. The results of the present investigation indicate defective GABA transmission in MS models depending from alteration of PV cells number and, in part, deriving from the effects of a chronic inflammation, and suggest that

pharmacological agents potentiating GABA signaling might be considered to limit neuronal damage in MS patients.

1. Introduction

Synaptic alterations are receiving increasing attention as early correlates of primarily neurodegenerative diseases but also of neuroinflammatory disorders. Inflammatory cytokines (Stellwagen et al., 2005; Lai et al., 2006; Stellwagen and Malenka, 2006; Cumiskey et al., 2007; Mizuno et al., 2008; Centonze et al., 2009), resident immune cells such as microglia (Centonze et al., 2009), and brain infiltrating T lymphocytes (Lewitus et al., 2007; Centonze et al., 2009), have been found to alter glutamate transmission, providing support to the emerging concept that glutamate-dependent excitotoxic damage plays a fundamental role in neuronal degeneration accompanying inflammatory disorders, such as multiple sclerosis (MS) (Srinivasan et al., 2005; Cianfoni et al., 2007; Newcombe et al., 2008), and its mouse model, experimental autoimmune encephalomyelitis (EAE) (Wallström et al., 1996; Bolton and Paul, 1997; Pitt et al., 2000; Smith et al., 2000; Matute et al., 2001; Centonze et al., 2009).

GABA is the main inhibitory neurotransmitter in the central nervous system (CNS), whose activity balances that of glutamate in neurons. To date, glutamate transmission has been studied in neurophysiological investigations in EAE mice (Centonze et al., 2009), while the possible changes of GABA signaling in this model of MS have been inferred on the basis of biochemical (Gottesfeld et al.,

1976), molecular (Wang et al., 2008), and morphological studies (Ziehn et al., 2010), but never addressed through direct recordings of synaptic activity.

The striatum is a sub-cortical gray matter structure whose activity is finely regulated by both glutamate and GABA inputs (Fisone et al., 2007; Tepper et al., 2007). It is highly sensitive to the neurodegenerative process associated with MS (Henry et al., 2008; Tao et al., 2009; Ceccarelli et al., 2010), and undergoes complex alterations of glutamate transmission and dendritic damage during EAE (Centonze et al., 2009). Importantly, these synaptic alterations occur in the absence of overt demyelinating lesions, and even before the appearance of the EAE-associated neurological deficits, indicating that they are not a mere consequence of axonal damage (Centonze et al., 2009).

Not only glutamate, but also GABAergic synaptic activity can be studied in the striatum by means of whole-cell patch clamp recordings from single neurons in slices. Striatal principal neurons (also known as medium spiny projection neurons, MSNs), in fact, receive GABAergic inputs from axon collateral of MSNs themselves and from GABAergic interneurons (Koos and Tepper, 1999; Tunstall et al., 2002; Guzman et al., 2003; Plenz, 2003; Tepper et al., 2004; Koos et al., 2004; Gustafson et al., 2006), which play a crucial role in limiting the excitatory drive originating from cortico-striatal glutamatergic inputs. Accordingly, blockade of GABAergic inhibition significantly elevates basal activity of MSNs in vivo (Nisenbaum and

Berger, 1992), which is driven by glutamate released from corticostriatal terminals (Wilson and Kawaguchi, 1996; Stern et al., 1998).

Given the complexity of the adult tissue, some of the intrinsic electrical features of a network of neurons can be analyzed in vitro, by taking advantage of using Multi Electrode Arrays (MEA) device. Indeed, primary neuronal cultures retain many of the properties found in their in vivo context (Wagenaar et al., 2006) and have advantages in terms of electrical recording and long term pharmacological manipulation. Neuronal network models display a spontaneous electrical activity that is governed by the balance between excitation and inhibition (Mazzoni et al., 2007).

Local immune response, derived from infiltrating blood derived cells – i.e. T helper 1 (Th1) lymphocytes, is characterized by a broad spectrum of pro-inflammatory cytokines that, acting on oligodendrocytes, astrocytes, resident microglia and neurons, elicit CNS derangement. IFN- γ , TNF- α and IL1- β represent key molecules of adaptive immunity and are secreted by Th1 cells infiltrating CNS of both EAE and MS active lesions. In addition, these pro-inflammatory molecules can also alter neuronal functioning. Indeed, TNF- α enhances synaptic efficacy of cultured neurons (Beattie et al., 2002); IL1- β increases neuronal excitability (Zhang et al., 2008) and IFN- γ causes long term modifications of synaptic activity and neuronal damages (Vikman et al., 2001; Mizuno et al., 2008). Thus, aim of the present investigation is to study GABA transmission in EAE and in Th1 pro-inflammatory treated neuronal cultures, to assess whether such molecules can trigger alterations of synaptic inhibition occurring in

these models, and to explore further synaptic mechanisms possibly contributing to neuronal damage occurring during neuro-inflammation.

2. Materials and methods

All efforts were made to minimize animal suffering and to reduce the number of mice used, in accordance with the European Communities Council Directive of 24 November, 1986 (86/609/ EEC).

2.1. EAE induction and clinical evaluation.

According to previous reports (Centonze et al., 2009; Rossi et al., 2009), EAE was induced in 6–8 weeks old C57BL/6 mice by subcutaneous immunization with 300 μ l of 200 μ g MOG₍₃₅₋₅₅₎ (Multiple Peptide System) in incomplete Freund's adjuvant containing 8mg ml⁻¹ Mycobacterium tuberculosis (strain H37Ra; Difco). Pertussis toxin (Sigma) (500 ng) was injected on the day of the immunization and again two days later. Body weight and clinical score (0 = healthy; 1 = limp tail; 2 = ataxia and/or paresis of hindlimbs; 3 = paralysis of hindlimbs and/or paresis of forelimbs; 4 = tetraparalysis; 5 = moribund or death) were recorded daily.

2.2. Electrophysiology

Mice were killed by cervical dislocation under halothane anesthesia, and corticostriatal coronal slices (200–300 μ m) were prepared from fresh tissue blocks of the brain with the use of a vibratome. A single slice was then transferred to a recording chamber and submerged in a continuously flowing artificial cerebrospinal fluid (ACSF) (34 °C, 2–3

ml/min) gassed with 95% O₂–5% CO₂. The composition of the control solution was (in mM): 126 NaCl, 2.5 KCl, 1.2 MgCl₂, 1.2 NaH₂PO₄, 2.4 CaCl₂, 11 glucose, 25 NaHCO₃. Whole-cell patch clamp recordings were made with borosilicate glass pipettes (1.8 mm o.d.; 2–5 MX) at the holding potential (HP) of 80 mV. To study spontaneous (sIPSCs) and miniature GABA_A-mediated inhibitory postsynaptic currents (mIPSCs), the recording pipettes were advanced toward medium-sized (20–30 μ m) striatal neurons and filled with internal solution of the following composition (mM): CsCl (110), K⁺-gluconate (30), ethylene glycol-bis (β -aminoethyl ether)-N,N,N',N'-tetra-acetic acid (EGTA; 1.1), HEPES (10), CaCl₂ (0.1), Mg-ATP (4), Na-GTP (0.3). MK-801 and CNQX were added to the external solution to block, respectively, NMDA and non-NMDA glutamate receptors.

Only data from putative medium spiny projection neurons (MSNs) were included in the present study. These neuronal subtypes represent over 95% of the entire population of striatal neurons, and were identified for their morphological and electrophysiological properties. Fast-spiking GABAergic interneurons (putative parvalbumin (PV)-positive cells) and large aspiny interneurons (putative cholinergic interneurons) were recognized for their typical firing activity and somatic size (Kawaguchi et al., 1995; Koos and Tepper, 1999), and discarded.

Shortly after the beginning of the recordings, cesium-based patch pipettes significantly altered the action potential properties of the neurons (Centonze et al., 2007), thereby preventing the physiological identification of the different striatal neuron subtypes. In particular,

we were unable to distinguish GABA interneurons from MSNs, while putative cholinergic interneurons were easily recognized in striatal slices because of their large somata (35–55 μm diameter). The identification of the MSNs included in the present study was therefore achieved immediately after rupture of the GX seal by evaluating the firing response to the injecting of depolarizing current and/or pharmacologically at the end of the recording, based on the notion that the group I metabotropic glutamate receptor agonist 3,5-DHPG (30 μM) does not alter the membrane properties of these cells, while causing membrane excitation in GABAergic and cholinergic interneurons (Centonze et al., 2007). Off-line analysis was performed on spontaneous and miniature synaptic events recorded during fixed time epochs (1– 2 min), sampled every 2–3 min (5–12 samplings) (Centonze et al., 2009; Rossi et al., 2009).

One to six cells per animal were recorded. For each type of experiment and time point, at least six control mice and EAE mice were employed. Throughout the text “n” refers to the number of cells, unless otherwise specified.

Drugs were applied by dissolving them to the desired final concentration in the bathing ACSF. Drugs were (in μM): CNQX (10), MK-801 (30), tetrodotoxin (TTX, 1) (Tocris Cookson, Bristol, UK). Bicuculline (10) (Sigma-RBI, St. Louis, USA). Tumor necrosis factor- α (TNF- α , 0.6) (Peprotech, Rocky Hill, NJ).

2.3. Cell culture and MEAs recording

Primary neuronal cell cultures were obtained from CD1 mice. Mice were sacrificed by inhalation of CO₂, and E17.5 embryos were

removed immediately by cesarean section. Brains were carefully dissected in cold HBSS (Gibco) supplemented with glucose 0.6% and 5 mM HEPES pH 7.4 (Sigma). The cerebral cortices of embryos were rapidly removed, chopped with a fine scissor and subsequently mechanically dissociated in single cells by using fire-polished Pasteur pipettes. Then, cells were re-suspended in culture medium containing 50% D-MEM (Gibco); 50% Ham's F12 (Gibco); 5 mM HEPES pH 7.4; 0.6% glucose; 1% Glutamax (Invitrogen); 30 nM Na-Selenite (Sigma); 20 nM Progesterone (Sigma); 60 nM Putrescine (Sigma); 100 µg/ml Transferine (Sigma) and 5 µM Insulin (Sigma). No antimitotic and antibiotic drugs were added to cultures. Neurons were plated onto poly-lysine (2 mg/ml; Sigma) and laminin (10 µg/ml; Sigma) coated Multi Electrodes Arrays (MEA, 60 Ti/Au/TiN 30 Im electrode diameter and spaced 200 µm each other, Multi-channel System) at the final density of 2×10^5 cells per chip and incubated in a humidified 5% CO₂ atmosphere at 37 °C. Cells were also plated on dishes for immune-fluorescence and RT-PCR experiments at the concentration of 400 cells/mm². Extracellular 5 min recordings of the neuronal activity were made 12 days after plating by using a MEA1060 signal amplification and data acquisitions system (Multi-Channel Systems, MCS); signals were amplified 1100x. The signals collected from micro-electrodes were digitalized at 25 kHz and subsequently processed off-line. Spikes were detected using MC Rack Software (Multi-Channel System, GmbH): the threshold was set, for each channel, to seven times the standard deviation of average noise amplitude during 500 ms at the beginning of each measurement (dead time value: 3 ms).

After the initial recording, cells were treated with the following pro-inflammatory cytokines: 20 ng/ml IFN- γ (Peprotec) (Butovsky et al., 2006); 100 ng/ml IL1- β (Euroclone) (Zhang et al., 2008) and 5 nM TNF- α (Peprotec) (Beattie et al., 2002), then recorded after 12 and 24 h. Control MEAs received saline as sham treatment. Then, some cultures were also treated with increasing amount of GABA (0.01, 0.1, 0.3, 1, 3, 10 and 100 μ M; Sigma) and subsequently recorded.

The off-line analysis was implemented in Matlab (The Mathworks, Natick, USA). The median number of active channels (mean frequency >0.03 Hz (Eytan and Marom, 2006)) and the total number of spikes were extracted for each culture, as previously done in literature (Chiappalone et al., 2006). Successively, a burst analysis was developed as reported in (Chiappalone et al., 2005, 2006); bursts were detected when the minimum number of spike was equal to 10 and the maximum Inter Spike Interval (ISI) was 100 ms. The median number of burst, the burst duration and the percentage of active channels displaying bursting activity were evaluated. Finally, network bursts (i.e. recurrent events of strong neuronal interaction) were identified if the product of the number of active channels and the number of spikes, evaluated in 25 ms bins, was bigger than 9 (van Pelt et al., 2005; Chiappalone et al., 2005) using a minimum Inter Network Burst Interval (INBI) of 100 ms. The network activity was assessed by means of the network burst length.

2.4. RT-PCR

Neurons were treated with pro-inflammatory cytokines as above described and then collected as previously reported (Muzio et al.,

2010). Briefly, total RNA was extracted from neuronal cultures (n = 3 independent cultures for each group) by using RNeasy Mini Kit (Qiagen) according to manufacturer's recommendations including DNase digestion. cDNA synthesis were performed by using ThermoScript™, RT-PCR System (Invitrogen) and Random Hexamer (Invitrogen) according the manufacturer's instructions in final a volume of 20 μ l. The LightCycler R 480 System (Roche) and SYBR Green JumpStart™ Taq ReadyMix™ for High Throughput QPCR (Sigma) were used together with the following primers: Histone H3 Forward: GGTGAAGAAACCTCAT CGTTACAGGCCTGG TAC Histone H3 Reverse: CTGCAAAGCACCAATAGCTGCACTCTG GA AGC Pv Forward: ACGCTTCTGGCCGCTGGAGAC Pv Reverse: CCTC CCTACAGGTGG TGTCCG.

2.5. Preparation and activation of BV2 microglia cell line

The BV2 immortalized murine microglial cell line was provided by Dr. F. Aloisi (Department of Cell Biology and Neuroscience, Istituto Superiore di Sanità, Rome, Italy). BV2 cells were infected with a retrovirus codifying the GFP gene and treated for 24 h with Th1-specific pro-inflammatory cytokines 100 U/ml IL1- β (Euroclone, Pero, Italy), 200U/ml TNF- α (Peprotech, Rocky Hill, NJ), 500U/ml IFN- γ (Becton Dickinson) (Th1 mix) known to peak during the acute phase of EAE (Furlan et al., 1999). Then, 105–106 cells were placed onto a single slice (30–60 min), before the electrophysiological recordings. In a previous study, incubation of striatal slices with 105–106 cytokine-treated BV2 microglial cells resulted in a significant alteration of

glutamatergic transmission, which was prevented by TNF- α blockade (Centonze et al., 2009).

2.6. Western blot

Striata (n = 4 for each experimental group) were collected and frozen in liquid nitrogen and stored at 80 °C until use. Brain samples were homogenized using a micropestel and lysed on ice in NP-40 complete lysis buffer (10% glycerol, 50 mM HEPES/NaOH [pH 8.0], 100 mM KCl, 1% NP-40, 2 mM EDTA, 2 mM DTT, 10 mM NaF, 1 mM Na₃VO₄) supplemented with protease inhibitor cocktail (Sigma–Aldrich, USA, P8340). Cellular debris were removed by centrifugation at 16,000 rpm, for 200 at 4 °C. All biochemical analysis have been performed as follows. Samples protein content was quantified by mean of Bradford colorimetric reaction. The volumes equivalent to 50 μ g proteins were added with 1:3 volume of NuPAGE® loading buffer (Invitrogen, NP0007) added with β -mercaptoethanol 715 mM and kept for 4 min at 95 °C. The electrophoresis has been performed in BioRad cell on 12% SDS–PAGE with 4% SDS–PAGE stacking gel and controlled with 20 II PiNK® prestained protein ladder (GeneDireX, PM005-0500). All gels were then transferred on Immobilon™-P Polyvinilidene Difluoride 0.45 μ m membrane (Sig–ma–Aldrich, P2938-1ROL) in a semi-dry transfer cell (TransBlot SD, BioRad) by applying a 20 V potential for 15 min. Western blot with specific antibodies followed. Used primary antibodies were anti- β actin (1:10000, Sigma–Aldrich, A5441), anti-PV (Sigma–Aldrich, P3088, 1:2000), anti-VGAT (1:5000, Synaptic Systems, Germany, #131011), anti-GAD67 (1:2000, Sigma–Aldrich, G5419).

Membranes were blocked with 5% milk in PBS Tween20 1‰ for 1 h at RT, and incubated with specific antibodies in 5% milk in PBS Tween20 1‰ o/n at 4 °C (15 min at RT for anti- β actin Ab), washed 3 x10 min with PBS Tween20 1‰ at RT, incubated with Goat anti-Mouse HRP-conjugated IgG (Millipore, AP308P, 1:5000) in 5% milk in PBS Tween20 1‰ for 1 h at RT (15 min at RT after incubation with anti-actin Ab) and finally washed 4 x10 min with PBS Tween20 1‰ at RT. Detection was performed incubating the membrane for 5 min with 2 ml ECL Plus (Amersham, RPN2132) and registering luminescence with Storm840 (Amersham). The ImageJ software was used to compare the protein expression levels. To control for loading, density values were normalized to actin signal.

2.7. Immunohistochemistry and microscopy

Mice from two different immunization experiments were sacrificed at the peak of the acute phase (20 dpi). They were deeply anesthetized with avertine and perfused through the aorta with ice-cold 4% paraformaldehyde. Brains were post-fixed for at least 4h at 4 °C and equilibrated with 30% sucrose overnight. Thirty micrometer-thick sections were permeabilized in PBS with Triton-X 0.25% (TPBS). All following incubations were performed in TPBS. Sections were pre-incubated with 10% normal donkey serum solution for 1 h at room temperature and incubated with the primary antibody mouse anti-PV (1:300, Sigma–Aldrich, P3088) overnight at +4 °C. After being washed for three times, 10 min each, sections were incubated with the secondary antibody Alexa-488-conjugated donkey anti-mouse (1:200, Invitrogen, USA) for 2 h at RT and rinsed. Sections were mounted

with Vectashield (Vector Labs, USA) on poly-L-lysine-coated slides, air-dried and coverslipped.

Neuronal cultures were fixed in paraformaldehyde 4% for 50 , washed three times in PBS1x, then blocked in PBS1x, FBS10%, BSA 1 mg/ml for 1 h. Primary antibodies were applied in the same buffer o/n at 4 °C. The next day, slides were washed three times in PBS1x before applying Alexafluor conjugated secondary antibodies and nuclei were stained with Dapi. The following primary antibodies were used: mouse anti-TuJ1 (1:1000. Millipore); Rabbit anti-CaB (1:500, Swantt); rabbit anti-Iba-1 (1:400, Wako).

Images from immunolabeled samples were acquired with a Leica TCR SP5 confocal imaging system (Leica Microsystem, Germany). A 5x objective (pixel resolution 2048 x 2048, pinhole of 2 airy units) was used to acquire anti-PV immunostaining stacks of the whole striatum from coronal sections. Each image stack was z-projected and exported in TIFF file format and adjusted for brightness and contrast as needed by NIH ImageJ software (<http://rsb.info.nih.gov/ij/>). Median filters were used to reduce noise on stacks and z-projections. PV-positive neurons were counted manually on the z-projections and divided by the surface of the striatum section. Measurements were repeated for 7–9 images from 4 to 5 sections per animal (n = 4–5 mice per group).

2.8. Statistical analysis

Gender-and age-matched animals only treated with Freund's adjuvant (CFA) were used as control group for the electrophysiological, western blotting, and immunohistochemical

data. Electrophysiological data were presented as the mean \pm SEM. Statistical analysis was performed using a paired or unpaired Student's t-test or Wilcoxon's test for comparisons between two groups. Multiple comparisons were analyzed by one-way ANOVA for independent and/or repeated measures followed by Tukey HSD. To determine whether two cumulative distributions of spontaneous synaptic activity were significantly different, the Kolmogorov–Smirnov (K-S test) was used. The significance level was established at $p < 0.05$.

Electrophysiological data recorded by MEA biochips were presented as single and median values. Statistical analysis on these data was performed using non-parametrical tests because of their verified non-gaussian distribution. Specifically, a Wilcoxon matched pair test was developed for paired data analysis (inside groups) and a Mann–Whitney U test was performed between treated and untreated cultures at 24 h. The significance level was established at $p < 0.05$. For GABA concentration–response curves, a non-linear regression was used to fit data in a variable slope sigmoidal model. The goodness-of-fit was assessed using the Coefficient of Determination R^2 . Moreover, the lowest concentration EC_{50} and the maximal ones were analyzed with Mann–Whitney U test, between treated and sham cultures. The significance was established at $p < 0.05$.

For confocal image and western blot analyses the difference between the experimental groups was evaluated by Student's t-test (the significance level was established at $p < 0.05$).

3. Results

3.1. Neurophysiological properties of GABA transmission in EAE

Spontaneous inhibitory postsynaptic currents (sIPSCs) were measured as an indicator of the physiological activity of GABA signaling in the striatum. When recorded from putative MSNs, sIPSCs of control mice ranged between 5 and 60 pA of amplitude and between 0.5 and 3 Hz of frequency (Fig. 1A–C), and could be entirely blocked following the application of bicuculline, selective antagonist of GABA-A receptors ($n = 12$) (not shown).

In EAE, striatal sIPSC frequency and amplitude were indistinguishable from those of control mice before the appearance of the motor deficits (7 dpi; $n = 16$; $p > 0.05$ for both frequency and amplitude) (Fig. 1A, C and D). However, in the symptomatic phases of the disease, spontaneous GABAergic currents were reduced. In particular, during acute neuro-inflammation (20–25 dpi; $n = 18$ for both groups), only sIPSC frequency was lower ($p < 0.01$) (Fig. 1A, C and D), while both frequency and amplitude were markedly inhibited in the later (chronic) phases of the disease (35, 50, 70 and 90 dpi; $n =$ at least 10 for each time point and experimental group; $p < 0.01$ for both frequency and amplitude (Fig. 1A–E).

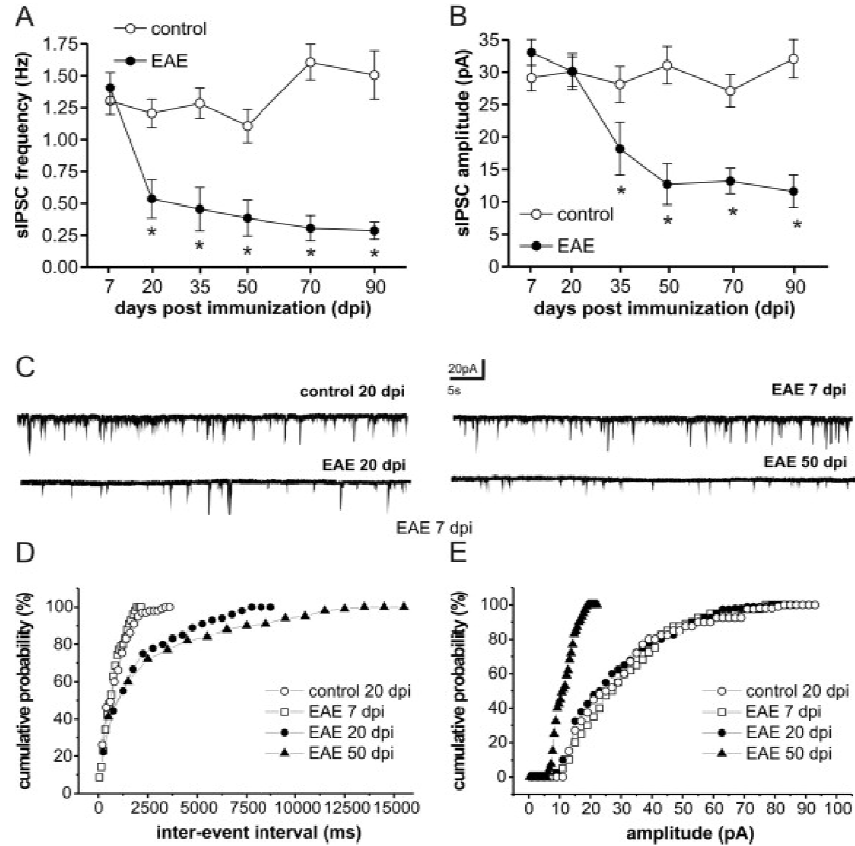


Fig 1. EAE alters GABAergic transmission in the striatum.

(A) The frequency of GABA-mediated sIPSCs recorded from striatal neurons was normal in the pre-symptomatic phase of EAE (7 dpi), but was down-regulated in the acute (20–25 dpi), and chronic stages of the disease (35, 50, 70, and 90 dpi). (B) sIPSC amplitude was unaffected in the pre-symptomatic and acute phases of EAE, while it was dramatically and irreversibly reduced in chronic EAE mice. (C) The electrophysiological traces are examples of sIPSCs (downward deflections) recorded from striatal neurons in control conditions and 7, 20, and 50 days p.i. with MOG. (D and E) Cumulative distributions of sIPSC inter-event interval (D) and amplitude (E) recorded in control condition and in the pre-symptomatic, acute and chronic stages of EAE. *Mean $p < 0.05$.

3.2. Th1 cytokines affect neuronal network functional properties

There is increasing evidence that a functional interaction exists between pro-inflammatory cytokines and the synaptic strength as demonstrated by many reports in which electrophysiological recording has been done on dissociated cultures treated with pro-inflammatory cues (Beattie et al., 2002; Stellwagen and Malenka, 2006; Zhang et al., 2008). We tested whether such signals can alter complex network functions including communication and integrative properties by investigating neuronal networks stably coupled to MEAs. Primary neuronal cultures were obtained from the dissociation of E17.5 cerebral cortices and kept in culture for 12 days. Then, we characterized these cultures for the presence of GABAergic neurons and glial cells by immunofluorescence. 13% (± 5.13) of plated cells expressed the GABAergic marker Calbindin (CaB) (Fig. 2A, $n = 3$). GFAP expression was observed on 7.04% (± 2.24) of total plated cells express, and very few cells, if any, expressed Iba-1, thus suggesting that microglial cells are barely detectable in our cultures (Fig. 2B and not shown). Electrophysiological spontaneous activity was measured on parallel cultures plated on MEA chips. Each culture was firstly recorded at day 12, then randomized MEAs were treated either with a cocktail of pro-inflammatory cytokines containing IL1- β , IFN- γ and TNF- α – i.e. Th1 treatment – or with the vehicle. Cytokines, mimicking typical inflammatory milieu of active neuro-inflammation, were used at concentrations that have been previously adopted for single cells electrophysiological recordings (Beattie et al., 2002; Stellwagen et al., 2006; Zhang et al., 2009).

MEAs were subsequently recorded 12 and 24 h after cytokines administration. Spikes recorded simultaneously from all electrodes were sorted and further analyzed accordingly to previously published algorithms (see Section 2). Possible stable alterations induced by inflammatory cues were investigated looking at the dynamic of these networks by studying correlative parameters among channels, spikes and bursting activity (see Section 2 for a detailed description of each parameter). Pro-inflammatory cytokines did not affect the median number of active electrodes in treated and control networks (Fig. 2D, $n = 14$), as well as the total number of spikes recorded in each group (Fig. 2E, $n = 14$). We next investigated the bursting activity of both treated and control networks. Bursts were detected in each recording and the percentage of active electrodes, displaying bursting activity, together with the median number of bursts recorded in each electrode were calculated in each group. However, these parameters were not altered in the presence of pro-inflammatory milieu (Fig. 2F and G, $n = 9$). We next measured the duration of burst for each electrode, but also in this case, we did not notice any differences between treated and control groups (Fig. 2H, $n = 9$). We next investigated more complex integrated properties of neuronal networks through the study of network burst activities variations (van Pelt et al., 2005; Chiappalone et al., 2005; Blankenship and Feller, 2010). Pro-inflammatory cytokines significantly increased the network burst length, that was approximately doubled in cultures treated for 24 h with Th1 cytokines (Fig. 2I, $n = 14$). In normal circumstances network bursts are sensitive to synaptic connectivity

and network bursts parameters have been analyzed in studies involving plasticity (Maeda et al., 1998). Since this parameter might be modulated by GABAergic signaling, we studied whether the alteration elicited by Th1 cues, depends on alteration of GABAergic signaling. Parallel networks were treated with the antagonist GABA-A receptor bicuculline. GABA receptor blockade alters the electrophysiological properties of untreated neuronal networks similarly to Th1 treatment (data not shown). Neuronal networks were also administered with increasing amount of GABA that induced significantly reduction of recorded spikes in untreated networks (Fig. 2J) and, above all, a dramatic reduction of network burst length in Th1 treated cultures (Fig. 2K). Altogether these results suggest that Th1 stimuli did not perturb single cell firing activity but alters network connectivity.

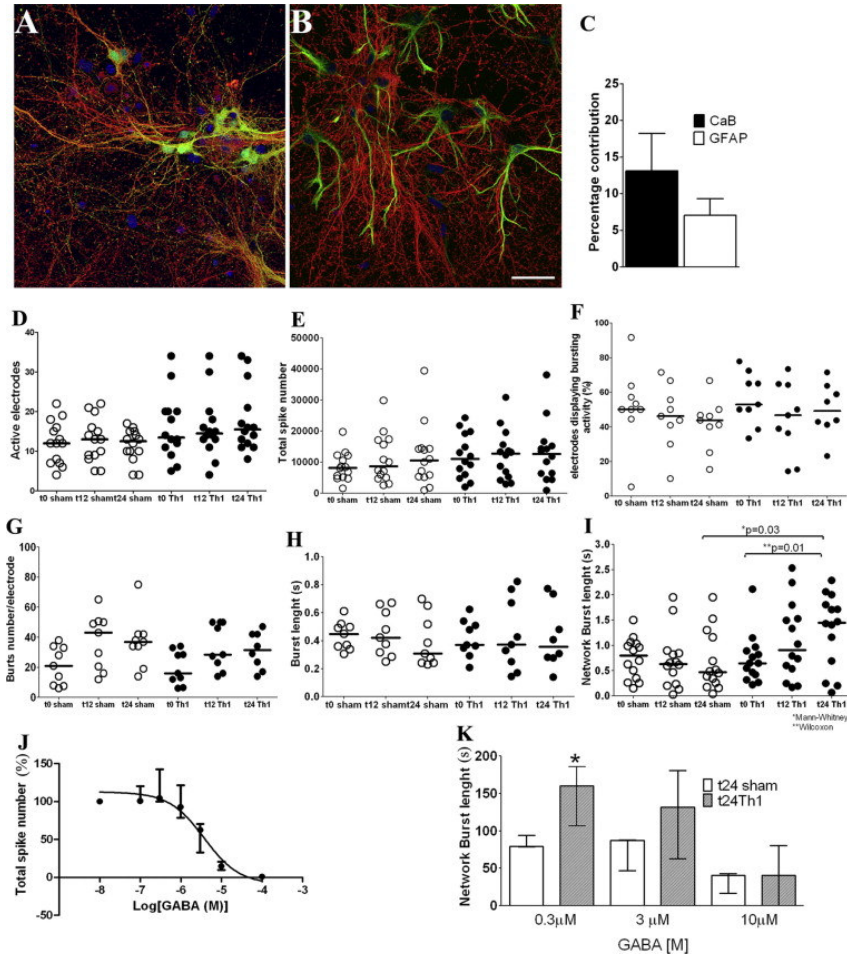


Fig 2. Pro-inflammatory cytokines affect the neuronal network homeostasis.

Primary neuronal cultures were assayed for Tuj1 (red) and CaB (green) by immune-fluorescence(A) after 12 days in vitro maturation. Panel (B) shows neurons assayed for Tuj1 (red) and GFAP (green). The percentages of CaB and GFAP expressing cells over the total cell number are plotted in histogram on panel (C). Electrophysiological activity was recorded on neurons plated on MEA chips after 12 days. Then cells were incubated with Th1 cytokines (solid circles) or saline (dashed circles), and subsequently recorded after 12 and 24 h (D–I). Active electrodes (D), total spike numbers (E), percentages of electrodes displaying burst activity (F), burst numbers per electrode (G) burst lengths (H) and network burst lengths (I) were calculated for each recording (5 min) and plotted on graphs as single dot.

3.3. Role of microglia and of TNF- α in EAE-induced inhibition of GABA transmission

We showed that resident microglia and the release of the pro-inflammatory cytokine TNF- α can alter glutamate transmission (Centonze et al., 2009) and that in vitro chronic administration of Th1

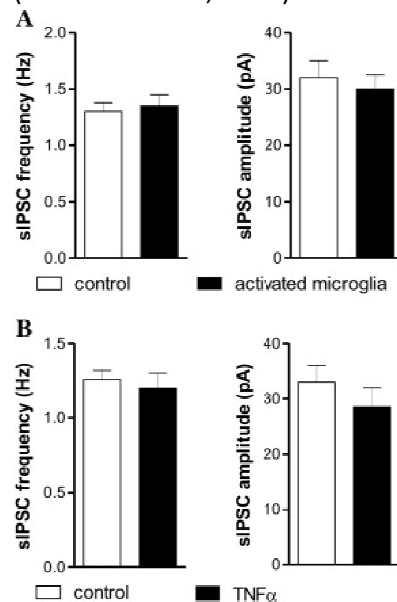


Fig 3. Activated BV2 microglia and TNF- α do not mimic EAE-induced inhibition of GABA transmission.

(A) The frequency and the amplitude of GABA-mediated sIPSCs were not altered by incubation of striatal slices with activated BV2 microglia. (B) The frequency and the amplitude of GABA-mediated sIPSCs were not altered by incubation of striatal slices with TNF- α .

cues to neuronal cultures can derange their homeostatic features. We wondered whether the abnormal GABA transmission, here reported, can be modulated also in vivo by similar mechanisms.

Acute incubation of striatal slices from control mice with activated BV2 microglia, however, failed to affect sIPSC frequency and

amplitude ($n = 12$; $p > 0.05$ for both parameters), indicating that microglia-released pro-inflammatory molecules cause an acute dysfunction of glutamate (Centonze et al., 2009) but are not sufficient to alter GABA transmission (Fig. 3A). In line with

this conclusion, acute incubation of striatal slices with TNF- α (3 h) also caused negligible effects on both frequency and amplitude of

sIPSCs ($n = 10$; $p > 0.05$ for both parameters) (Fig. 3B), although a previous study showed that this cytokine is able to downregulate GABA transmission in the hippocampus (Stellwagen et al., 2005).

3.4. Differential involvement of GABA inputs to MS cells in EAE principal

Axon collaterals from MSNs themselves and GABAergic interneurons represent the two main sources of GABA inputs to striatal principal neurons (Plenz, 2003; Tepper et al., 2004; Gustafson et al., 2006). The two inputs differentially influence the activity of MSNs, since inhibition from interneurons predominantly targets their somatic region (Bennett and Bolam, 1994; Kubota and Kawaguchi, 2000; Gustafson et al., 2006), while inputs from axon collaterals of neighbor MSNs preferentially target distant dendrites (Koos et al., 2004; Gustafson et al., 2006).

Based on the notion that somatic synaptic contacts give rise to sIPSCs of higher amplitude than contacts to distant dendrites (Koos et al., 2004), we tried to determine which inputs were preferentially impaired in EAE mice. Amplitude-frequency histograms of sIPSCs from control and EAE mice were significantly different, as sIPSC of higher amplitude were preferentially reduced in EAE (Fig. 4A and B). We also compared the effects of the voltage-dependent sodium channel blocker TTX on sIPSC recorded from control and EAE mice. When recorded in slices, in fact, MSNs are quiescent and do not generate action potential (AP). Striatal GABAergic interneurons,

conversely, have generally more depolarized resting membrane potential (RMP) and give rise more frequently to spontaneous APs (Kawaguchi et al., 1995; Koos and Tepper, 1999). Thus, AP-dependent GABAergic inputs to MSNs are likely to stem from interneurons, while AP-independent events might be of both interneuronal or MSN axon collateral origin. Blockade of AP with TTX, significantly reduced the frequency of sIPSC in both control and EAE mice ($n = 15$ from both groups, $p < 0.01$). The effect of TTX, however, was more pronounced in neurons from control mice, suggesting that a larger proportion of sIPSC recorded from EAE mice are AP-independent (Fig. 4C). Based on the notion that somatic synaptic contacts give rise to sIPSCs of higher amplitude than contacts to distant dendrites (Koos et al., 2004), we tried to determine which inputs were preferentially impaired in EAE mice. Amplitude-frequency histograms of sIPSCs from control and EAE mice were significantly different, as sIPSC of higher amplitude were preferentially reduced in EAE (Fig. 4A and B). We also compared the effects of the voltage-dependent sodium channel blocker TTX on sIPSC recorded from control and EAE mice. When recorded in slices, in fact, MSNs are quiescent and do not generate action potential (AP). Striatal GABAergic interneurons, conversely, have generally more depolarized resting membrane potential (RMP) and give rise more frequently to spontaneous APs (Kawaguchi et al., 1995; Koos and Tepper, 1999). Thus, AP-dependent GABAergic inputs to MSNs are likely to stem from interneurons, while AP-independent events might be of both interneuronal or MSN axon collateral origin. Blockade of AP with TTX, significantly reduced the

frequency of sIPSC in both control and EAE mice ($n = 15$ from both groups, $p < 0.01$). The effect of TTX, however, was more pronounced in neurons from control mice, suggesting that a larger proportion of sIPSC recorded from EAE mice are AP-independent (Fig. 4C).

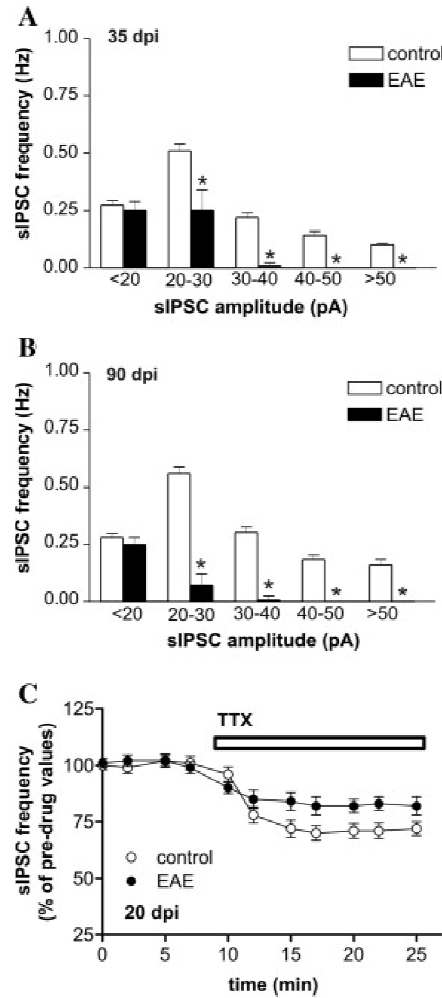


Fig 4. Interneuron GABAergic inputs were preferentially impaired in EAE mice.

(A and B) sIPSC amplitude-frequency histograms in control and EAE mice at 35 (A) and at 90 (B) dpi. (C) The graph shows that the effects of the voltage-dependent sodium channel blocker TTX on sIPSC frequency was more pronounced in neurons from control mice than in EAE mice. $*p < 0.05$.

3.5. Density of GABA synapses and PV-positive interneurons in the striatum of EAE mice

To assess if the observed inhibition of GABA transmission could result from lower number of GABAergic synapses in mice with EAE, we studied markers of GABA transmission by means of western blot experiments. No difference was detected in vesicular GABA transporter (V-GAT), a marker of GABAergic synapses (Tafoya et al., 2006; Centonze et al., 2008) and in glutamate acid decarboxylase 67 (GAD67) – the main enzyme in GABA biosynthesis – at 7 and 20 dpi (not shown). We next wanted to see whether the number of GABAergic neurons were reduced in EAE, to provide a plausible explanation of our neurophysiological findings. MSNs represent over 95% of the entire population of striatal neurons (Kawaguchi et al., 1995; Wilson and Kawaguchi, 1996; Tepper et al., 2004), and our previous study in EAE showed that the total number of striatal neurons was not reduced during the acute and chronic phases of the disease (Centonze et al., 2009). Here, we investigated striatal PV⁺ GABAergic interneurons (Kawaguchi et al., 1995). PV⁺ interneurons were significantly reduced in EAE mice (at 20 dpi) down to 74% of the controls (EAE = 24.6 neurons/mm²; control = 33.5 neurons/mm²; n = 4 and 5 mice, respectively; t = 5.76; p = 0.0007) (Fig. 5A and B). Moreover, we observed a predictable striatal atrophy (p < 0.05), consisting in a reduction of 8% of the striatal surface on coronal sections in EAE mice compared to controls (EAE = 3.8 mm²; control = 3.5 mm²; n = 4 and 5 mice, respectively; t = 2.94; p = 0.021) (not shown).

To confirm the immunohistochemical data, we analyzed by western blot the PV expression levels in the striatum of both pre-symptomatic and acute EAE mice. Consistently, PV signal did not vary significantly at 7 dpi between control and EAE mice ($p = 0.504$), while it was significantly reduced at 20 dpi ($p < 0.05$) (Fig. 5C and D). We next investigated the expression of PV in neuronal cultures by RT-PCR assay. Total mRNA extracts were obtained from cultures treated with Th1 cytokines for 12 and 24 h ($n = 3$ for each group) and parallel cultures treated with vehicle. PV expression was measured by RT-PCR and each RNA extract was normalized by assaying the expression of the housekeeping gene Histone H3 (Supplementary Fig. 1). Accordingly with data obtained in vitro, pro-inflammatory cytokines treatment significantly reduced the expression levels of PV (Supplementary Fig. 1).

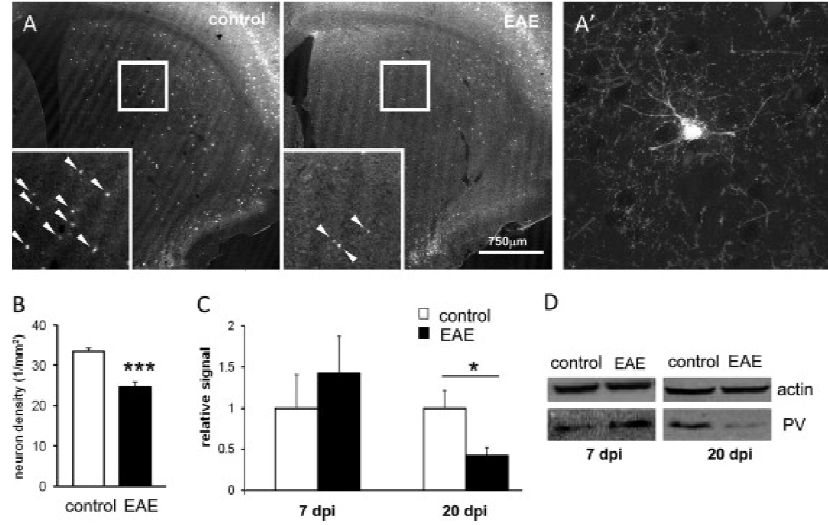


Fig 5. Reduction of PV-positive GABAergic interneurons in the striatum of EAE mice.

PV was labeled on striatum sections from immunized and control animals (A). An exemplificative picture of a stained neuron is shown at high magnification in A' (objective 63_x, zoom 2_x). The number of positive neurons (A, insert, arrowheads), counted on confocal microscopy images and expressed as density (1/mm²) was significantly reduced in EAE mice compared to control in the acute phase of EAE (20 dpi) (B; mean ± SEM; n = 4 and 5 mice, respectively; ***p < 0.001). (C and D) A significant reduction was observed also by western blot analysis for PV signal in the striatum of EAE mice compared to control in the acute (20 dpi, *p < 0.05; mean ± SEM; n = 4) but not in pre-symptomatic phase (7 dpi, p = 0.504, mean ± SEM; n = 4).

4. Discussion

Previous studies have postulated impaired GABA transmission in MS and in EAE. GABA is reduced in the cerebrospinal fluid of MS subjects (Qureshi and Baig, 1988), and [3H] GABA uptake (Gottesfeld et al., 1976), and protein and mRNA expression of the GABA transporter-1 (GAT-1) are dramatically reduced in the spinal cord of EAE mice (Wang et al., 2008). Furthermore, potentiation of GABA signaling significantly ameliorates EAE clinical course, through a mechanism likely involving a direct neuroprotective effect and an inhibitory action on antigen-presenting cells and the resulting inflammatory response (Bhat et al., 2010). The present study is the first combined neurophysiological and morphological investigation of inhibitory transmission in the brains of EAE mice and in network of neurons. Our data demonstrate irreversible alterations of GABA transmission in the striatum of EAE mice, providing further evidence that gray matter structures of the nervous system undergo profound rearrangements of synaptic transmission during immune-mediated attack of the central myelin. Exacerbated glutamate-mediated transmission, in fact, has been previously reported in EAE striata, in the absence of overt demyelinating foci, but in association with microglial activation and TNF- α release (Centonze et al., 2009; Rossi et al., 2009). However, the mechanisms at the basis of enhanced glutamate and reduced GABA transmission do not seem to overlap and the kinetic of glutamate transmission up-regulation and GABA down-regulation were, however, different during EAE. In fact,

glutamate transmission hyperfunctioning was evident in the pre-symptomatic and acute phases (when the activation of resident microglia was maximal), while GABAergic hypofunctioning was present in the acute and especially marked in the chronic phases of the disease (when microglial cells return to the resting state) (Centonze et al., 2009). We also showed that a cocktail of pro-inflammatory cytokines can perturb the GABAergic system in vitro, when chronically administered for 24 h. In line with this evidence, we failed to replicate the neurophysiological abnormalities of GABAergic sIPSCs following short incubation of striatal slices with either activated BV2 microglia or TNF- α . Altogether, these data suggest that chronic stimulation of neuronal networks, that is possible only in vitro by using neuronal cultures, determines profound alteration of GABA transmission, needing more time to take place and lasting longer. Based on these considerations, it is therefore conceivable that microglia and pro-inflammatory molecules released by microglia contribute to alter GABAergic transmission in the intact brain during EAE. Our results are in agreement with other reports showing that prolonged treatments with a prototypic pro-inflammatory cytokine – i.e. TNF- α -induced severe derangement of neuronal morphology, altering the dendritic branching (Neumann et al., 2003) and perturbing spatial learning (Aloe et al., 1999; Golan et al., 2004). These data might suggest different neuroprotective strategies in the early and late stages of MS, since the unbalance towards neuronal excitation, which characterizes the entire course of EAE since its pre-symptomatic phase, likely primes excitotoxic damage by increasing

neuronal vulnerability to MS-specific mitochondrial dysfunction (Vyshkina et al., 2005), or to the neurotoxic effects of inflammation (Xiong and McNamara, 2002; Zhu et al., 2003).

Striatal GABAergic MSNs form functional synapses through their recurrent axon collaterals, establishing a feedback control over striatal neuron activity (Tunstall et al., 2002; Guzman et al., 2003; Koos et al., 2004; Gustafson et al., 2006). Inputs from GABAergic interneurons are another important source of synaptic inhibition of MSNs, giving rise to a feed-forward inhibitory pathway that is independent of striatal output (Koos and Tepper, 1999; Plenz, 2003; Tepper et al., 2004; Gustafson et al., 2006). Our data seem to indicate that the feedback and feed-forward GABAergic control over striatal output is differentially affected in EAE, because sIPSCs of larger amplitude and sensitive to TTX were predominantly reduced in these mice, as expected for a preferential involvement of inhibitory interneuronal activity (Bennett and Bolam, 1994; Kubota and Kawaguchi, 2000; Koos et al., 2004; Gustafson et al., 2006). In line with this hypothesis, the total number of striatal neurons, largely composed of projection MSNs (Kawaguchi et al., 1995; Wilson and Kawaguchi, 1996; Tepper et al., 2004), is not reduced in EAE (Centonze et al., 2009), while we found that GABAergic interneurons are markedly underrepresented in the striatum. It is noticeable, however, that although distinct physiological properties of evoked IPSCs originating from axon collaterals of projection neurons and from GABAergic interneurons have been described by using paired recordings (Koos et al., 2004), our recordings of sIPSCs do not allow

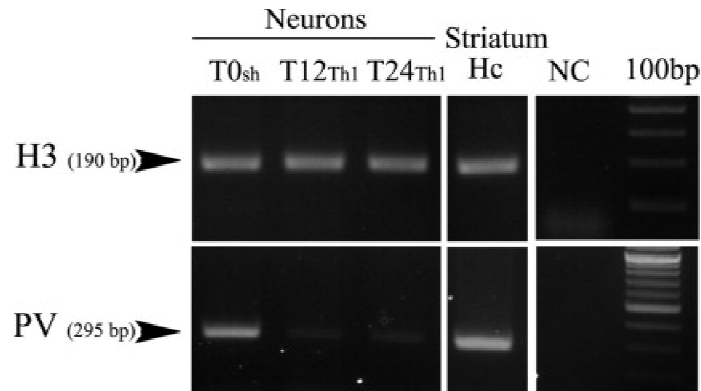
to conclusively discriminate between the two input sources, and thus GABAergic dysfunction might also involve inputs from axon collaterals of MSNs, and might be more generalized than postulated in the present study.

A significant reduction in the number of PV-positive striatal cells accompanied impaired GABA signaling seen in electrophysiological, morphological and western blot experiments. Furthermore, PV expression was also severely reduced in neuronal cultures treated with of pro-inflammatory cytokines. These data point to GABAergic interneurons as the primary cell-type population compromised by EAE, and are in good agreement with previous findings showing selective loss of PV interneurons, and reduced extension of PV-positive neurites in the normal appearing gray matter and in the motor cortex of MS patients (Dutta et al., 2006; Clements et al., 2008). Defective GABAergic transmission within the motor cortex has also been postulated in MS patients on the basis of neurophysiological findings with paired-pulse transcranial magnetic stimulation (Caramia et al., 2004). Furthermore, loss of PV-positive interneurons was also observed in the hippocampus of EAE mice, in association with significant defects of hippocampus-related memory abilities (Ziehn et al., 2010). Interestingly, the widely accepted excitotoxic hypothesis of neuronal damage in MS (Srinivasan et al., 2005; Cianfoni et al., 2007; Newcombe et al., 2008) and in EAE (Wallström et al., 1996; Bolton and Paul, 1997; Pitt et al., 2000; Smith et al., 2000; Matute et al., 2001; Centonze et al., 2009) is hardly compatible with the high vulnerability displayed by PV interneurons

in these inflammatory neurodegenerative disorders, because PV and other calcium-buffering proteins have a protective role against a deleterious increase of intraneuronal calcium (Friedman and Segal, 2010). Thus, the reasons of the selective susceptibility of PV interneurons to degenerate in MS and in EAE has to be further investigated. The evidence, however, that cytokines signaling, per se, is able to alter GABAergic transmission and consequently circuit functioning, as demonstrated by “in vitro” experiments, gives additional interest to the possibility that this mechanism is at the base of late stages of MS pathogenesis. The general GABAergic down-regulation induced by cytokines chronic treatment that emerges from this study, is of impulse for the search of drugs able to control this alteration. The “in vitro” model of cortical neurons treatment with cytokines and the paradigm for GABAergic alteration study could turn to be helpful for future drug screening studies.

In conclusion, the results of the present investigation indicate defective GABA transmission in a reliable mouse model of MS and in neuronal networks in vitro, and suggest that pharmacological agents potentiating GABA signaling might be considered an alternative valuable therapeutic option to limit neuronal damage in MS patients.

Appendix A. Supplementary data



Supplementary Fig 1. PV expression levels are down-regulated in neuronal cultures treated with Th1 cytokines.

Total mRNA extracts were obtained from neuronal cultures and used to study the expression of PV by RT-PCR. The first row shows the expression of the housekeeping gene Histone H3. The second row shows the expression of PV. Measures were done in untreated (1st lane); Th1 treated (12 h of treatments are in 2nd lane; 24 h of treatments are in the 3rd lane); healthy striatal microdissections were used as positive control ($n = 3$, 4th lane) and negative controls are in 5th lanes. While H3 expression was similar in treated and sham treated cultures, PV expression levels were significantly down-regulated in neurons receiving pro-inflammatory cytokines.

Acknowledgments

We thank Vladimiro Batocchi for helpful technical assistance. This investigation was supported by the Italian National Ministero dell'Università e della Ricerca to D.C.; by the Italian National Ministero della Salute to D.C., by Fondazione Italiana Sclerosi Multipla (FISM) to R.F., G.M. and L.M. (L.M. was supported by FISM grant number 2009/R/18), and by BMW-Italy to G.M.

References

- Aloe, L., Properzi, F., Probert, L., Akassoglou, K., Kassiotis, G., Micera, A., Fiore, L., 1999. Learning abilities, NGF and BDNF brain levels in two lines of TNF α transgenic mice, one characterized by neurological disorders, the other phenotypically normal. *Brain Res.* 840, 125–137.
- Bennett, B.D., Bolam, J.P., 1994. Synaptic input and output of parvalbuminimmunoreactive neurons in the neostriatum of the rat. *Neuroscience* 62, 707–719.
- Beattie, E.C., Stellwagen, D., Morishita, W., Bresnahan, J.C., Ha, B.K., Von Zastrow, M., Beattie, M.S., Malenka, R.C., 2002. Control of synaptic strength by glial TNF α . *Science* 295, 2282–2285.
- Bhat, R., Axtell, R., Mitra, A., Miranda, M., Lock, C., Tsien, R.W., Steinman, L., 2010. Inhibitory role for GABA in autoimmune inflammation. *Proc. Natl. Acad. Sci. USA* 107, 2580–2585.
- Blankenship, A., Feller, M., 2010. Mechanisms underlying spontaneous patterned activity in developing neural circuits. *Nat. Rev. Neurosci.* 11, 18–29.
- Bolton, C., Paul, C., 1997. MK-801 limits neurovascular dysfunction during experimental allergic encephalomyelitis. *J. Pharmacol. Exp. Ther.* 282, 397–402.
- Butovsky, O., Ziv, Y., Schwartz, A., Landa, G., Talpalar, A.E., Pluchino, S., Martino, G., Schwartz, M., 2006. Microglia activated by IL-4 or IFN- γ differentially induce neurogenesis and oligodendrogenesis from adult stem/progenitor cells. *Mol. Cell. Neurosci.* 31, 149–160.
- Caramia, M.D., Palmieri, M.G., Desiato, M.T., Boffa, L., Galizia, P., Rossini, P.M., Centonze, D., Bernardi, G., 2004. Brain excitability changes in the relapsing and remitting phases of multiple sclerosis: a study with transcranial magnetic stimulation. *Clin. Neurophysiol.* 115, 956–965.
- Ceccarelli, A., Rocca, M.A., Neema, M., Martinelli, V., Arora, A., Tauhid, S., Ghezzi, A., Comi, G., Bakshi, R., Filippi, M., 2010. Deep gray matter T2 hypointensity is

- present in patients with clinically isolated syndromes suggestive of multiple sclerosis. *Mult. Scler.* 16, 39–44.
- Centonze, D., Muzio, L., Rossi, S., Cavasinni, F., De Chiara, V., Bergami, A., Musella, A., D'Amelio, M., Cavallucci, V., Martorana, A., Bergamaschi, A., Cencioni, M.T., Diamantini, A., Butti, E., Comi, G., Bernardi, G., Cecconi, F., Battistini, L., Furlan, R., Martino, G., 2009. Inflammation triggers synaptic alteration and degeneration in experimental autoimmune encephalomyelitis. *J. Neurosci.* 29, 3442–3452.
- Centonze, D., Rossi, S., Mercaldo, V., Napoli, I., Ciotti, M.T., De Chiara, V., Musella, A., Prosperetti, C., Calabresi, P., Bernardi, G., Bagni, C., 2008. Abnormal striatal GABA transmission in the mouse model for the fragile X syndrome. *Biol. Psychiatry* 63, 963–973.
- Centonze, D., Rossi, S., Prosperetti, C., Gasperi, V., De Chiara, V., Bari, M., Tschertter, A., Febbraro, F., Bernardi, G., Maccarrone, M., 2007. Endocannabinoids limit metabotropic glutamate 5 receptor-mediated synaptic inhibition of striatal principal neurons. *Mol. Cell. Neurosci.* 35, 302–310.
- Chiappalone, M., Novellino, A., Vajda, I., Vato, A., Martinoia, S., van Pelt, J., 2005. Burst detection algorithms for the analysis of spatio-temporal patterns in cortical networks of neurons. *Neurocomputing* 65, 653–662.
- Chiappalone, M., Bove, M., Vato, A., Tedesco, M., Martinoia, S., 2006. Dissociated cortical networks show spontaneously correlated activity patterns during in vitro development. *Brain Res.* 1093, 41–53.
- Cianfoni, A., Niku, S., Imbesi, S.G., 2007. Metabolite findings in tumefactive demyelinating lesions utilizing short echo time proton magnetic resonance spectroscopy. *A.J.N.R. Am. J. Neuroradiol.* 28, 272–277.
- Clements, R.J., McDonough, J., Freeman, E.J., 2008. Distribution of parvalbumin and calretinin immunoreactive interneurons in motor cortex from multiple sclerosis post-mortem tissue. *Exp. Brain Res.* 187, 459–465.
- Cumiskey, D., Curran, B.P., Herron, C.E., O'Connor, J.J., 2007. A role for inflammatory mediators in the IL-18 mediated attenuation of LTP in the rat dentate gyrus. *Neuropharmacology* 52, 1616–1623.
- Dutta, R., McDonough, J., Yin, X., Peterson, J., Chang, A., Torres, T., Gudz, T., Macklin, W.B., Lewis, D.A., Fox, R.J., Rudick, R., Mirnics, K., Trapp, B.D., 2006. Mitochondrial dysfunction as a cause of axonal degeneration in multiple sclerosis patients. *Ann. Neurol.* 59, 478–489.
- Eytan, D., Marom, S., 2006. Effective topology underlying synchronization in networks of cortical neurons. *J. Neurosci.* 26, 8465–8476.

- Fisone, G., Håkansson, K., Borgkvist, A., Santini, E., 2007. Signaling in the basal ganglia: postsynaptic and presynaptic mechanisms. *Physiol. Behav.* 92, 8–14.
- Friedman, L.K., Segal, M., 2010. Early exposure of cultured hippocampal neurons to excitatory amino acids protects from later excitotoxicity. *Int. J. Dev. Neurosci.* 28, 195–205.
- Furlan, R., Martino, G., Galbiati, F., Poliani, P.L., Smirardo, S., Bergami, A., Desina, G., Comi, G., Flavell, R., Su, M.S., Adorini, L., 1999. Caspase-1 regulates the inflammatory process leading to autoimmune demyelination. *J. Immunol.* 163, 2403–2409.
- Golan, H., Levav, T., Mendelsohn, A., Huleihel, M., 2004. Involvement of tumor necrosis factor alpha in hippocampal development and function. *Cereb. Cortex* 14 (1), 97.
- Gottesfeld, Z., Teitelbaum, D., Webb, C., Arnon, R., 1976. Changes in the GABA system in experimental allergic encephalomyelitis-induced paralysis. *J. Neurochem.* 27, 695–699.
- Gustafson, N., Gireesh-Dharmaraj, E., Czubayko, U., Blackwell, K.T., Plenz, D., 2006. A comparative voltage and current-clamp analysis of feedback and feedforward synaptic transmission in the striatal microcircuit in vitro. *J. Neurophysiol.* 95, 737–752.
- Guzman, J.N., Hernandez, A., Galarraga, E., Tapia, D., Laville, A., Vergara, R., Aceves, J., Vargas, J., 2003. Dopaminergic modulation of axon collaterals interconnecting spiny neurons of the rat striatum. *J. Neurosci.* 23, 8931–8940.
- Henry, R.G., Shieh, M., Okuda, D.T., Evangelista, A., Gorno-Tempini, M.L., Pelletier, D., 2008. Regional grey matter atrophy in clinically isolated syndromes at presentation. *J. Neurol. Neurosurg. Psychiatry* 79, 1236–1244.
- Kawaguchi, Y., Wilson, C.J., Augood, S.J., Emson, P.C., 1995. Striatal interneurons: chemical, physiological and morphological characterization. *Trends Neurosci.* 18, 527–535.
- Koos, T., Tepper, J.M., 1999. Inhibitory control of neostriatal projection neurons by GABAergic interneurons. *Nat. Neurosci.* 2, 467–472.
- Koos, T., Tepper, J.M., Wilson, C.J., 2004. Comparison of IPSCs evoked by spiny and fast-spiking neurons in the neostriatum. *J. Neurosci.* 24, 7916–7922.
- Kubota, Y., Kawaguchi, Y., 2000. Dependence of GABAergic synaptic areas on the interneuron type and target size. *J. Neurosci.* 20, 375–386.
- Lai, A.Y., Swayze, R.D., El-Husseini, A., Song, C., 2006. Interleukin-1 beta modulates AMPA receptor expression and phosphorylation in hippocampal neurons. *J. Neuroimmunol.* 175, 97–106.

- Lewitus, G.M., Zhu, J., Xiong, H., Hallworth, R., Kipnis, J., 2007. CD4(+)CD25(+) effector T-cells inhibit hippocampal long-term potentiation in vitro. *Eur. J. Neurosci.* 26, 1399–1406.
- Mazzoni, A., Broccard, F., Garcia-Perez, E., Bonifazi, P., Ruaro, M., Torre, V., 2007. On the dynamics of the spontaneous activity in neuronal networks. *PLoS One* 5, e439.
- Matute, C., Alberdi, E., Domercq, M., Pérez-Cerdá, F., Pérez-Samartín, A., Sánchez-Gómez, M.V., 2001. The link between excitotoxic oligodendroglial death and demyelinating diseases. *Trends Neurosci.* 24, 224–230.
- Maeda, E., Kuroda, Y., Robinson, H., Kawana, A., 1998. Modification of parallel activity elicited by propagating bursts in developing networks of rat cortical neurones. *Eur. J. Neurosci.* 10 (2), 488–496.
- Mizuno, T., Zhang, G., Takeuchi, H., Kawanokuchi, J., Wang, J., Sonobe, Y., Jin, S., Takada, N., Komatsu, Y., Suzumura, A., 2008. Interferon-gamma directly induces neurotoxicity through a neuron specific, calcium-permeable complex of IFN-gamma receptor and AMPA GluR1 receptor. *FASEB J.* 22, 1797–1806.
- Muzio, L., Cavaiani, F., Marinaro, C., Bergamaschi, A., Bergami, A., Porcheri, C., Cerri, F., Dina, G., Quattrini, A., Comi, G., Furlan, R., Martino, G., 2010. Cxcl10 enhances blood cells migration in the sub-ventricular zone of mice affected by experimental autoimmune encephalomyelitis. *Mol. Cell. Neurosci.* 43, 268–280.
- Neumann, H., Schweigreiter, R., Yamashita, T., Rosenkranz, K., Wekerle, H., Barde, Y., 2003. Tumor necrosis factor inhibits neurite outgrowth and branching of hippocampal neurons by a Rho-dependent mechanism. *J. Neurosci.* 22 (3), 854.
- Newcombe, J., Uddin, A., Dove, R., Patel, B., Turski, L., Nishizawa, Y., Smith, T., 2008. Glutamate receptor expression in multiple sclerosis lesions. *Brain Pathol.* 18, 52–61.
- Nisenbaum, E.S., Berger, T.W., 1992. Functionally distinct subpopulations of striatal neurons are differentially regulated by GABAergic and dopaminergic inputs-I. In vivo analysis. *Neuroscience* 48, 561–578.
- Pitt, D., Werner, P., Raine, C.S., 2000. Glutamate excitotoxicity in a model of multiple sclerosis. *Nat. Med.* 6, 67–70.
- Plenz, D., 2003. When inhibition goes incognito: feedback interaction between spiny projection neurons in striatal function. *Trends Neurosci.* 26, 436–443.
- Qureshi, G.A., Baig, M.S., 1988. Quantitation of free amino acids in biological samples by high-performance liquid chromatography. Application of the method in evaluating amino acid levels in

- cerebrospinal fluid and plasma of patients with multiple sclerosis. *J. Chromatogr.* 459, 237–244.
- Rossi, S., Furlan, R., De Chiara, V., Musella, A., Lo Giudice, T., Mataluni, G., Cavinini, F., Cantarella, C., Bernardi, G., Muzio, L., Martorana, A., Martino, G., Centonze, D., 2009. Exercise attenuates the clinical, synaptic and dendritic abnormalities of experimental autoimmune encephalomyelitis. *Neurobiol. Dis.* 36, 51–59.
- Smith, T., Groom, A., Zhu, B., Turski, L., 2000. Autoimmune encephalomyelitis ameliorated by AMPA antagonists. *Nat. Med.* 6, 62–66.
- Srinivasan, R., Sailasuta, N., Hurd, R., Nelson, S., Pelletier, D., 2005. Evidence of elevated glutamate in multiple sclerosis using magnetic resonance spectroscopy at 3 T. *Brain* 128, 1016–1025.
- Stellwagen, D., Beattie, E.C., Seo, J.Y., Malenka, R.C., 2005. Differential regulation of AMPA receptor and GABA receptor trafficking by tumor necrosis factor- α . *J. Neurosci.* 25, 3219–3228.
- Stellwagen, D., Malenka, R.C., 2006. Synaptic scaling mediated by glial TNF- α . *Nature* 440, 1054–1059.
- Stern, E.A., Jaeger, D., Wilson, C.J., 1998. Membrane potential synchrony of simultaneously recorded striatal spiny neurons in vivo. *Nature* 394, 475–478.
- Tafoya, L.C., Mamelì, M., Miyashita, T., Guzowski, J.F., Valenzuela, C.F., Wilson, M.C., 2006. Expression and function of SNAP-25 as a universal SNARE component in GABAergic neurons. *J. Neurosci.* 26, 7826–7838.
- Tao, G., Datta, S., He, R., Nelson, F., Wolinsky, J.S., Narayana, P.A., 2009. Deep gray matter atrophy in multiple sclerosis: a tensor based morphometry. *J. Neurol. Sci.* 282, 39–46.
- Tepper, J.M., Abercrombie, E.D., Bolam, J.P., 2007. Basal ganglia macrocircuits. *Prog. Brain Res.* 160, 3–7.
- Tepper, J.M., Koos, T., Wilson, C.J., 2004. GABAergic microcircuits in the neostriatum. *Trends Neurosci.* 27, 662–669.
- Tunstall, M.J., Oorschot, D.E., Kean, A., Wickens, J.R., 2002. Inhibitory interactions between spiny projection neurons in the rat striatum. *J. Neurophysiol.* 88, 1263–1269.
- van Pelt, J., Vajda, I., Wolters, P.S., Corner, M.A., Ramakers, G.J.A., 2005. Dynamics and plasticity in developing neuronal networks in vitro. *Prog. Brain Res.* 147, 173–188.
- Vikman, K., Owe-Larsson, B., Brask, J., Kristensson, K., Hill, R., 2001. Interferon- γ -induced changes in synaptic activity and AMPA receptor clustering in hippocampal cultures. *Brain Res.* 895, 18–29.
- Vyshkina, T., Banisori, I., Shugart, Y.Y., Leist, T.P., Kalman, B., 2005. Genetic variants of Complex I in multiple sclerosis. *J. Neurol. Sci.* 228, 55–64.

- Wallström, E., Diener, P., Ljungdahl, A., Khademi, M., Nilsson, C.G., Olsson, T., 1996. Memantine abrogates neurological deficits, but not CNS inflammation, in Lewis rat experimental autoimmune encephalomyelitis. *J. Neurol. Sci.* 137, 89–96.
- Wang, Y., Feng, D., Liu, G., Luo, Q., Xu, Y., Lin, S., Fei, J., Xu, L., 2008. Gammaaminobutyric acid transporter 1 negatively regulates T cell-mediated immune responses and ameliorates autoimmune inflammation in the CNS. *J. Immunol.* 181, 8226–8236.
- Wagenaar, D., Pine, J., Potter, S., 2006. An extremely rich repertoire of bursting patterns during the development of cortical cultures. *BMC Neurosci.* 7–11, 1–18.
- Wilson, C.J., Kawaguchi, Y., 1996. The origins of two-state spontaneous membrane potential fluctuations of neostriatal spiny neurons. *J. Neurosci.* 16, 2397–2410.
- Xiong, Z.Q., McNamara, J.O., 2002. Fleeting activation of ionotropic glutamate receptors sensitizes cortical neurons to complement attack. *Neuron* 36, 363–374.
- Zhang, R., Yamada, J., Hayashi, Y., Wu, Z., Koyama, S., Nakanishi, H., 2008. Inhibition of NMDA-induced outward currents by interleukin-1 β in hippocampal neurons. *Biochem. Biophys. Res. Commun.* 372, 816–820.
- Zhu, B., Luo, L., Moore, G.R., Paty, D.W., Cynader, M.S., 2003. Dendritic and synaptic pathology in experimental autoimmune encephalomyelitis. *Am. J. Pathol.* 162, 1639–1650.
- Ziehn, M.O., Avedisian, A.A., Tiwari-Woodruff, S., Voskuhl, R.R., 2010. Hippocampal CA1 atrophy and synaptic loss during experimental autoimmune encephalomyelitis, EAE. *Lab. Invest.* 90, 774–786.

CHAPTER 4

Summary, conclusions and future perspectives

Previous study uncovered the contribution of pro-inflammatory cytokines in promoting synaptic degeneration and dendritic spines loss in EAE affected mice (Centonze et al 2009a). Beside these results, it was highlighted the protective effects deriving from the blockage of AMPA receptors during acute neuroinflammation, and established a functional connection between pro-inflammatory cues and harmful molecular cascades, that are fostering neurodegenerative processes during acute EAE (Centonze et al 2009b).

Since GABA is reduced in the cerebrospinal fluid of MS subjects (Qureshi and Baig, 1988), protein and mRNA expression of the GABA transporter-1 (GAT-1) are dramatically reduced in the spinal cord of EAE mice (Wang et al., 2008) and potentiation of GABA signaling significantly ameliorates EAE clinical course (Bhat et al., 2010), also the GABAergic transmission seems to be impaired in EAE. Actually, we found irreversible alteration of GABA synaptic transmission in gray matter of the striatum of EAE mice, that during inflammation, accordingly with the previous studies on striata glutamate-mediated transmission (Centonze et al 2009a) (Rossi et al., 2009), is reorganized. However, the GABAergic and glutamatergic

transmission changed with different kinetics: glutamate transmission hyperfunctioning was evident in the pre-symptomatic and acute phases of EAE disease when the activation of resident microglia was maximal, while GABAergic hypofunctioning was present in the acute and especially marked in the chronic phases of the disease when microglial cells return to the resting state (Centonze et al., 2009). We also showed that a cocktail of pro-inflammatory cytokines can perturb the GABAergic system *in vitro*, when chronically administered for 24 h. In line with this evidence, we failed to replicate the neurophysiological abnormalities of GABAergic sIPSCs following short incubation of striatal slices with either activated BV2 microglia or TNF- α , thus suggesting that to obtain GABAergic alteration long lasting cytokines exposure is needed. Our results are in agreement with other reports showing that prolonged treatments with a prototypic pro-inflammatory cytokine -i.e. TNF- α - induced severe derangement of neuronal morphology, altering the dendritic branching (Neumann et al., 2003) and perturbing spatial learning (Aloe et al., 1999; Golan et al., 2004).

Moreover a significant reduction in the number of PV-positive striatal cells accompanied impaired GABA signaling seen in electrophysiological, morphological and western blot experiments and also *in vitro* PV expression was severely reduced in neuronal cultures treated with pro-inflammatory cytokines. This study evidences that chronic treatment with pro-inflammatory cytokines

induce a GABAergic down-regulation that seems to affect mainly PV expressing neurons.

Another aspect of EAE pathogenesis during the acute phase of inflammation that we investigated is the contribution of CNS acidosis. Since mitochondria dysfunctions and lactate accumulation in cerebrospinal fluid of MS patient were well established (Dutta et al 2006, Paling et al 2011, Simone et al 1996), we hypothesize that these features together with inflammatory milieu create an acidification state. Furthermore, the presence of sustained acidification in chronic EAE mice has been recently described by measuring the pH within the spinal cord of EAE affected mice at the peak of the inflammation introducing a micro-pH meter (Fries et al 2007). Fries and colleague found an acidic pH within a range around 6.6; however, this is an invasive technique and the technical method may, *per se*, generate bleeding and a subsequent general acidosis of tissues. To measure pH fluctuation in intact brain with a non-invasive technique on EAE mice demonstrating the presence of a persistent acidosis also in the brain, we used an unconventional MR-Spectroscopy based approach, based on the IEPA probe (Garcia-Martin et al 2001). Accordingly to Fries and collaborators findings we observed that in the areas of CNS lesions, that are gadolinium positive, IEPA probe measured acid environment with a pH value around 6.6. In addition, in these areas we found an accumulation of CD45⁺ inflammatory cells. Since ASIC1a is activated at the pH that we found using MRS (pH6.6), we next investigated the contribution of ASIC1a activation to the

neurodegenerative processes by treating EAE mice with Diminazene Aceturate (DA), which is a new potent and specific ASICs inhibitor belonging to the family of diarylamidines. In this framework, previous studies demonstrated protective effects deriving from the inhibition of ASICs in EAE (Friese et al 2007, Vergo et al 2011) and MS patients (Arun et al 2013). These studies proposed the use of Amiloride for the blockage of ASICs during acute inflammation. Amiloride, however, displays a broad spectrum of action, being able to block epithelial sodium channels (ENaC), the Na^+/H^+ antiporter 1 in the heart, $\text{Na}^+/\text{Ca}^{2+}$ exchanger and voltage-gated Ca^{2+} channels, in addition to ASICs inhibition, thus posing questions about its specificity and suggesting additional studies. DA exerts the blockage of ASIC1a, -1b -2a, and -3 currents in transfected CHO cells, with the following efficiency $1b > 3 > 2a > 1a$, therefore the effects that we observed are all dependent to ASICs family blockage. Our results indicate that DA is able to mediate beneficial effects in the CNS of EAE mice, inducing myelin preservation and reducing axonal loss. It is interestingly to note that our treatment caused a rapid improvement of walking performances in mice affected by EAE, suggesting that beside axonal preservation, DA was also effective to counteract harmful electrophysiological alterations elicited by acidosis. However, we cannot exclude that since DA block also ASIC2a/b and ASIC3, the inhibition of these channels together with ASIC1a blockage can participate to avoid the establishment of the CNS damage and pain perception in EAE disease.

Moreover we studied the electrophysiological changes elicited by low pH, using *in vitro* networks of neurons coupled with Micro Electrode Arrays devices. Our electrophysiological data suggest that acidic treatment causes long term alterations of the neuronal connectivity, that were reverted by administering neurons with DA. Indeed, we demonstrated that the homeostasis of the pre-synaptic compartment is severely affected in neurons exposed to low pH, thus showing that extracellular acidosis can modulate the synaptic stability.

Since DA do not cause any side effects in mice, is neuroprotective and improves walking performances in EAE mice, it shed light on new perspectives for MS treatment through specific ASICs blockage. Furthermore, ASICs are involved in various pathology - as stroke, epilepsy, Huntington's disease, Parkinson's disease, migraine, spinal cord injury, glioblastoma (Wemmie et al 2013)- therefore the discovery of new molecules able to block these channels open new perspective to innovative therapies in a wide spectrum of pathologies.

References

- Aloe, L., Properzi, F., Probert, L., Akassoglou, K., Kassiotis, G., Micera, A., Fiore, L., 1999. Learning abilities, NGF and BDNF brain levels in two lines of TNF α transgenic mice, one characterized by neurological disorders, the other phenotypically normal. *Brain Res.* 840, 125–137.
- Arun T, Tomassini V, Sbardella E, de Ruiter MB, Matthews L, et al. 2013. Targeting ASIC1 in primary progressive multiple sclerosis: evidence of neuroprotection with amiloride. *Brain* 136: 106-15
- Bhat, R., Axtell, R., Mitra, A., Miranda, M., Lock, C., Tsien, R.W., Steinman, L., 2010. Inhibitory role for GABA in autoimmune inflammation. *Proc. Natl. Acad. Sci. USA* 107, 2580–2585.
- Centonze D, Muzio L, Rossi S, Cavasinni F, De Chiara V, et al. 2009a. Inflammation Triggers Synaptic Alteration and Degeneration in Experimental Autoimmune Encephalomyelitis. *Journal of Neuroscience* 29: 3442-52
- Centonze D, Muzio L, Rossi S, Furlan R, Bernardi G, Martino G. 2009b. The link between inflammation, synaptic transmission and neurodegeneration in multiple sclerosis. *Cell Death and Differentiation* 17: 1083-91
- Dutta R, McDonough J, Yin X, Peterson J, Chang A, et al. 2006. Mitochondrial dysfunction as a cause of axonal degeneration in multiple sclerosis patients. *Ann Neurol* 59: 478-89
- Friesse MA, Craner MJ, Etzensperger R, Vergo S, Wemmie JA, et al. 2007. Acid-sensing ion channel-1 contributes to axonal degeneration in autoimmune inflammation of the central nervous system. *Nature Medicine* 13: 1483-89
- Garcia-Martin ML, Herigault G, Remy C, Farion R, Ballesteros P, et al. 2001. Mapping extracellular pH in rat brain gliomas in vivo by ¹H magnetic resonance spectroscopic imaging: comparison with maps of metabolites. *Cancer Res* 61: 6524-31
- Golan, H., Levav, T., Mendelsohn, A., Huleihel, M., 2004. Involvement of tumor necrosis factor alpha in hippocampal development and function. *Cereb. Cortex* 14 (1), 97.
- Neumann, H., Schweigreiter, R., Yamashita, T., Rosenkranz, K., Wekerle, H., Barde, Y., 2003. Tumor necrosis factor inhibits neurite outgrowth and branching of hippocampal neurons by a Rho-dependent mechanism. *J. Neurosci.* 22 (3), 854.

- Paling D, Golay X, Wheeler-Kingshott C, Kapoor R, Miller D. 2011. Energy failure in multiple sclerosis and its investigation using MR techniques. *Journal of Neurology* 258: 2113-27
- Qureshi, G.A., Baig, M.S., 1988. Quantitation of free amino acids in biological samples by high-performance liquid chromatography. Application of the method in evaluating amino acid levels in cerebrospinal fluid and plasma of patients with multiple sclerosis. *J. Chromatogr.* 459, 237–244.
- Rossi, S., Furlan, R., De Chiara, V., Musella, A., Lo Giudice, T., Mataluni, G., Cavašinni, F., Cantarella, C., Bernardi, G., Muzio, L., Martorana, A., Martino, G., Centonze, D., 2009. Exercise attenuates the clinical, synaptic and dendritic abnormalities of experimental autoimmune encephalomyelitis. *Neurobiol. Dis.* 36, 51–59.
- Simone IL, Federico F, Trojano M, Tortorella C, Liguori M, et al. 1996. High resolution proton MR spectroscopy of cerebrospinal fluid in MS patients. Comparison with biochemical changes in demyelinating plaques. *Journal of the Neurological Sciences* 144: 182-90
- Vergo S, Craner MJ, Etzensperger R, Attfield K, Friesse MA, et al. 2011. Acid-sensing ion channel 1 is involved in both axonal injury and demyelination in multiple sclerosis and its animal model. *Brain* 134: 571-84
- Wang, Y., Feng, D., Liu, G., Luo, Q., Xu, Y., Lin, S., Fei, J., Xu, L., 2008. Gammaaminobutyric acid transporter 1 negatively regulates T cell-mediated immune responses and ameliorates autoimmune inflammation in the CNS. *J. Immunol.* 181, 8226–8236.
- Wemmie JA, Taugher RJ, Kreple CJ. 2013. Acid-sensing ion channels in pain and disease. *Nat Rev Neurosci* 14: 461-71

CHAPTER 5

Publications

Impaired striatal GABA transmission in experimental autoimmune encephalomyelitis.

Rossi S, Muzio L, De Chiara V, Grasselli G, Musella A, Musumeci G, Mandolesi G, **De Ceglia R**, Maida S, Biffi E, Pedrocchi A, Menegon A, Bernardi G, Furlan R, Martino G, Centonze D.

Brain, Behavior, and Immunity 2011 Jul; 25(5):947-56.

doi: 10.1016/j.bbi.2010.10.004. Epub 2010 Oct 20.

A novel environmental chamber for neuronal network multisite recordings.

Biffi E, Regalia G, Ghezzi D, **De Ceglia R**, Menegon A, Ferrigno G, Fiore GB, Pedrocchi A.

Biotechnology and Bioengineering 2012 Oct; 109(10):2553-66.

doi: 10.1002/bit.24526. Epub 2012 Apr 24.

Subventricular zone neural progenitors protect striatal neurons from glutamatergic excitotoxicity.

Butti E, Bacigaluppi M, Rossi S, Cambiaghi M, Bari M, Cebrian Silla A, Brambilla E, Musella A, **De Ceglia R**, Teneud L, De Chiara V, D'Adamo P, Garcia-Verdugo JM, Comi G, Muzio L, Quattrini A, Leocani L, Maccarrone M, Centonze D, Martino G.

Brain 2012 Nov; 135(Pt 11):3320-35.

doi: 10.1093/brain/aws194. Epub 2012 Sep 24.

Acknowledgements

Durante il dottorato ho conosciuto numerose persone e ho imparato molto da ciascuna di loro. Cercherò quindi di ringraziarle, sperando di non tralasciare nessuno...

Innanzitutto ringrazio il Prof. Gianvito Martino che mi ha dato la possibilità di svolgere questo lavoro nel suo laboratorio e che mi ha sempre dato consigli e supporto durante questi anni di tesi. Senza la sua selezione iniziale non sarei qui oggi!

Ringrazio Luca Muzio per avermi seguito passo-passo durante lo svolgimento di questo progetto. I momenti di screzio durante questi anni credo che ci abbiano aiutato a trovare un certo equilibrio, anche se ogni tanto mi capita di sbilanciarlo nuovamente... Ti ringrazio per avermi insegnato gran parte delle competenze che ho oggi nel mio bagaglio di conoscenze. Spero di riuscirle a sfruttare al meglio.

Ringrazio la Prof.ssa Granucci per essere stata il mio Supervisor e per il supporto e la disponibilità che mi ha da sempre dimostrato.

Ringrazio la Prof.ssa Verderio per aver accettato di essere mio Mentor e per tutti i suggerimenti dati durante il dottorato.

Un grazie speciale va alle "muzine", frequentatrici della Baia, vecchie e nuove... Grazie a Cinzia che anche se non è più fisicamente in lab mi ha sempre sostenuto fin dai primi giorni quando sono arrivata in lab. Cinzy sei veramente una persona speciale non ci sono parole per spiegare l'aiuto, il conforto e il supporto che mi hai dato... soprattutto per il legame di amicizia che abbiamo realizzato... sono veramente felice di averti incontrato... Semplicemente Grazie...

Grazie ad Anniniiii, "aiutoooo aiutoooo" che senza audio non rende molto, ma tu sai cosa significa, soprattutto nel tardo pomeriggio! Abbiamo condiviso tanti momenti insieme e spero che nonostante la distanza riusciremo in qualche modo a crearne di nuovi...

Ora le nuove entrate... oramai mica tanto nuove, ma comunque... Benny, Chiara e Vale... che dire... in questo ultimo anno sono successe veramente tante cose, ma il fatto di affrontarle insieme, ci ha permesso di superarle. Ragazze ricordatevi sempre che l'unione fa la forza, e chi c'è nel bancone di fianco può sempre sostenerti! E' la squadra che permette di vincere... e nonostante tutto

noi siamo una piccola-piccola squadra! Grazie per tutto quello che mi avete dato anche inconsapevolmente!

E grazie al nostro CTDM o GMC che dir si voglia! Andre in questi anni siamo anche diventati compagni di bancone... ahahiah... grazie per tutto il supporto che mi hai dato, lavorativamente e non... per tutte le caxxte dette e radio Capital che assolutamente FEDELEMENTE ci ha accompagnato!

Grazie a Francesca R., Elena e Annamaria per i suggerimenti e il sostegno in tutti questi anni...

Grazie a tutti i tesisti vecchi e nuovi o come sono stati definiti (ST) vero Giulia! Anche se ST non lo siete per nulla... Grazie a Giulia, Gianluca, Mattia, Antonio, Giuseppe, Bruno, Giacomo e tutti gli altri che mancano perché siete veramente tanti... grazie a tutti voi perché anche se non lo sapete ognuno di voi mi ha insegnato qualcosa!

Grazie ai ragazzi stranieri Bruno, Gabriela e Amir che hanno portato un po' di MONDO in lab..

Grazie a Melania, Chiara M. (anche se nn sei più in lab), Dona, Marco, Luca JP, Francesca G., Arianna e tutti i ragazzi del lab per tutti i momenti passati insieme e per i consigli e gli scambi di opinione e il vivere il lab in orari alternativi!

Grazie a Livia, per le nostre chiacchierate, scambi di opinione, suggerimenti, idee e soprattutto citochine: risospensione e diluizione. Ahahaha!!! Dai che siamo alla fine!! Ce la possiamo fareeeeeee!!!! DEVI solo STARE MOLTO CALMO!!

Un grazie particolare a Cecilia con cui ho condiviso tanto, soprattutto l'angolo del bancone all'inizio e che ci ha portate vicine-vicine, vero???? Amiccccceeee! Adesso abbiamo condiviso anche i MEA, ma soprattutto il pdf della cover... vero Ce'! Ahahiah! Grazie Ceci per i consigli scientifici ma anche per il sostegno e le battute sparate ogni giorno che ci permettono e ci hanno permesso di affrontare con il sorriso anche le situazioni peggiori! Grazie!

Un grazie speciale alla Buttina... difficile dire a parole quello che penso... Grazie di tutto, di esserci sempre, dal consiglio in lab e soprattutto fuori dal lab o nel lab ma che non riguarda il lab... un po' complicato ma penso che si capisca! Chi lo avrebbe mai detto... Abbiamo costruito una splendida amicizia incredibilmente inaspettata... Grazie...

Grazie agli Ingegneri di fiducia Emy e Giuly. Sempre presenti e tempestive! Ci sono un sacco di novità Piccole e grandi da quando ci siamo conosciute, specialmente con te, Emy... è stato piacevole ed istruttivo lavorare con voi.. chissà in futuro che non ci rincontreremo, lavorativamente parlando ovviamente, come amicizia sono certa di sì!

Grazie anche a Simo, Caprots, Marikina, Maggy e Laura che nonostante l'anno veramente difficile, al di là degli anni che passano, sono-e-siamo sempre tanto vicine...

Bhè i vostri nomi sono superflui, sicuramente vi riconoscerete da sole... per voi non credo ci siano parole, ma proverò comunque a scrivere qualcosa:

Grazie per le cene improvvisate, per gli abbracci arrivati anche se non richiesti, per le pizze di supporto al sabato sera, per le incazzature per farmi smuovere, per i ti voglio bene, per le telefonate e i messaggi ai momenti più o meno giusti, per le cose dette e non dette, per tutti i momenti trascorsi insieme, per tutti i momenti in cui mi avete risollevato quando avevo toccato il fondo... Ragazze GRAZIE DI ESSERE SEMPRE-SEMPRE-SEMPRE presenti... vi voglio bene... R.E.D.V.

Infine Grazie con la G maiuscola alla mia famiglia, ma soprattutto a mamma, papà e a "occhiali-occhiali che si muovono-il NULLA". Grazie di esserci adesso ed esserci sempre stati fin dal principio, grazie al "NULLA" per essersi presentato a casa a Milano sconvolgendo i vecchi equilibri e instaurandone dei nuovi. Un semplice ma sincero GRAZIE...